(12) INTERNATIONAL APPLICATION PUBLISHED UNDER THE PATENT COOPERATION TREATY (PCT)

(19) World Intellectual Property Organization
International Bureau

(43) International Publication Date
28 September 2023 (28.09.2023)

WIPO | PCT

(10) International Publication Number
WO 2023/183681 A2

(51) International Patent Classification:
B22F 1/054 (2022.01) *C22C 19/05* (2006.01)

(21) International Application Number:
PCT/US2023/062662

(22) International Filing Date:
15 February 2023 (15.02.2023)

(25) Filing Language: English

(26) Publication Language: English

(30) Priority Data:
63/310,432 15 February 2022 (15.02.2022) US

(71) Applicant: **MASSACHUSETTS INSTITUTE OF TECHNOLOGY** [US/US]; 77 Massachusetts Ave., Cambridge, Massachusetts 02139 (US).

(72) Inventors: **SCHUH, Christopher A.**; 4 Plainview Road, Wayland, Massachusetts 01778 (US). **NAUNHEIM, Yannick**; 70 Pacific St, Cambridge, Massachusetts 02139 (US).

(74) Agent: **FOX, Harold H.**; 1440 New York Ave NW, Suite 200, Washington, District of Columbia 20005 (US).

(81) Designated States *(unless otherwise indicated, for every kind of national protection available)*: AE, AG, AL, AM, AO, AT, AU, AZ, BA, BB, BG, BH, BN, BR, BW, BY, BZ, CA, CH, CL, CN, CO, CR, CU, CV, CZ, DE, DJ, DK, DM, DO, DZ, EC, EE, EG, ES, FI, GB, GD, GE, GH, GM, GT, HN, HR, HU, ID, IL, IN, IQ, IR, IS, IT, JM, JO, JP, KE, KG, KH, KN, KP, KR, KW, KZ, LA, LC, LK, LR, LS, LU, LY, MA, MD, MG, MK, MN, MW, MX, MY, MZ, NA, NG, NI, NO, NZ, OM, PA, PE, PG, PH, PL, PT, QA, RO, RS, RU, RW, SA, SC, SD, SE, SG, SK, SL, ST, SV, SY, TH, TJ, TM, TN, TR, TT, TZ, UA, UG, US, UZ, VC, VN, WS, ZA, ZM, ZW.

(84) Designated States *(unless otherwise indicated, for every kind of regional protection available)*: ARIPO (BW, CV, GH, GM, KE, LR, LS, MW, MZ, NA, RW, SC, SD, SL, ST, SZ, TZ, UG, ZM, ZW), Eurasian (AM, AZ, BY, KG, KZ, RU, TJ, TM), European (AL, AT, BE, BG, CH, CY, CZ, DE, DK, EE, ES, FI, FR, GB, GR, HR, HU, IE, IS, IT, LT, LU, LV, MC, ME, MK, MT, NL, NO, PL, PT, RO, RS, SE, SI, SK, SM, TR), OAPI (BF, BJ, CF, CG, CI, CM, GA, GN, GQ, GW, KM, ML, MR, NE, SN, TD, TG).

Declarations under Rule 4.17:
— *as to the identity of the inventor (Rule 4.17(i))*
— *as to applicant's entitlement to apply for and be granted a patent (Rule 4.17(ii))*
— *as to the applicant's entitlement to claim the priority of the earlier application (Rule 4.17(iii))*

Published:
— *without international search report and to be republished upon receipt of that report (Rule 48.2(g))*

(54) **Title:** NANO-PHASE SEPARATING NI POWDER AND THE METHODOLOGY TO IDENTIFY THEM

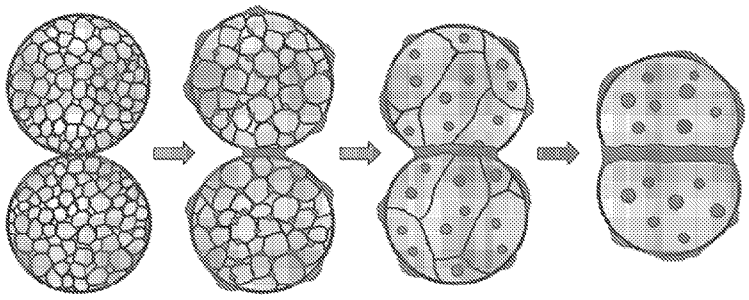

FIG. 1A

(57) **Abstract:** Alloys can be designed to serve as structural metals both in cryogenic and high temperature applications.

WO 2023/183681 A2

NANO-PHASE SEPARATING NI POWDER AND THE METHODOLOGY TO IDENTIFY THEM

CLAIM OF PRIORITY

[0001] This application claims priority to U.S. Provisional Patent Application No. 63/310,432, filed February 15, 2022, which is incorporated by reference in its entirety.

GOVERNMENT SPONSORSHIP STATEMENT

[0002] This invention was made with Government support under Grant No. 80MSFC19C0050 awarded by NASA Goddard Space Flight Center. The Government has certain rights in the invention.

FIELD OF THE INVENTION

[0003] The invention relates to phase separating powders and methods of identifying them.

BACKGROUND

[0004] Sintered nanocrystalline materials are often subjected to pressure or other post-sintering processing techniques to achieve higher density materials.

SUMMARY

[0005] In one aspect, a method of designing a metal alloy powder having a miscibility gap at low temperature can include identifying a first metal element and a second metal to form a metal alloy, selecting a third metal having a miscibility gap with the metal alloy, and mechanically alloying the third metal and the metal alloy to form a metal alloy powder having a nanoscale grain size.

[0006] In certain circumstances, the metal alloy powder can be engineered to have a phase separation temperature at which diffusion of the third metal occurs to phase separate as a nanoscale phase.

[0007] In certain circumstances, the nanoscale phase can redissolve at a transition temperature

higher than the phase separation temperature.

[0008] In certain circumstances, the metal alloy can be a nano-phase separating powder.

[0009] In certain circumstances, the first metal can include nickel.

[0010] In certain circumstances, the second metal can include chromium, cobalt, vanadium, silver, molybdenum, tungsten, or iron.

[0011] In certain circumstances, the third metal can include copper.

[0012] In certain circumstances, the metal alloy powder can include manganese.

[0013] In certain circumstances, the metal alloy powder can include vanadium.

[0014] In certain circumstances, the metal alloy powder can include molybdenum.

[0015] In certain circumstances, the metal alloy powder can include tungsten.

[0016] In certain circumstances, the metal alloy powder can include silver.

[0017] In certain circumstances, the metal alloy powder can include zirconium.

[0018] In certain circumstances, the metal alloy powder can include iron.

[0019] In certain circumstances, the metal alloy can include a ternary nano-phase separating powder.

[0020] In certain circumstances, the metal alloy can include a quaternary nano-phase separating powder.

[0021] In certain circumstances, the first metal can have a concentration of about 25 at% to about 95 at% of the alloy.

[0022] In certain circumstances, the second metal can have a concentration of about 25 at% to about 95 at% of the alloy.

[0023] In certain circumstances, the third metal can have a concentration of about 5 at% to about 50 at% of the alloy.

[0024] In certain circumstances, the metal alloy powder can include an oxygen scavenging metal.

[0025] In another aspect, a method of nano-phase separation sintering of a powder can include providing a fine grained powder including a first metal element and a second metal forming a metal alloy and a third metal having a miscibility gap with the metal alloy, and sintering the fine grained powder to form a sintered product.

[0026] In another aspect, a metal alloy powder for sintering can include a mechanically alloyed powder including a first metal element and a second metal forming a metal alloy and a third metal having a miscibility gap with the metal alloy.

[0027] In certain circumstances, the fine grained powder can be a mechanically alloyed powder.

[0028] In certain circumstances, the sintered product achieves at least 80% density at low temperatures without the need for an applied pressure during the sintering.

[0029] In certain circumstances, the sintered product achieves at least 90% density at low temperatures without the need for an applied pressure during the sintering.

[0030] In certain circumstances, the mechanically alloyed powder is a nano-phase separating powder.

[0031] In certain circumstances, the mechanically alloyed powder can include nickel, chromium, iron, copper, vanadium, molybdenum, tungsten, silver, zirconium, or combinations thereof.

[0032] In certain circumstances, sintering can include nano-phase separation sintering.

[0033] In certain circumstances, grain size of the metal alloy powder and grain size of the sintered powder can be substantially the same.

[0034] In certain circumstances, the metal alloy powder can include: NiCu having 5 at% to 20 at% Cr; NiCu having 5 at% to 45 at% Fe; NiCu having 5 at% to 45 at% Co; NiFeCu having 5at% or 8at% Mn; NiCu having 5 at% to 15 at% V; or NiCu having 5at% to 45 at% Co.

[0035] In certain circumstances, the mechanically powder is a quaternary nano-phase separating powder.

[0036] In certain circumstances, the metal alloy powder can include NiCu having 5at% to 45 at% Co and up to 5at% Mn.

[0037] In another aspect, a sintered product can include the powder described above.

[0038] Other aspects, embodiments, and features will be apparent from the following description, the drawings, and the claims.

BRIEF DESCRIPTION OF THE DRAWINGS

[0039] FIG. 1A is a schematic illustrating nano-phase separation sintering, including phase separation, neck formation, sintering and densification.

[0040] FIG. 1B depicts a phase diagram.

[0041] FIG. 1C is a schematic illustrating an example of the general process described herein.

[0042] FIG. 2A depicts a Ni-Cu phase diagram.

[0043] FIG. 2B is a graph illustrating a behavior of the system.

[0044] FIG. 3 depicts a phase diagram.

[0045] FIG. 4A is a graph showing densification rate.

[0046] FIG. 4B is a graph showing change in relative density.

[0047] FIG. 5A depicts a Ni-Cr phase diagram.

[0048] FIG. 5B depicts a Cu-Cr phase diagram.

[0049] FIG. 6A depicts a Ni-Cu phase diagram at 5 at% Cr.

[0050] FIG. 6B depicts a Ni-Cu phase diagram at 10 at% Cr.

[0051] FIG. 6C depicts a Ni-Cu phase diagram at 15 at% Cr.

[0052] FIG. 6D depicts a phase diagram of 60 at% Ni and 15% Cr.

[0053] FIG. 6E is a table showing the compositions of stable phases at 550°C.

[0054] FIG. 6F is a graph showing the temperature dependence of densification at 5°C/min to 1200°C and 40°C/min cooling.

[0055] FIG. 7A depicts a Ni-Fe phase diagram.

[0056] FIG. 7B depicts a Cu-Fe phase diagram.

[0057] FIG. 8A depicts a Ni-Cu phase diagram at 5 at% Fe.

[0058] FIG. 8B depicts a Ni-Cu phase diagram at 20 at% Fe.

[0059] FIG. 8C depicts a Ni-Cu phase diagram at 42 at% Fe.

[0060] FIG. 8D depicts a Ni-Cu phase diagram at 42at% Fe.

[0061] FIG. 8E is a table showing the compositions of stable phases at 550°C.

[0062] FIG. 8F is a graph showing the temperature dependence of densification at 5°C/min to 945°C and 40°C/min cooling.

[0063] FIG. 8G is a graph showing the change in relative density over time at 5°C/min heating.

[0064] FIG. 8H is a graph showing the temperature dependence of densification at 10°C/min

to 1000°C and 40°C/min cooling.

[0065] FIG. 8I is a graph showing the change in relative density over time at 5°C/min heating to a final relative density of 0.5864%.

[0066] FIG. 8J is a graph showing the temperature dependence of densification at 15°C/min to 1000°C and 40°C/min cooling.

[0067] FIG. 8K is a graph showing the change in relative density over time at 15°C/min heating to a final relative density of 0.5477%.

[0068] FIG. 8L is a graph showing the temperature dependence of densification at 20°C/min to 1000°C and 40°C/min cooling.

[0069] FIG. 8M is a graph showing the change in relative density over time at 20°C/min heating to a final relative density of 0. 4276%.

[0070] FIG. 8N is a graph showing the temperature dependence of densification at 5°C/min to 1100°C and 40°C/min cooling.

[0071] FIG. 8O is a graph showing the change in relative density over temperature at 5°C/min heating.

[0072] FIG. 8P is a graph showing the change in relative density over time at 5°C/min heating.

[0073] FIG. 8Q is a graph showing the temperature dependence of densification at 10°C/min to 1100°C and 40°C/min cooling.

[0074] FIG. 8R is a graph showing the change in relative density over temperature at 10°C/min heating.

[0075] FIG. 8S is a graph showing the change in relative density over time at 15°C/min.

[0076] FIG. 8T is a graph showing the temperature dependence of densification at 20°C/min to 1100°C and 40°C/min cooling.

[0077] FIG. 8U is a graph showing the temperature dependence of densification at 20°C/min to 1100°C and 40°C/min cooling.

[0078] FIG. 8V is a graph showing the change in relative density over time at 20°C/min.

[0079] FIG. 9A depicts a Ni-Co phase diagram.

[0080] FIG. 9B depicts a Cu-Co phase diagram.

[0081] FIG. 10A depicts a Ni-Cu phase diagram at 5 at% Co.

[0082] FIG. 10B depicts a Ni-Cu phase diagram at 20 at% Co.

[0083] FIG. 10C depicts a Ni-Cu phase diagram at 44 at% Co.

[0084] FIG. 11A depicts a Ni-V phase diagram.

[0085] FIG. 11B depicts a Cu-V phase diagram.

[0086] FIG. 12A depicts a Ni-Cu phase diagram at 6 at% V.

[0087] FIG. 12B depicts a Ni-Cu phase diagram at 10 at% V.

[0088] FIG. 12C depicts a Ni-Cu phase diagram at 13 at% V.

[0089] FIG. 12D depicts a Ni-Cu phase diagram and 13 at% V. At 15 at% Cu.

[0090] FIG. 12E is a table showing the stable phases at 1150°C.

[0091] FIG. 12F is a graph showing the temperature dependence of the densification rate for

10 at 5°C/min to 1200°C and 40°C/min cooling.

[0092] FIG. 12G is a graph showing the temperature dependences of the change in relative density.

[0093] FIG. 13 is a chart showing the diffusion rates and temperature range for metals described herein.

[0094] FIG. 14A depicts a phase diagram for Fe-Cu with 40 at% Ni from an Fe database.

[0095] FIG. 14B depicts a phase diagram for Fe-Cu with 40 at% Ni from a Ni database.

[0096] FIG. 14C depicts a phase diagram for Fe-Cu with 40 at% Ni from a Cu database.

[0097] FIG. 14D depicts a phase diagram for Fe-Cu with 40 at% Ni from a high entropy alloy database.

[0098] FIG. 15 depicts a Cr-Cu phase diagram at 60 at% Ni.

[0099] FIG. 16 depicts a Co-Cu phase diagram at 40 at% Ni.

[00100] FIG. 17 depicts a Cu-V phase diagram at 75 at% Ni.

[00101] FIGS. 18A, 18B and 18C are graphs showing densification after pretreatment with hydrogen at different heating rates.

[00102] FIG. 19 is a graph showing the impact on density of 5 at% and 8 at% Mn to a Ni-Fe-Cu composition.

[00103] FIG. 20 is a graph showing the densification behavior of the addition of Mn in a 37.5 at% Ni - 37.5 at% Co – 20 at% Cu – 5 at% Mn composition heated to 1200°C.

[00104] FIGS. 21, 22, 23 and 24 are micrographs of the composition of FIG. 20.

[00105] FIGS. 25-28 are graphs showing the mechanical properties of the sintered products of 37.5 at% Ni 37.5 at% Fe 20 at% Cu 5 at% Mn.

DESCRIPTION

[00106] Ternary, and higher order, metal alloys are designed to serve as structural metals both in cryogenic and high temperature applications. The more specific properties of these alloys can include the capability to be rapidly sintered from powder and achieve full density at low temperatures without the need for an applied pressure during the sintering process, which enables the processability of these alloys in additive manufacturing operations in bulk form.

[00107] As described herein, design a Ni based alloy suitable for use in space applications can be primarily made up of Ni to replace Inconel/superalloys. The materials can lead to improved processing. For example, accelerated (low-temperature) sintering from powder can allow for 3D printing using bound metal deposition without sag of structure. The materials can also have improved mechanical properties. Nanocrystallinity can provide increased strength and light-weighting structure over Inconel. The materials show improved thermal stability and scalability of the sintered parts/components.

[00108] Nanophase sintering demonstrates the need for the secondary phase to be transient. It can be important to avoid a contiguious secondary phase which can cause to a material to fail without harnessing the hard-won gains in Ni. Importantly, the Ni-Cu system thermodynamically it meets the criteria. However, kinetically diffusion is too slow in pure Ni-Cu allows in the two-phase region, which forms necks due to the low transus temperature.

[00109] Rapid densification can be achieved through nano-phase separation and the design of ternary Ni systems, quaternary Ni systems, or higher order Ni systems. The Ni-Cu phase diagram exhibits a miscibility gap having a Ni- and a Cu-rich phase at low temperatures and a single phase

at temperatures above 400 °C over the entire compositional range. The phase separating element is Cu to form interparticle necks between the powders. Cu is chosen, because it i) precipitates into a second phase at low temperatures, ii) has a relatively small activation energy for diffusion in Ni and a lower melting temperature, which makes it favorable to create new precipitates at the interparticle necks, and iii) promotes rapid diffusion of Ni into the interparticle necks after reaching the single solid-solution phase field. It thus satisfies all proposed thermodynamic criteria for nano-phase separation.

[00110] In order to enable the diffusional nature of the phase separation kinetics, a third element can be chosen to elevate the transus temperature and to extend the two-phase field (miscibility gap) of the binary system Ni-Cu. Exemplary, calculated pseudo-binary phase diagrams for the systems containing various alloying amounts of Fe, Cr, Mn, V, W, Ag, Mo, or Co are described herein. Any of these ternary, or higher order, Ni phase diagrams can exhibit a two-phase field and a single-phase field at higher temperatures for a certain compositional range, like the binary Ni-Cu system. Any of these ternary or greater systems exhibits a transition from a dual to a single phase-field for a range of compositions that is taking place at a higher temperature than for any possible composition in the binary system Ni-Cu.

[00111] To prepare these alloys, powders of Ni, Cu and one of the elements described herein are mechanically alloyed, producing supersaturated powders with an evenly dispersed alloying components and a refined grain size in the order of a few nanometers. All alloy powders are subsequently cold isostatically pressed into the shape of a pellet (green body). Upon sintering, the supersaturated powders will decompose into a two-phase microstructure with a main Ni containing phase and a Cu-rich phase forming interparticle necks. The Cu-rich phase will make contact between neighboring particles. These necks serve as rapid diffusion pathways and redissolve for

temperatures higher than the transus, the main densification mechanism of the ternary or greater Ni alloys. The low temperature phase decomposition and the interdiffusion between the two phases promotes rapid densification to reach > 98% relative densities.

[00112] Thermo-Calc Software can be used to assess the equilibrium bulk phase diagrams of the ternary, or higher order, nano-phase separating Ni alloys with all of the following described characteristics and properties, such as volume fraction and chemical composition of the involved phases. Calculations, for example, Thermo-Calc, can be used as design tool to identify and predict potential alloy candidates for nano-phase separating ternary, or higher order, Ni systems.

[00113] Criteria to identify alloying elements for the design of ternary, or higher order, nano-phase separating Ni alloys can include one or more of the following features. The third alloying element should extend the thermodynamic stability of the low-temperature miscibility gap phase field of the binary system Ni-Cu, while maintaining a single phase solid-solution at high homologous temperatures of the alloy. Another factor to consider is a low-temperature miscibility gap is comprised of a Ni and a Cu-rich containing phase. In addition, a ternary, or higher order, alloying element can be chosen to elevate the transition temperature from a dual to single phase to such a degree that the thermodynamic equilibrium is reached. For example, phase decomposition into a dual-phase structure can kinetically take place. Another consideration is that, in addition to the dual-phase at low-temperature and the single phase at high temperature, no other phases (i.e. intermetallic phases) should form, that thermodynamically or kinetically impede nano-phase separation of the ternary or greater Ni powders. It can be important to identify a compositional range for appropriate volume fraction of the second phase forming in the low-temperature miscibility gap, or identify a compositional range for appropriate composition for the involved phases, thermodynamic and kinetic implications for nano-phase separation sintering, or both.

[00114] Processing steps for making and testing these alloys is described herein. Mechanical alloying of elemental nickel, copper, and iron (vanadium, cobalt, molybdenum, tungsten, silver, zirconium, manganese, or chromium) powders can be achieved via high-energy ball-milling technique and formation of a (forced) supersaturated solid solution. This can be followed by production of a green body (powder pellet) in the desired shape via cold isostatic pressing of the powder. Next, sintering of the powder pellets in a controlled atmosphere (Argon with some amount of forming gas) can take place. In general, a heating cycle to the desired temperature can include initial (phase separation) and secondary (interdiffusion, redissolution) densification take place at 500-700 °C and above 850 °C, respectively, reaching full density at a temperature of 1100 °C. Temperature and heating rate details can vary, as discussed herein and as understood in practice.

[00115] The methods and materials described herein can be useful in commercial applications. The ternary, or higher order, nano-phase separating Ni alloys can be designed to facilitate rapid consolidation of powder in bulk form without application of pressure during sintering, which are suitable characteristics for the application in additive manufacturing processes. The sintered ternary, or higher order, Ni alloys can be used as structural alloys in many applications that require high thermal, mechanical and corrosive stability, such as for components of turbines, engines and nuclear reactors. The simplified processibility of the ternary, or higher order, Ni alloys can reduce the complexity of 3d printing typically associated with Ni-base superalloys, which can require an additional isothermal precipitation treatment to adjust appropriate phase fraction of a dual-phase structure. The technology is of special interest for high technology and space applications, because they plan on incorporating components printed from powders of these ternary or greater Ni alloys. A favored printing technique will be bound metal deposition, which can enable large scale

production of components with relative complex geometries and shapes.

[00116] A method of designing a metal alloy powder having a miscibility gap at low temperature can include identifying a first metal element and a second metal to form a metal alloy, selecting a third metal having a miscibility gap with the metal alloy, and mechanically alloying the third metal and the metal alloy to form a metal alloy powder having a nanoscale grain size.

[00117] For example, a Ni-Cu alloy can include one or more of a third metal, which can be chromium, cobalt, vanadium, silver, molybdenum, tungsten, or iron. The third metal is selected based on the ternary phase diagram properties that will allow nano-phase separation to occur, as described herein. In certain embodiments, iron can be a preferred metal in the alloy. In other embodiments, chromium can be a preferred metal in the alloy. In other embodiments, cobalt can be a preferred metal in the alloy. In other embodiments, vanadium can be a preferred metal in the alloy. In other embodiments, silver can be a preferred metal in the alloy. In other embodiments, molybdenum can be a preferred metal in the alloy. In other embodiments, tungsten can be a preferred metal in the alloy. The composition of the metal alloy can be selected to be a nano-phase separating powder, such as a ternary nano-phase separating powder or a quaternary nano-phase separating powder.

[00118] In certain circumstances, the alloy can include an oxygen scavenging metal. The oxygen scavenging metal can be at a low concentration of the alloy, for example, 5 at%, 4 at%, 3 at%, 2 at%, 1 at%, or lower. The oxygen scavenging metal can be manganese or zirconium. The oxygen scavenging metal can be added to a ternary alloy to for a quaternary alloy.

[00119] In certain circumstances, the metal alloy powder can be engineered to have a phase separation temperature at which diffusion of the third metal occurs to phase separate as a nanoscale phase. Moreover, it can be preferred that the nanoscale phase can redissolve at a transition

temperature higher than the phase separation temperature.

[00120] According to certain embodiments, the mechanical alloying (e.g., ball milling) is performed at a relatively low temperature. For example, in some embodiments, the mechanical alloying (e.g., ball milling) is performed while the particles are at a temperature of less than or equal to 150° C, less than or equal to 100° C, less than or equal to 75° C, less than or equal to 50° C, less than or equal to 40° C, less than or equal to 35° C, less than or equal to 30° C, less than or equal to 25° C, or less than or equal to 20° C. In some embodiments, the mechanical working (e.g., ball milling) is performed while the particles are at a temperature of at least 0° C. In some embodiments, the mechanical alloying (e.g., ball milling) can be performed at a temperature of the surrounding, ambient environment.

[00121] In certain embodiments, the mechanical alloying (e.g., ball milling) may be conducted for a time of greater than or equal to 6 hours (e.g., greater than or equal to 8 hours, greater than or equal to 10 hours, greater than or equal to 12 hours, or greater than or equal to 15 hours). In certain embodiments, the mechanical alloying (e.g., ball milling) may be conducted for a time of less than or equal to 18 hours. In some embodiments, the mechanical alloying (e.g., ball milling) may be conducted for a time of 6 hour to 18 hours.

[00122] In some embodiments, the mechanical alloying (e.g., ball milling) can be conducted in an inert atmosphere, for example, an argon atmosphere.

[00123] In certain circumstances, the nanoscale feature or nanophase can be 100 nm, 90 nm, 80 nm, 70 nm, 60 nm, 50 nm, 40 nm, 30 nm, 20 nm, 10 nm, 5 nm or smaller. The nanophase, nanoscale feature, or nanocrystal can refer to the size of a crystal (or a "grain") being less than or equal to about 1000 nm—e.g., 500 nm, 200 nm, 100 nm, 50 nm, 20 nm, 10 nm, 5 nm, 2 nm, etc.

For example, the grain size may be between 1000 nm and about 2 nm—e.g., about 500 nm and about 2 nm, about 200 nm and about 2 nm, about 100 nm and about 2 nm, about 50 nm and about 2 nm, about 30 nm and about 2 nm, about 20 and about 2 nm, about 10 nm and about 2 nm. In some embodiments, the size may refer to the largest dimension of the grain. The size of the grains referred herein may be determined as an "average" and may be measured by any suitable techniques. The dimensions may refer the diameter, length, width, height, depending on the geometry of the grain. In some instances (and as provided below), a stable nanocrystalline material may also refer to a material comprising an amorphous phase.

[00124] The alloy can be composed of three, four or more metals. Each metal can have a concentration of about 25 at% (atomic percent) to about 95 at% of the alloy. When two metal components of a ternary alloy each has a concentration of about 25 at% to about 95 at% of the alloy, the third metal component can have a concentration of about 5 at% to about 50 at% of the alloy. For example, each metal concentration can be at least 5 at%, at least 10 at%, at least 15 at%, at least 20 at%, at least 25 at%, at least 30 at%, at least 35 at%, at least 40 at%, at least 45 at%, at least 50 at%, at least 55 at%, at least 60 at%, at least 65 at%, at least 70 at%, at least 75 at%, at least 80 at%, at least 85 at%, at least 90 at%, or at least 95 at%.

[00125] In another aspect, a method of nano-phase separation sintering of a powder can include providing a fine grained powder including a first metal element and a second metal forming a metal alloy and a third metal having a miscibility gap with the metal alloy, and sintering the fine grained powder to form a sintered product.

[00126] In another aspect, a metal alloy powder for sintering can include a mechanically alloyed powder including a first metal element and a second metal forming a metal alloy and a third metal having a miscibility gap with the metal alloy.

[00127] In certain circumstances, the sintered product achieves at least 80%, at least 85%, at least 90%, at least 95%, at least 97%, or at least 98% density. These densities can be achieved at low temperatures without the need for an applied pressure during the sintering. In certain circumstances, sintering can include nano-phase separation sintering.

[00128] According to certain embodiments, sintering the plurality of particles involves heating the particles to a sintering temperature of less than or equal to 2200° C., less than or equal to 2000° C., less than or equal to 1900° C., less than or equal to 1800° C., less than or equal to 1700° C., less than or equal to 1600° C., less than or equal to 1500° C., less than or equal to 1400° C., less than or equal to 1300° C., less than or equal to 1200° C., less than or equal to 1100° C., less than or equal to 1000° C., less than or equal to 900° C., less than or equal to 850° C., less than or equal to 800° C., or less than or equal to 750° C. According to certain embodiments, sintering the plurality of particles involves heating the particles to a sintering temperature of greater than or equal to 750° C., greater than or equal to 850° C., greater than or equal to 1000° C., greater than or equal to 1200° C., greater than or equal to 1450° C., or greater than or equal to 1600° C. Combinations of these ranges are also possible. For example, in some embodiments, sintering the plurality of particles involves heating the particles to a sintering temperature that is greater than or equal to 750° C. and less than or equal to 2200° C. In some embodiments, the temperature of the sintered material is within these ranges for at least 10%, at least 25%, at least 50%, at least 75%, at least 90%, or at least 99% of the sintering time.

[00129] According to certain embodiments, sintering the plurality of particles involves maintaining the particles within the range of sintering temperatures for less than 72 hours, less than 48 hours, less than or equal to 24 hours, less than or equal to 12 hours, less than or equal to 6 hours, less than or equal to 4 hours, less than or equal to 3 hours, less than or equal to 2 hours, or

less than or equal to 1 hour (and/or, in some embodiments, for at least 10 minutes, at least 20 minutes, at least 30 minutes, at least 50 minutes, at least 3 hours, or at least 6 hours). Combinations of these ranges are also possible. For example, in some embodiments, sintering the plurality of particles involves heating the particles to a first sintering temperature that is greater than or equal to 600° C. and less than or equal to 1100° C. for a sintering duration greater than or equal to 6 hours and less than or equal to 24 hours.

[00130] In certain circumstances, the rate of heating can be 2° C/min, 3° C/min, 4° C/min, 5° C/min, 10° C/min, 15° C/min, or 20° C/min.

[00131] In certain circumstances, grain size of the metal alloy powder and grain size of the sintered powder can be substantially the same. The grain size can be a nano-scale grain size. The powder can be a fine grained powder.

[00132] The alloys described herein can be the alloys may be at least one of Ni—Cu—Fe, Ni—Cu—Co, Ni—Cu—Cr, Ni—Cu—V, Ni—Cu—Ag, Ni—Cu—Mo, Ni—Cu—W, Ni—Cu—Mn, Ni—Cu—Zr, Ni—Cu—Fe—Mn, Ni—Cu—Co—Mn, Ni—Cu—Cr—Mn, Ni—Cu—V—Mn, Ni—Cu—Ag—Mn, Ni—Cu—Mo—Mn, or Ni—Cu—W—Mn.

[00133] In the alloy, the Ni content can be 15 at%, 20 at%, 30 at%, 35 at%, 40 at%, 45 at%, 50 at%, 55 at%, 60 at%, 65 at%, 70 at%, 75at%, 80 at%, 85 at%, 90 at%, or 95 at% of the composition.

[00134] In the alloy, the Cu content can be 15 at%, 20 at%, 30 at%, 35 at%, 40 at%, 45 at%, 50 at%, 55 at%, 60 at%, 65 at%, 70 at%, 75at%, 80 at%, 85 at%, 90 at%, or 95 at% of the composition.

[00135] In the alloy, the Fe content can be 1 at%, 2 at%, 3 at%, 4 at%, 5 at%, 6 at%, 7 at%, 8 at%, 9 at%, 10 at%, 11 at%, 13 at%, 14 at%, 15 at%, 20 at%, 30 at%, 35 at%, 40 at%, 45 at%, 50 at%, 55 at%, 60 at%, 65 at%, 70 at%, 75at%, 80 at%, 85 at%, 90 at%, or 95 at% of the composition.

[00136] In the alloy, the Co content can be 1 at%, 2 at%, 3 at%, 4 at%, 5 at%, 6 at%, 7 at%, 8 at%, 9 at%, 10 at%, 11 at%, 13 at%, 14 at%, 15 at%, 20 at%, 30 at%, 35 at%, 40 at%, 45 at%, 50 at%, 55 at%, 60 at%, 65 at%, 70 at%, 75at%, 80 at%, 85 at%, 90 at%, or 95 at% of the composition.

[00137] In the alloy, the Cr content can be 1 at%, 2 at%, 3 at%, 4 at%, 5 at%, 6 at%, 7 at%, 8 at%, 9 at%, 10 at%, 11 at%, 13 at%, 14 at%, 15 at%, 20 at%, 30 at%, 35 at%, 40 at%, 45 at%, 50 at%, 55 at%, 60 at%, 65 at%, 70 at%, 75at%, 80 at%, 85 at%, 90 at%, or 95 at% of the composition.

[00138] In the alloy, the V content can be 1 at%, 2 at%, 3 at%, 4 at%, 5 at%, 6 at%, 7 at%, 8 at%, 9 at%, 10 at%, 11 at%, 13 at%, 14 at%, 15 at%, 20 at%, 30 at%, 35 at%, 40 at%, 45 at%, 50 at%, 55 at%, 60 at%, 65 at%, 70 at%, 75at%, 80 at%, 85 at%, 90 at%, or 95 at% of the composition.

[00139] In the alloy, the Mo content can be 1 at%, 2 at%, 3 at%, 4 at%, 5 at%, 6 at%, 7 at%, 8 at%, 9 at%, 10 at%, 11 at%, 13 at%, 14 at%, 15 at%, 20 at%, 30 at%, 35 at%, 40 at%, 45 at%, 50 at%, 55 at%, 60 at%, 65 at%, 70 at%, 75at%, 80 at%, 85 at%, 90 at%, or 95 at% of the composition.

[00140] In the alloy, the W content can be 1 at%, 2 at%, 3 at%, 4 at%, 5 at%, 6 at%, 7 at%, 8 at%, 9 at%, 10 at%, 11 at%, 13 at%, 14 at%, 15 at%, 20 at%, 30 at%, 35 at%, 40 at%, 45 at%, 50 at%, 55 at%, 60 at%, 65 at%, 70 at%, 75at%, 80 at%, 85 at%, 90 at%, or 95 at% of the composition.

[00141] In certain circumstances, NiCu can have 5 at% to 20 at% Cr; NiCu can have 5 at% to 45 at% Fe; NiCu can have 5 at% to 45 at% Co; NiFeCu can have 5at% or 8at% Mn; NiCu can have 5 at% to 15 at% V; or NiCu can have 5at% to 45 at% Co. For example, the metal alloy powder can include: NiCu having 5at%, 10at% 11at%, 12at%, 13at%, 14at%, 15at%, 16at%, 17at%, 18at%, or 19at% Cr; NiCu having 5 at%, 10at% 12at%, 14at%, 16at%, 18at%, 20at%, 22at%, 24at%, 26at%, 28at%, 30at%, 32at%, 34at%, 36at%, 38at%, 40at%, or 42at% Fe; NiCu having 5at%, 10at% 12at%, 14at%, 16at%, 18at%, 20at%, 22at%, 24at%, 26at%, 28at%, 30at%,

32at%, 34at%, 36at%, 38at%, 40at%, 42at%, or 44at% Co; NiFeCu having 5at% or 8at% Mn; NiCu having 6at%, 7at%, 8at%, 9at%, 10at%, 11at%, 12at%, or 13at% V; or NiCu having 5at%, 10at% 12at%, 14at%, 16at%, 18at%, 20at%, 22at%, 24at%, 26at%, 28at%, 30at%, 32at%, 34at%, 36at%, 38at%, 40at%, 42at%, or 44at% Co.

5 **[00142]** In certain circumstances, the mechanically powder is a quaternary nano-phase separating powder. For example, the metal alloy powder can include NiCu having 5at%, 10at% 12at%, 14at%, 16at%, 18at%, 20at%, 22at%, 24at%, 26at%, 28at%, 30at%, 32at%, 34at%, 36at%, 38at%, 40at%, 42at%, or 44at% Co and up to 5at% Mn.

[00143] Referring to FIG. 1A, generalized requirements for nano-phase separation sintering are 10 illustrated, including phase separation, neck formation, sintering and densification. The characteristics of the alloy are important to perform these steps. For example, nanocrystallinity can ensure rapid diffusion to the particle surface. Moreover, supersaturation can allow a desired second phase to form at necks. Mechanical alloying can facilitate both of these important factors.

[00144] Referring to FIG. 1B, a phase diagram suggests the interplay between concentration, 15 tempature, phase separation, reduced surface energy and high solubility that least to the phase seperation enhanced sintering described herein.

[00145] FIG. 1C illustrates an example of the general process example with Fe.

[00146] Ternary and higher order Ni-Cu alloy systems are of particular interest. Requirements for the selection of the ternary element include the following. The ternary element should possess 20 a high positive heat of mixing with Cu. This can increase the transition temperature from miscibility gap to the solid solution phase field. The ternary element should also ideally form a solid solution with Ni. This property can favor an interdiffusion as required for nano-phase

separation sintering.

[00147] FIG. 2A shows a Ni-Cu phase diagram. FIG. 2B illustrates a behavior of the system. For example, increased mobility leads to decreased undercooling and increased undercooling leads to decreased mobility.

[00148] For example, a 70 at% Ni, 15 at% Cu and 15 at% Co alloy was studied. The phase diagram for the system is shown in FIG. 3. The alloy was heated at different rates (5, 10, 15°C/min) up to 1000°C then cooled 40°C/min. FIG. 4A shows the densification rate at 10K/min to 1000°C, then 40K/min cooling. FIG. 4B shows the change in relative density.

[00149] A Cr alloy was also studied. FIG. 5A is a Ni-Cr phase diagram. FIG. 5B is a Cu-Cr phase diagram. Other phase diagrams at other Cr concentrations can be found at FIGS. 6A-6C. FIG. 6A is a Ni-Cu phase diagram at 5 at% Cr. FIG. 6B is a Ni-Cu phase diagram at 10 at% Cr. FIG. 6C is a Ni-Cu phase diagram at 15 at% Cr.

[00150] An alloy of 60 at% Ni, 25 at% Cu and 15 at% Cr was studied. A phase diagram of 60 at% Ni and 15% Cr is shown in FIG. 6D. FIG. 6E is a table showing the compositions of stable phases at 550°C. FIG. 6F shows the temperature dependence of densification at 5°C/min to 1200°C and 40°C/min cooling.

[00151] An Fe alloy was studied. FIG. 7A is a Ni-Fe phase diagram. FIG. 7B is a Cu-Fe phase diagram. Other phase diagrams at other Fe concentrations can be found at FIGS. 8A-8C. FIG. 8A is a Ni-Cu phase diagram at 5 at% Fe. FIG. 8B is a Ni-Cu phase diagram at 20 at% Fe. FIG. 8C is a Ni-Cu phase diagram at 42 at% Fe.

[00152] FIG. 8D is a Ni-Cu phase diagram at 42at% Fe. FIG. 8E is a table showing the compositions of stable phases at 550°C. One set of experiments were conducted at 15 at% Cu.

FIG. 8F shows the temperature dependence of densification at 5°C/min to 945°C and 40°C/min cooling. FIG. 8G shows the change in relative density over time at 5°C/min heating. FIG. 8H shows the temperature dependence of densification at 10°C/min to 1000°C and 40°C/min cooling. FIG. 8I shows the change in relative density over time at 5°C/min heating to a final relative density of 0.5864%. FIG. 8J shows the temperature dependence of densification at 15°C/min to 1000°C and 40°C/min cooling. FIG. 8K shows the change in relative density over time at 15°C/min heating to a final relative density of 0.5477%. FIG. 8L shows the temperature dependence of densification at 20°C/min to 1000°C and 40°C/min cooling. FIG. 8M shows the change in relative density over time at 20°C/min heating to a final relative density of 0. 4276%.

[00153] Another set of experiments were conducted at 15 at% Cu. FIG. 8N shows the temperature dependence of densification at 5°C/min to 1100°C and 40°C/min cooling. FIG. 8O shows the change in relative density over temperature at 5°C/min heating. FIG. 8P shows the change in relative density over time at 5°C/min heating. FIG. 8Q shows the temperature dependence of densification at 10°C/min to 1100°C and 40°C/min cooling. FIG. 8R shows the change in relative density over temperature at 10°C/min heating. FIG. 8S shows the change in relative density over time at 15°C/min. FIG. 8T shows the temperature dependence of densification at 20°C/min to 1100°C and 40°C/min cooling. FIG. 8U shows the temperature dependence of densification at 20°C/min to 1100°C and 40°C/min cooling. FIG. 8V shows the change in relative density over time at 20°C/min.

[00154] A Co alloy was studied. FIG. 9A is a Ni-Co phase diagram. FIG. 9B is a Cu-Co phase diagram. Other phase diagrams at other Co concentrations can be found at FIGS. 10A-10C. FIG. 10A is a Ni-Cu phase diagram at 5 at% Co. FIG. 10B is a Ni-Cu phase diagram at 20 at% Co. FIG. 10C is a Ni-Cu phase diagram at 44 at% Co.

[00155] A V alloy was studied. FIG. 11A is a Ni-V phase diagram. FIG. 11B is a Cu-V phase diagram. Other phase diagrams at other V concentrations can be found at FIGS. 12A-12C. FIG. 12A is a Ni-Cu phase diagram at 6 at% V. FIG. 12B is a Ni-Cu phase diagram at 10 at% V. FIG. 12C is a Ni-Cu phase diagram at 13 at% V. FIG. 12D is a Ni-Cu phase diagram and 13 at% V. At 15 at% Cu, FIG. 12E shows the stable phases at 1150°C. FIG. 12F shows the temperature dependence of the densification rate for 10 at 5°C/min to 1200°C and 40°C/min cooling. FIG. 12G shows the temperature dependences of the change in relative density.

[00156] Based on the experiments described herein, Ni self-diffusion impacts the limit of accelerated densification.

[00157] FIG. 13 is a chart showing the diffusion rates and temperature range for metals described herein.

[00158] The phase diagram information can vary depending on the source of the data. FIG. 14A is a phase diagram for Fe-Cu with 40 at% Ni from an Fe database. FIG. 14B is a phase diagram for Fe-Cu with 40 at% Ni from a Ni database. FIG. 14C is a phase diagram for Fe-Cu with 40 at% Ni from a Cu database. FIG. 14D is a phase diagram for Fe-Cu with 40 at% Ni from a high entropy alloy database.

[00159] Other phase diagrams can be created. FIG. 15 is a Cr-Cu phase diagram at 60 at% Ni. FIG. 16 is a Co-Cu phase diagram at 40 at% Ni. FIG. 17 is a Cu-V phase diagram at 75 at% Ni.

[00160] Pretreatment of an alloy in a reducing atmosphere can improve the sintering performance of the alloy. For example, pretreatment with hydrogen gas at 300°C for 24 hours can reduce swelling. FIGS. 18A, 18B and 18C show densification after pretreatment with hydrogen at different heating rates.

[00161] As noted above, and oxygen scavenger can be included in an alloy. FIG. 19 shows the impact on density of 5 at% and 8 at% Mn to a Ni-Fe-Cu composition.

[00162] In another example, FIG. 20 shows the densification behavior of the addition of Mn in a 37.5 at% Ni - 37.5 at% Co – 20 at% Cu – 5 at% Mn composition heated to 1200°C. Microstructures are shown in the images of FIGS. 21, 22, 23 and 24.

[00163] The mechanical properties of the sintered products described herein have been tested. Results of mechanical testing of 37.5 at% Ni 37.5 at% Fe 20 at% Cu 5 at% Mn are shown in FIGS. 25-28.

[00164] Experimental methods

[00165] This work focuses on the sintering of a model nanocrystalline material produced through a relatively standard route with standard inputs, so as to focus on the physics of the kinetic competition outlined above. Ni is selected as the base metal for its technological relevance, and because it occupies a unique position: for microcrystalline materials debinding easily precedes sintering, but for nanocrystalline materials the onset of sintering is at the low end of the debinding range, so that the conflation of organic burnout and sintering is expected to be nearly unavoidable.

[00166] Nanocrystalline Ni-Fe alloy powders were produced through high-energy ball milling. Nickel powder (Alfa Aesar, 99.9% purity, 3–7 μm particle size) was milled on a SPEX 8000D Mixer/Mill and with a ball-to-powder ratio of 10:1 (5 g powder batch) with hardened steel vials and media. High-energy ball-milling was conducted in a glovebox maintained under an ultra-high purity Ar atmosphere to limit atmospheric oxygen contamination. To balance fracturing and cold-welding of the powder particles during high-energy ball milling, approximately 5 weight percent (wt%) ethanol (C_2H_6O) was added as a process control agent (PCA). Note that this is the only

organic species used in the present work, and is therefore the primary source of carbon in the system.

[00167] The powder was milled for 20 h and then imaged using a Merlin Zeiss high-resolution scanning electron microscope (HR-SEM) in secondary electron (SE) mode to estimate the as-milled powder size of 51 (± 23) μm. The as-milled grain size of about 23 nm was determined on a Panalytical X'Pert PRO using Cu-Kα radiation with a wavelength λ=1.5418 Å and a step size of 0.0167° operated at 45 kV and 40 mA for voltage and current, respectively. The average grain size was determined from the peak broadening corrected by the lattice strain using a classical Williamson-Hall analysis and instrumental contributions using a NIST LaB6 as reference. Although pure Ni is the input to this process, the wear of the steel media/vials for these milling conditions leads to the production of Ni-Fe solid solution alloy powders. The final composition of powders was determined using an energy-dispersive x-ray (EDX) spectrometry detector in the SEM, under the same condi¬tions as described before. The accumulation of Fe contamination as function of ball-milling time. All of the powders reported in this paper were produced under the same 20 h milling conditions and have an iron content of 9.75 atomic percent (at%) (±0.41), which was generally confirmed by wavelength dispersive spectroscopy measurements. Wavelength dispersive spectroscopy (WDS) analysis was based on four separate measurements, which were all comparable. The analysis was performed on a JEOL JSM7900F Scanning electron microscope with an Oxford Wave WDS spectrometer (voltage of 20 kV, probe current of 1.25 nA). For each element analyzed, the Kα line was used with standard references for all elements that were expected to be part of the alloy through wear of the initial Ni powder with the grinding media. The experiments on the pressed compacts reported in the following include powders from three independent but otherwise identical ball-milling batches. X-ray diffraction confirmed that the as-

milled powders were FCC solid solutions.

[00168] The ball-milled powders were pressed into cylindrical specimens with dimensions of approximately 6 and 1.5 mm for diameter and height, respectively, to an initial relative density in the range of - 55.8–58.9% using a uniaxial hydraulic press (model YLJ-15 L from MTI Corporation) with a pressure of - 400–450 MPa acting on the pellets, and no additional added binder phases. The initial relative densities of the pressed specimens were determined from the ratio of initial and theoretical density (8.80 g/cm^3, accounting for the Fe content) based on mass and dimension measurements. TMA data are presented by converting a raw change in length into a relative density assuming an isotropic shape change, which was generally confirmed after each experiment with caliper measurements.

[00169] Details of one or more embodiments are set forth in the accompanying drawings and description. Other features, objects, and advantages will be apparent from the description, drawings, and claims. Although a number of embodiments of the invention have been described, it will be understood that various modifications may be made without departing from the spirit and scope of the invention. It should also be understood that the appended drawings are not necessarily to scale, presenting a somewhat simplified representation of various features and basic principles of the invention.

WHAT IS CLAIMED IS:

1. A method of designing a metal alloy powder having a miscibility gap at low temperature comprising:

identifying a first metal element and a second metal to form a metal alloy;

selecting a third metal having a miscibility gap with the metal alloy; and

mechanically alloying the third metal and the metal alloy to form a metal alloy powder having a nanoscale grain size.

2. The method of claim 1, wherein the metal alloy powder is engineered to have a phase separation temperature at which diffusion of the third metal occurs to phase separate as a nanoscale phase.

3. The method of claim 2, wherein the nanoscale phase redissolves at a transition temperature higher than the phase separation temperature.

4. The method of claim 1, wherein the metal alloy is a nano-phase separating powder.

5. The method of any one of the preceding claims, wherein the first metal includes nickel.

6. The method of any one of the preceding claims, wherein the second metal includes chromium, cobalt, vanadium, silver, molybdenum, tungsten, or iron.

7. The method of any one of the preceding claims, wherein third metal includes copper.

8. The method of any one of the preceding claims, wherein the metal alloy powder includes manganese.

9. The method of any one of the preceding claims, wherein the metal alloy powder includes vanadium.

10. The method of any one of the preceding claims, wherein the metal alloy powder includes molybdenum.

11. The method of any one of the preceding claims, wherein the metal alloy powder includes tungsten.

12. The method of any one of the preceding claims, wherein the metal alloy powder includes silver.

13. The method of any one of the preceding claims, wherein the metal alloy powder includes zirconium.

14. The method of any one of the preceding claims, wherein the metal alloy powder includes iron.

15. The method of any one of the preceding claims, wherein the metal alloy includes a ternary nano-phase separating powder.

16. The method of any one of the preceding claims, wherein the metal alloy includes a quaternary nano-phase separating powder.

17. The method of any one of the preceding claims, wherein the first metal has a concentration of about 25 at% to about 95 at% of the alloy.

18. The method of any one of the preceding claims, wherein the second metal has a concentration of about 25 at% to about 95 at% of the alloy.

19. The method of any one of the preceding claims, wherein the third metal has a concentration of about 5 at% to about 50 at% of the alloy.

20. The method of any one of the preceding claims, wherein the metal alloy powder includes an oxygen scavenging metal.

21. A method of nano-phase separation sintering of a powder comprising:

providing a fine grained powder including a first metal element and a second metal forming a metal alloy and a third metal having a miscibility gap with the metal alloy; and

sintering the fine grained powder to form a sintered product.

22. The method of claim 21, wherein the fine grained powder is a mechanically alloyed powder.

23. The method of claim 21, wherein the sintered product achieves at least 80% density at low temperatures without the need for an applied pressure during the sintering.

24. The method of claim 21, wherein the sintered product achieves at least 90% density at low temperatures without the need for an applied pressure during the sintering.

25. The method of any one of claims 21-24, wherein the fine grained powder is a nano-phase separating powder.

26. The method of any one of claims 21-25, wherein the fine grained powder includes nickel, chromium, iron, copper, vanadium, molybdenum, tungsten, silver, zirconium, manganese, or combinations thereof.

27. The method of any one of claims 21-26, wherein sintering includes nano-phase separation sintering.

28. The method of any one of claims 21-27, wherein grain size of the metal alloy powder and grain size of the sintered powder is substantially the same.

29. A metal alloy powder for sintering comprising:

a mechanically alloyed powder including a first metal element and a second metal forming a metal alloy and a third metal having a miscibility gap with the metal alloy.

30. The powder of claim 29, wherein the mechanically alloyed powder is a nano-phase separating powder.

31. The powder of claims 29 or 30, wherein the mechanically alloyed powder includes nickel, chromium, iron, copper, vanadium, molybdenum, tungsten, silver, zirconium, manganese, or combinations thereof.

32. The powder of any one of claims 29-30, wherein the mechanically powder is a ternary nano-phase separating powder.

33. The powder of any one of claims 29-30, wherein the metal alloy powder includes:

NiCu having 5at%, 10at% 11at%, 12at%, 13at%, 14at%, 15at%, 16at%, 17at%, 18at%, or 19at% Cr;

NiCu having 5 at%, 10at% 12at%, 14at%, 16at%, 18at%, 20at%, 22at%, 24at%, 26at%, 28at%, 30at%, 32at%, 34at%, 36at%, 38at%, 40at%, or 42at% Fe;

NiCu having 5at%, 10at% 12at%, 14at%, 16at%, 18at%, 20at%, 22at%, 24at%, 26at%, 28at%, 30at%, 32at%, 34at%, 36at%, 38at%, 40at%, 42at%, or 44at% Co;

NiFeCu having 5at% or 8at% Mn;

NiCu having 6at%, 7at%, 8at%, 9at%, 10at%, 11at%, 12at%, or 13at% V; or

NiCu having 5at%, 10at% 12at%, 14at%, 16at%, 18at%, 20at%, 22at%, 24at%, 26at%, 28at%, 30at%, 32at%, 34at%, 36at%, 38at%, 40at%, 42at%, or 44at% Co.

34. The powder of any one of claims 29-31, wherein the mechanically powder is a quaternary nano-phase separating powder.

35. The powder of any one of claims 29-31, wherein the metal alloy powder includes:

NiCu having 5at%, 10at% 12at%, 14at%, 16at%, 18at%, 20at%, 22at%, 24at%, 26at%, 28at%, 30at%, 32at%, 34at%, 36at%, 38at%, 40at%, 42at%, or 44at% Co and up to 5at% Mn.

36. A sintered product comprising the powder of any one of claims 29-35.

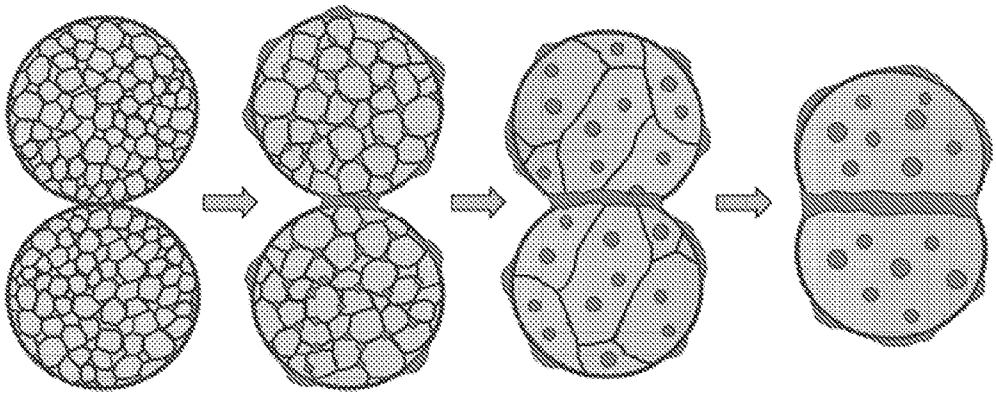

FIG. 1A

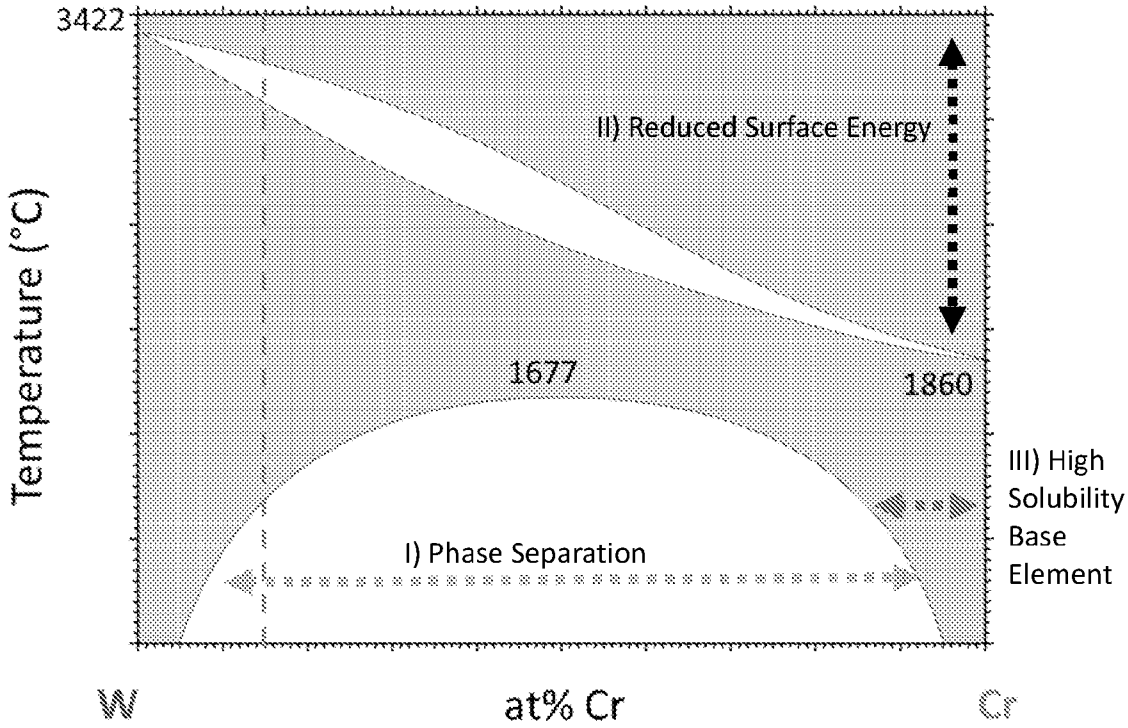
3422
II) Reduced Surface Energy
Temperature (°C)
1677
1860
III) High Solubility Base Element
I) Phase Separation
W
at% Cr
Cr

FIG. 1B

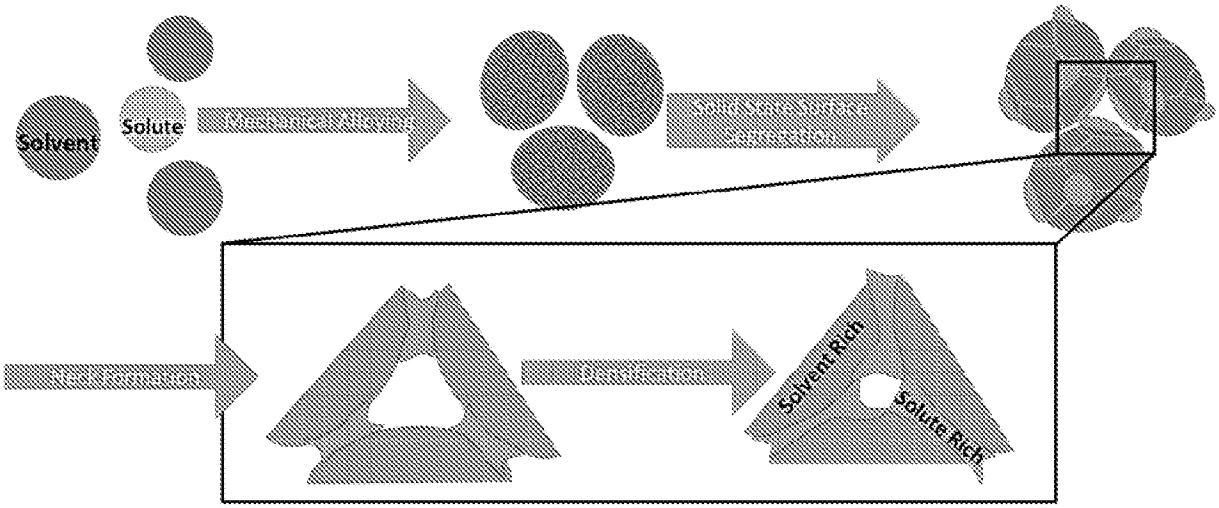
Solvent
Solute
Mechanical Alloying
Solid State Surface Segregation
Neck Formation
Densification
Solvent Rich
Solute Rich

FIG. 1C

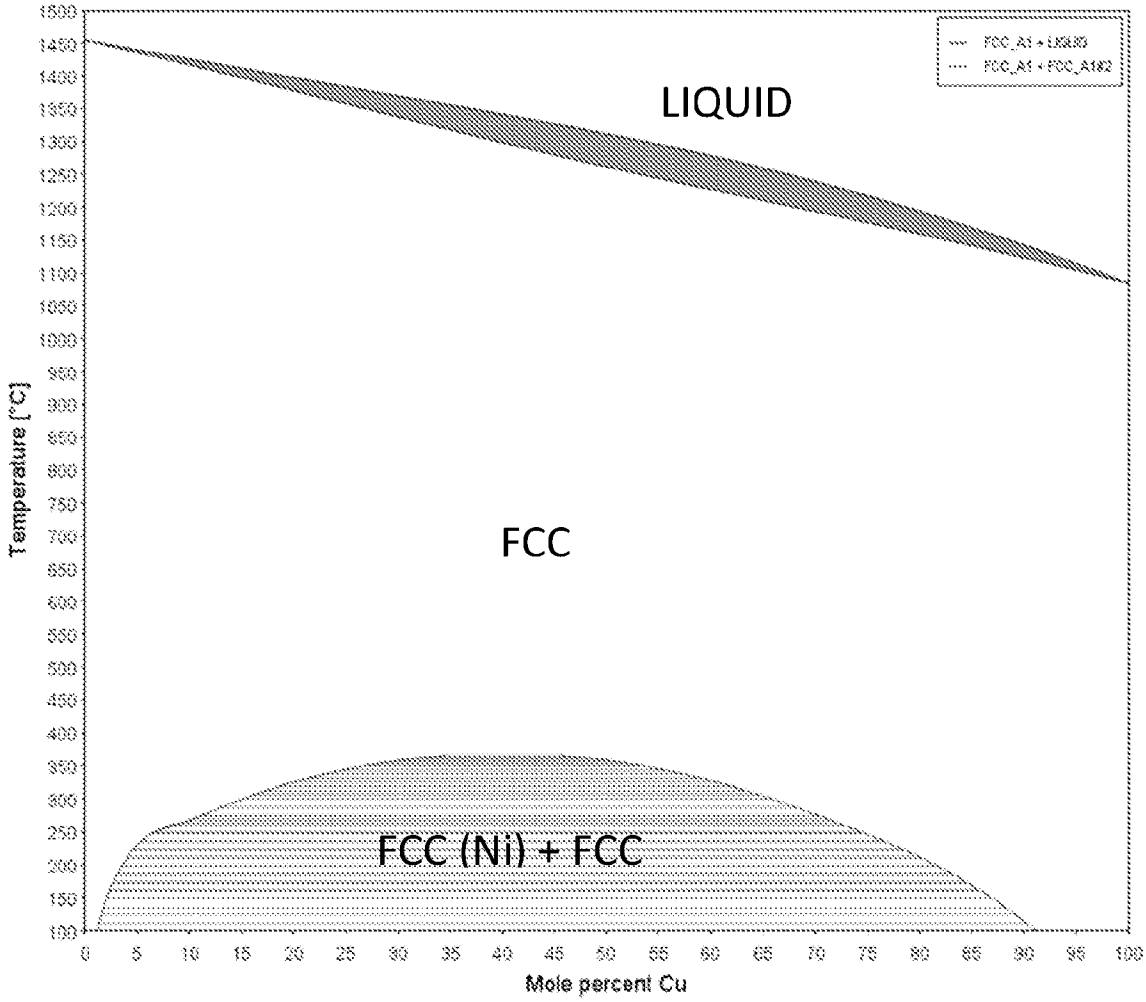

FIG. 2A

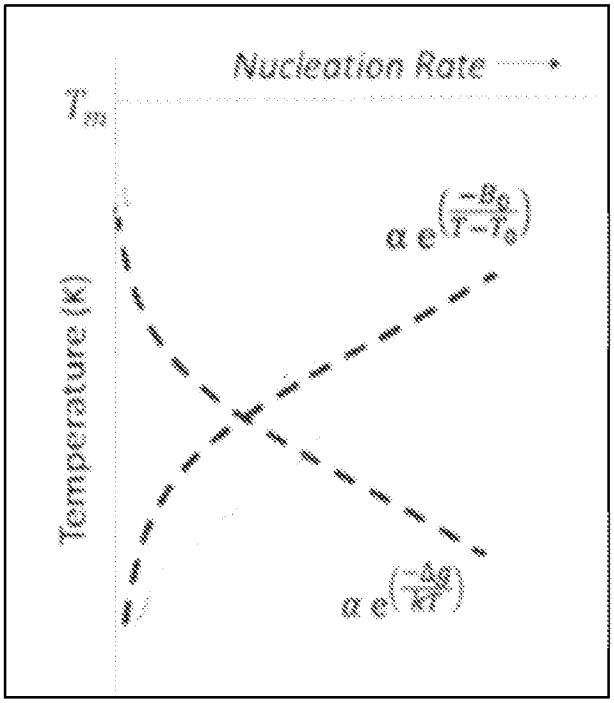

↑ Increased mobility
decreased undercooling

Increased undercooling
decreased mobility

FIG. 2B

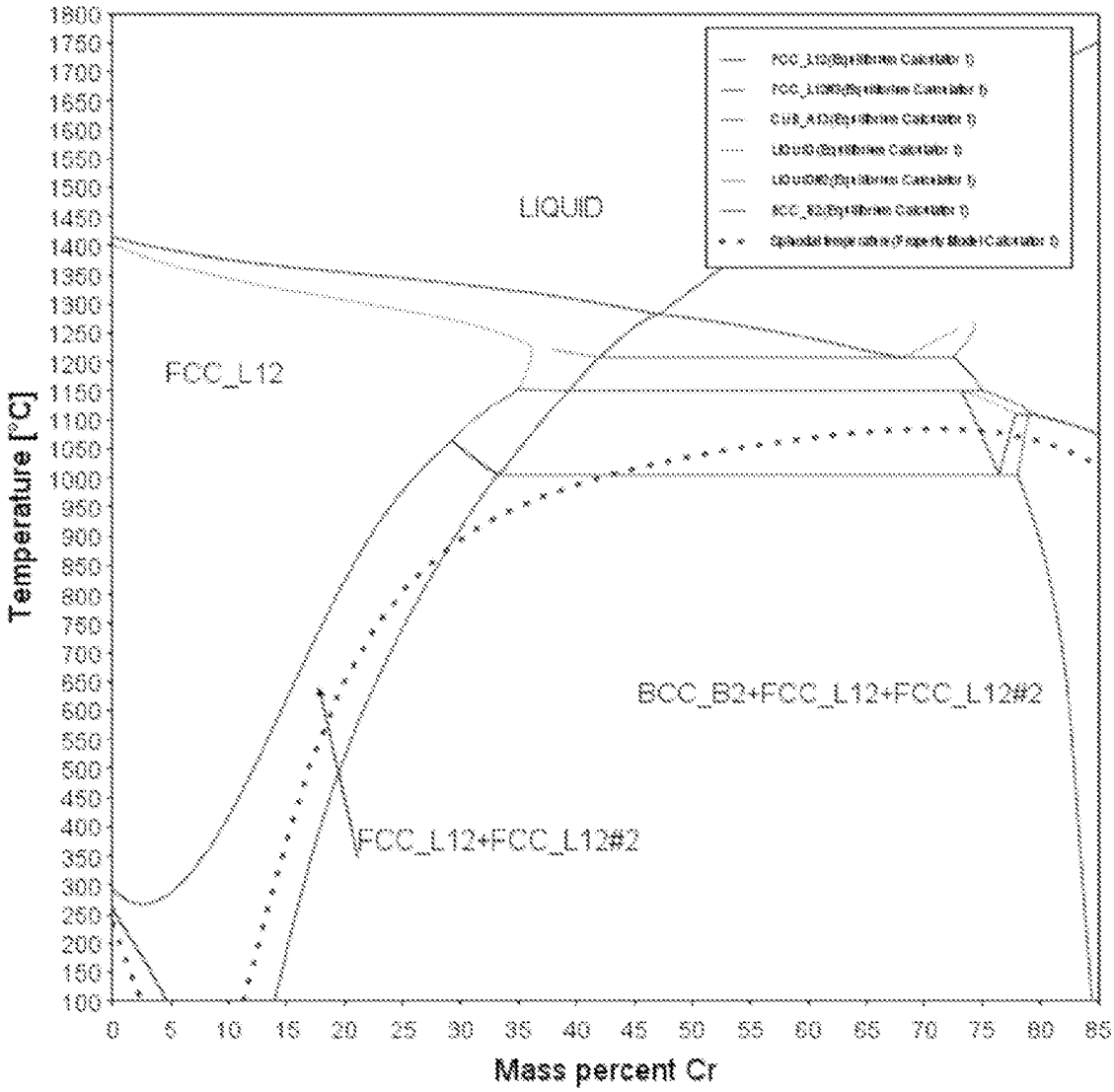
LIQUID
FCC_L12
BCC_B2+FCC_L12+FCC_L12#2
FCC_L12+FCC_L12#2
Temperature [°C]
Mass percent Cr

FIG. 3

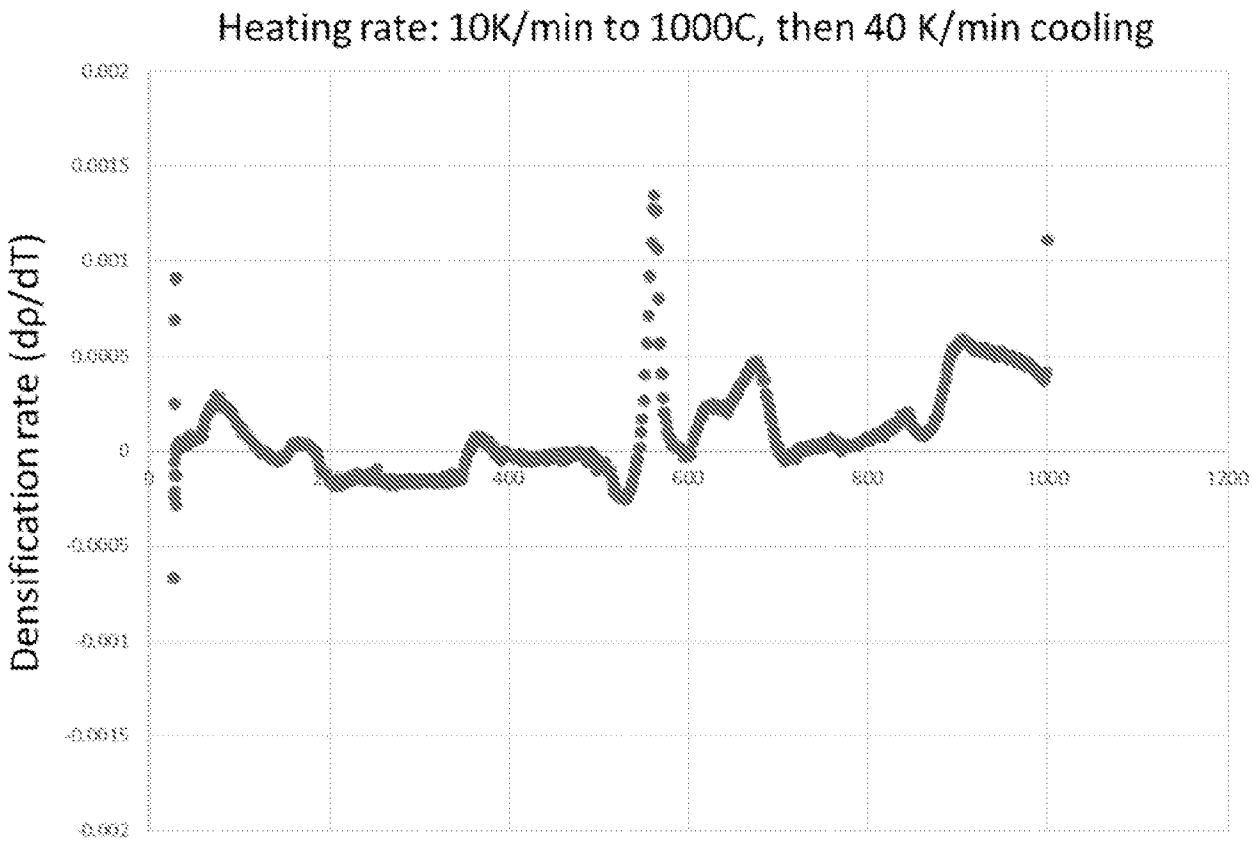
Heating rate: 10K/min to 1000C, then 40 K/min cooling
Densification rate (dρ/dT)
0.002
0.0015
0.001
0.0005
0
-0.0005
-0.001
-0.0015
-0.002
0
200
400
600
800
1000
1200

FIG. 4A

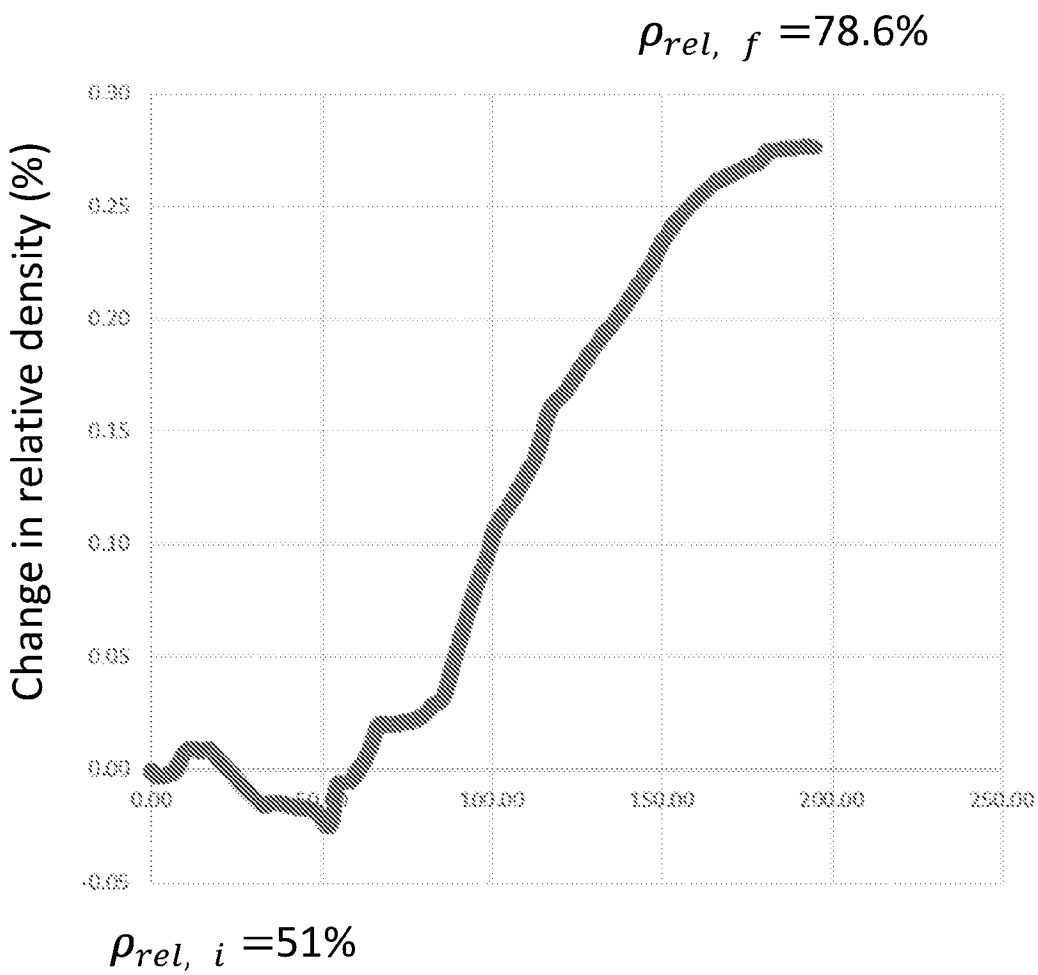
$\rho_{rel,\ f}$ =78.6%
Change in relative density (%)
0.30
0.25
0.20
0.15
0.10
0.05
0.00
-0.05
0.00
50.00
100.00
150.00
200.00
250.00
$\rho_{rel,\ i}$ =51%

FIG. 4B

Ni-Cr

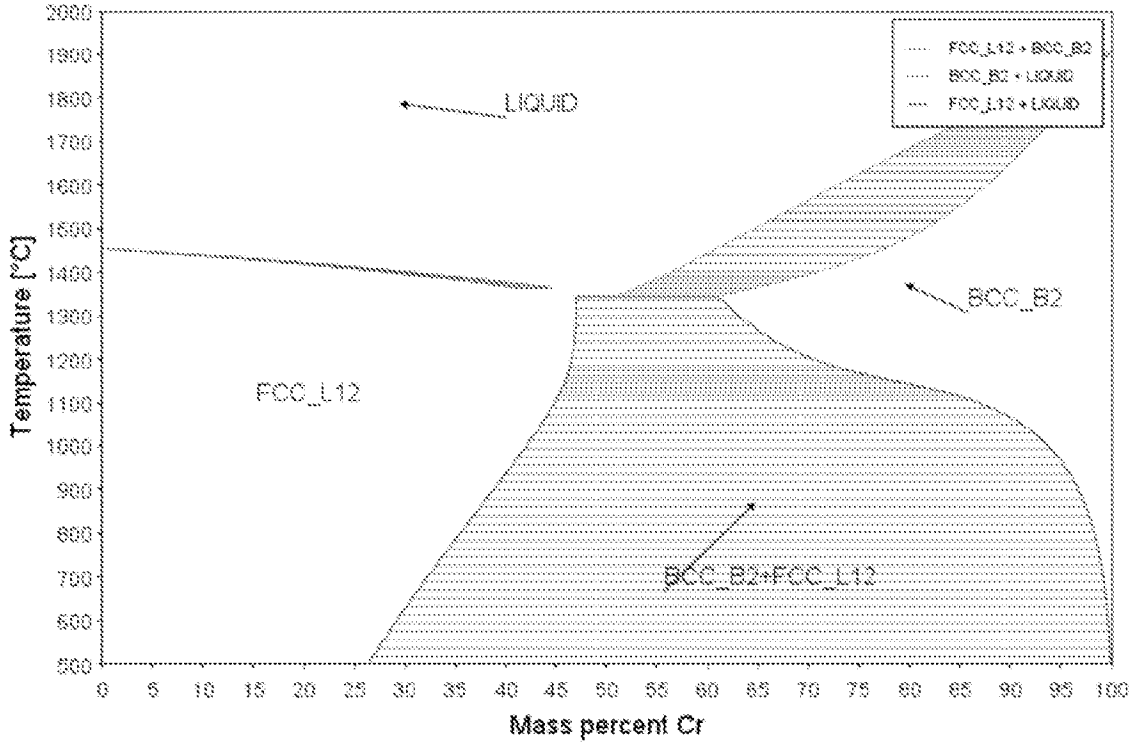
LIQUID
FCC_L12
BCC_B2
BCC_B2+FCC_L12
Temperature [°C]
Mass percent Cr

FIG. 5A

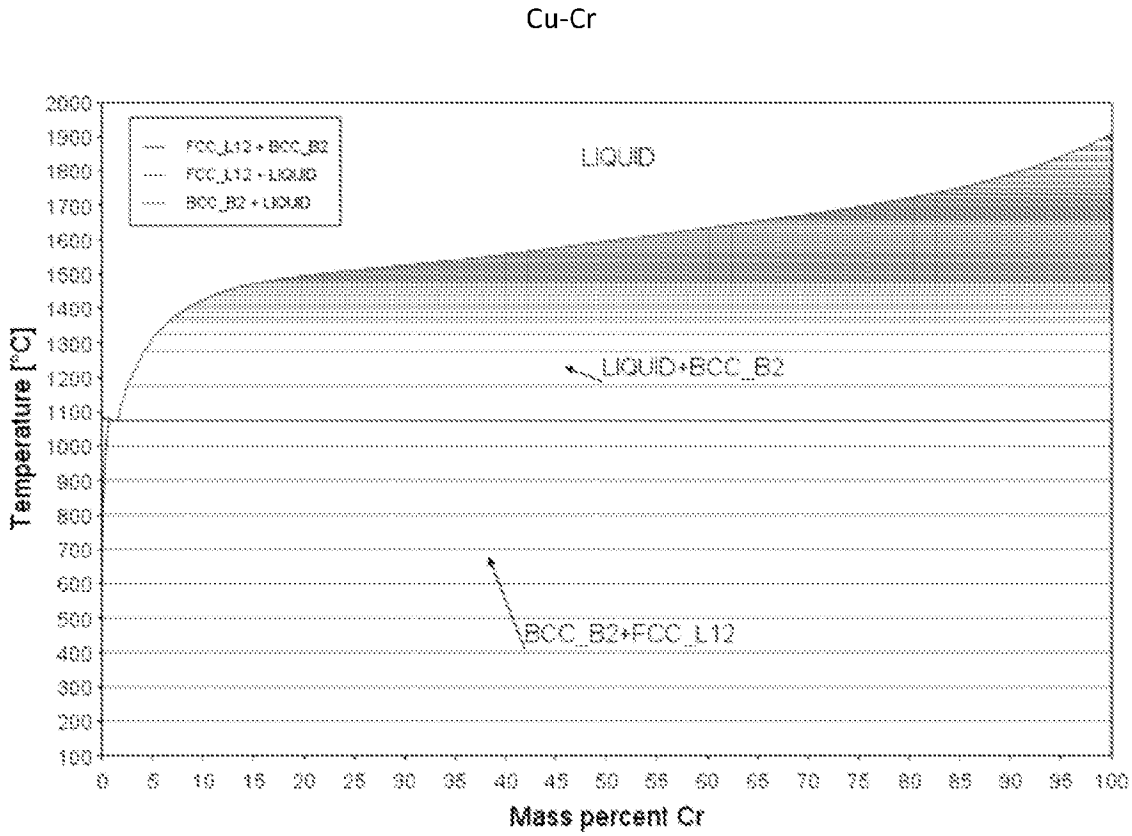
Cu-Cr
FCC_L12 + BCC_B2
FCC_L12 + LIQUID
BCC_B2 + LIQUID
LIQUID
LIQUID+BCC_B2
BCC_B2+FCC_L12
Temperature [°C]
Mass percent Cr
2000
1900
1800
1700
1600
1500
1400
1300
1200
1100
1000
900
800
700
600
500
400
300
200
100
0 5 10 15 20 25 30 35 40 45 50 55 60 65 70 75 80 85 90 95 100

FIG. 5B

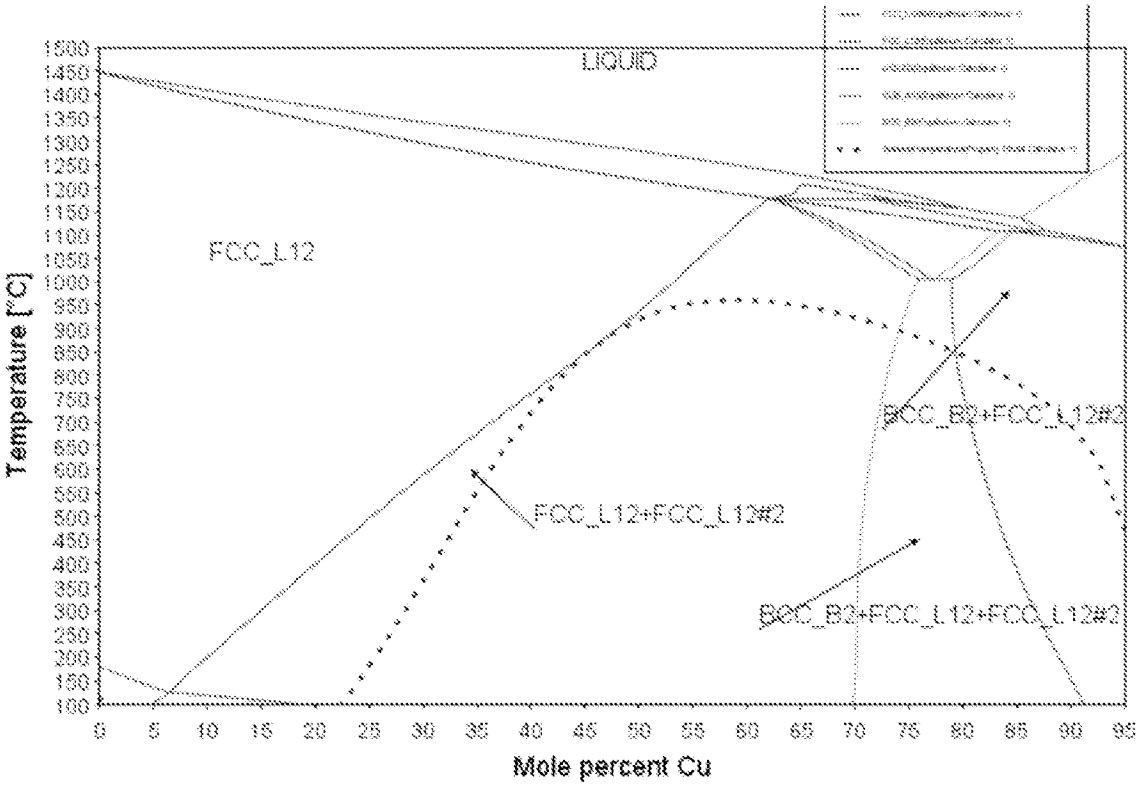
LIQUID
FCC_L12
BCC_B2+FCC_L12#2
FCC_L12+FCC_L12#2
BCC_B2+FCC_L12+FCC_L12#2
Temperature [°C]
Mole percent Cu

FIG. 6A

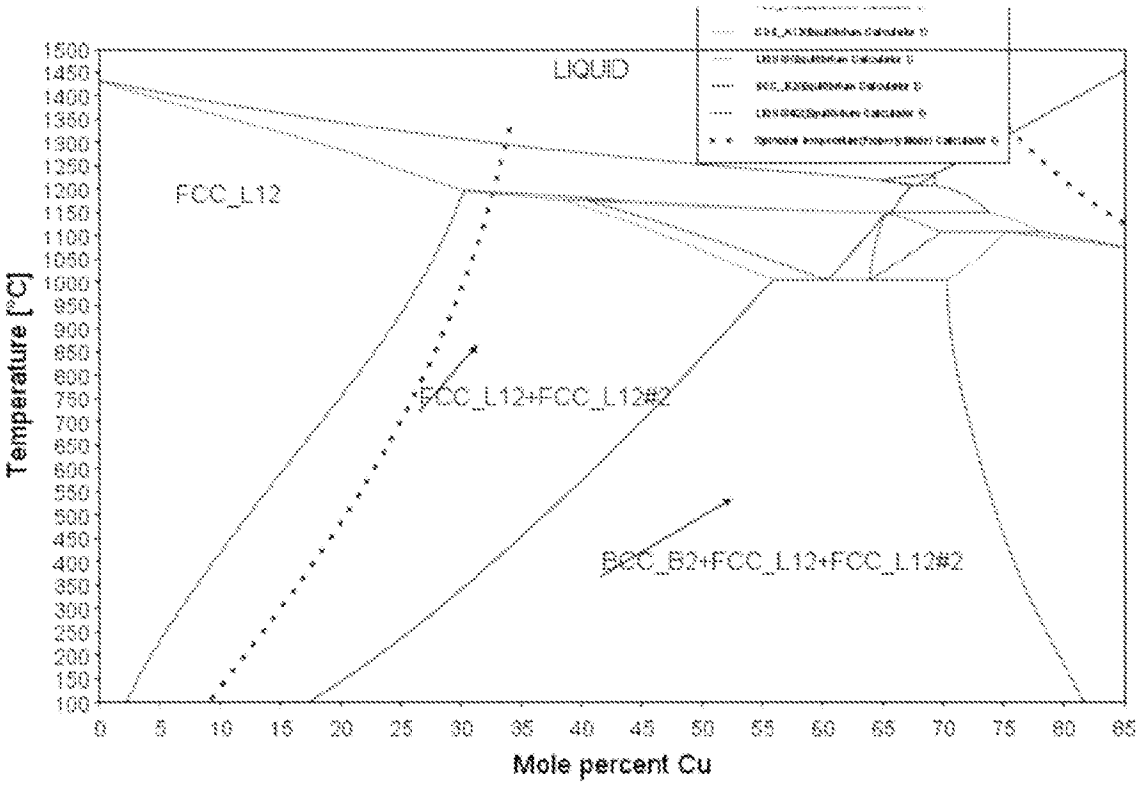
LIQUID
FCC_L12
FCC_L12+FCC_L12#2
BCC_B2+FCC_L12+FCC_L12#2
Temperature [°C]
Mole percent Cu
1500
1450
1400
1350
1300
1250
1200
1150
1100
1050
1000
950
900
850
800
750
700
650
600
550
500
450
400
350
300
250
200
150
100
0
5
10
15
20
25
30
35
40
45
50
55
60
65
70
75
80
85

FIG. 6B

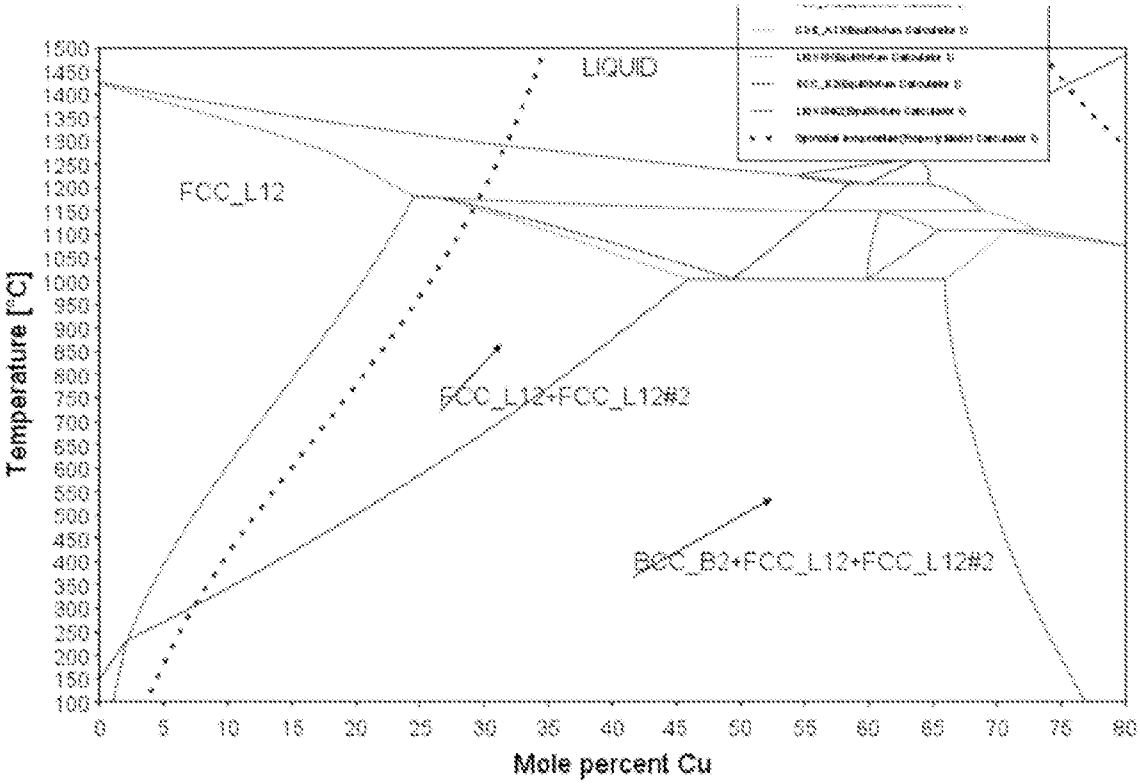
LIQUID
FCC_L12
FCC_L12+FCC_L12#2
BCC_B2+FCC_L12+FCC_L12#2
Temperature [°C]
Mole percent Cu
1500
1450
1400
1350
1300
1250
1200
1150
1100
1050
1000
950
900
850
800
750
700
650
600
550
500
450
400
350
300
250
200
150
100
0
5
10
15
20
25
30
35
40
45
50
55
60
65
70
75
80

FIG. 6C

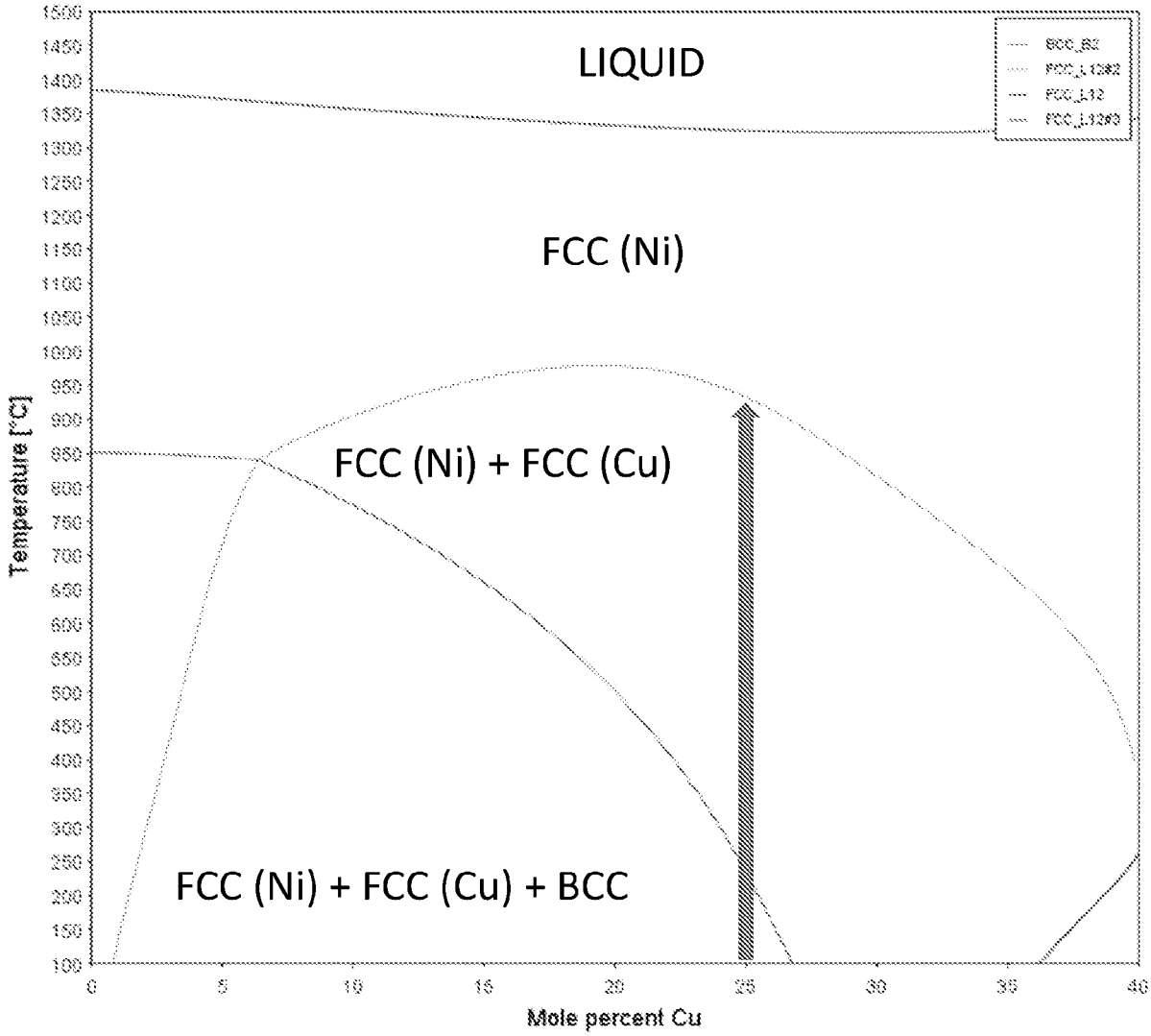
LIQUID
FCC (Ni)
FCC (Ni) + FCC (Cu)
FCC (Ni) + FCC (Cu) + BCC
Temperature [°C]
Mole percent Cu
1500
1450
1400
1350
1300
1250
1200
1150
1100
1050
1000
950
900
850
800
750
700
650
600
550
500
450
400
350
300
250
200
150
100
0
5
10
15
20
25
30
35
40

FIG. 6D

550C

Stable Phases

	Moles	*Mass*	*Volume Fraction*
FCC (Cu)	0.20654	12.95992	0.21317

Composition

Component	*Mole Fraction*	*Mass Fraction*
Cu	0.83685	0.84750
Ni	0.16221	0.15172
Cr	0.00094	0.00078

	Moles	*Mass*	*Volume Fraction*
FCC (Ni,Cr)	0.79346	45.93274	0.78683

Composition

Component	*Mole Fraction*	*Mass Fraction*
Ni	0.71396	0.72383
Cr	0.18959	0.17029
Cu	0.09645	0.10588

FIG. 6E

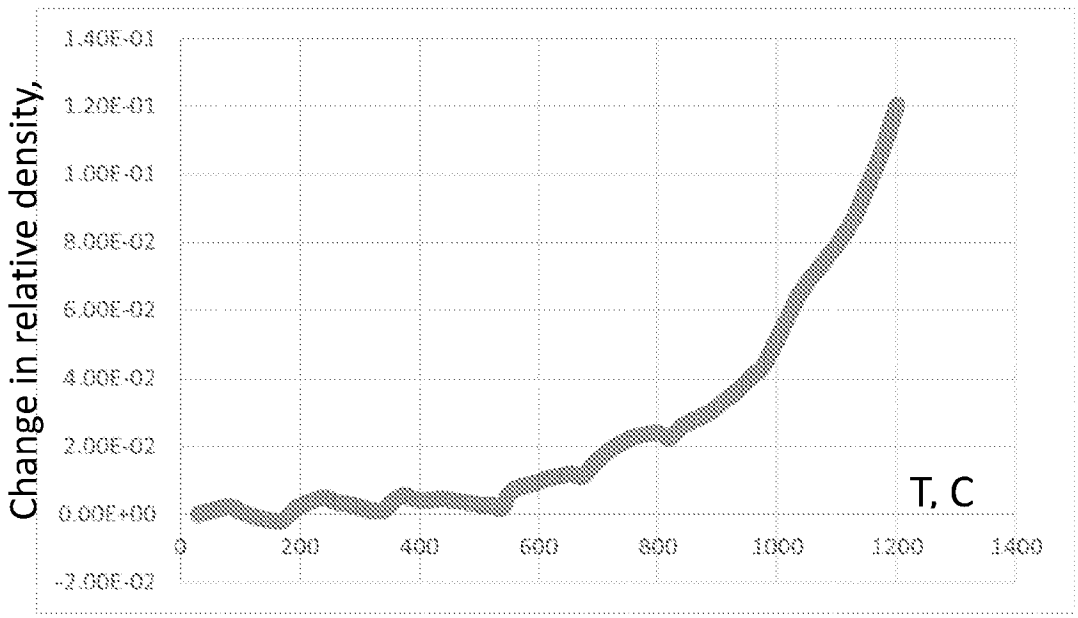

FIG. 6F

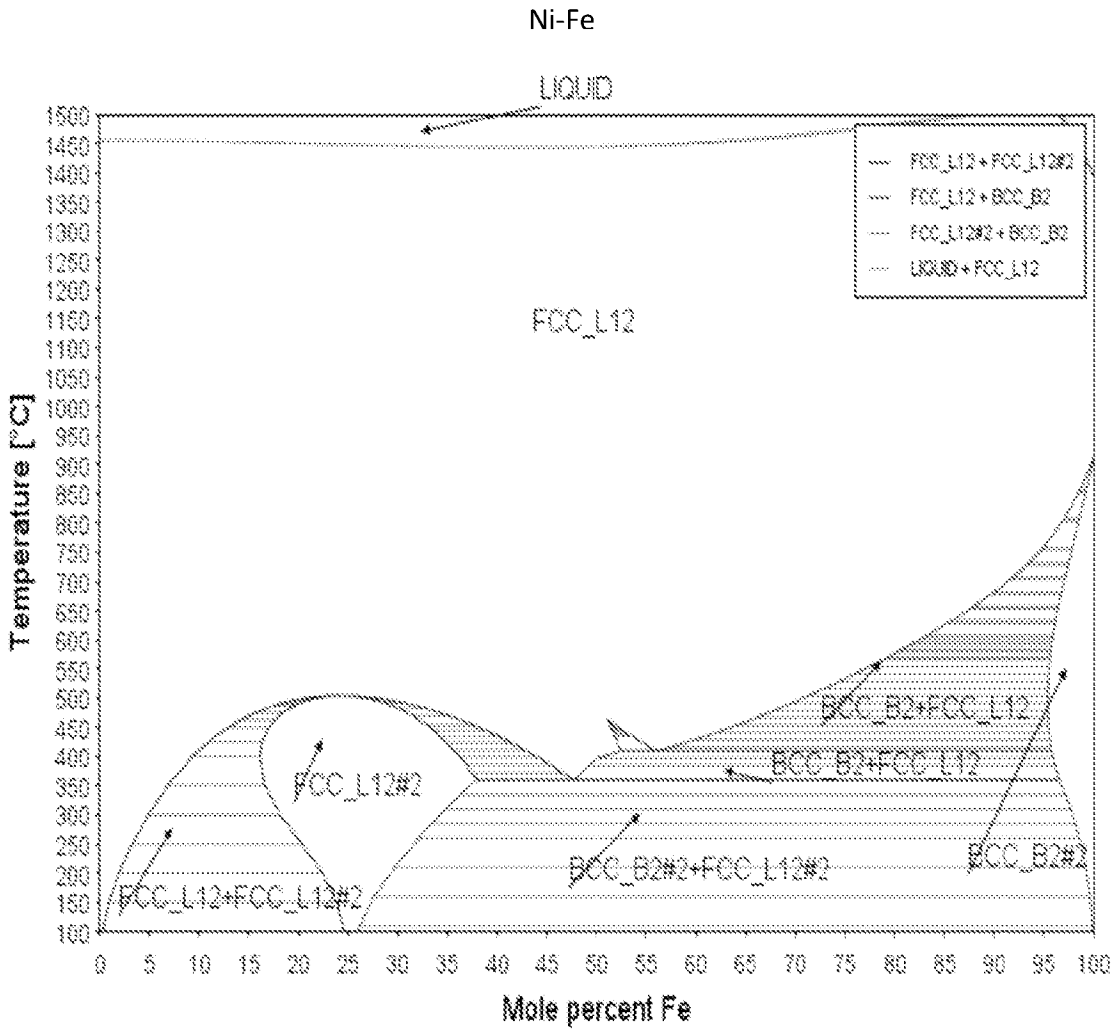
Ni-Fe
LIQUID
FCC_L12
FCC_L12#2
BCC_B2+FCC_L12
BCC_B2+FCC_L12
BCC_B2#2+FCC_L12#2
BCC_B2#2
FCC_L12+FCC_L12#2
Temperature [°C]
Mole percent Fe

FIG. 7A

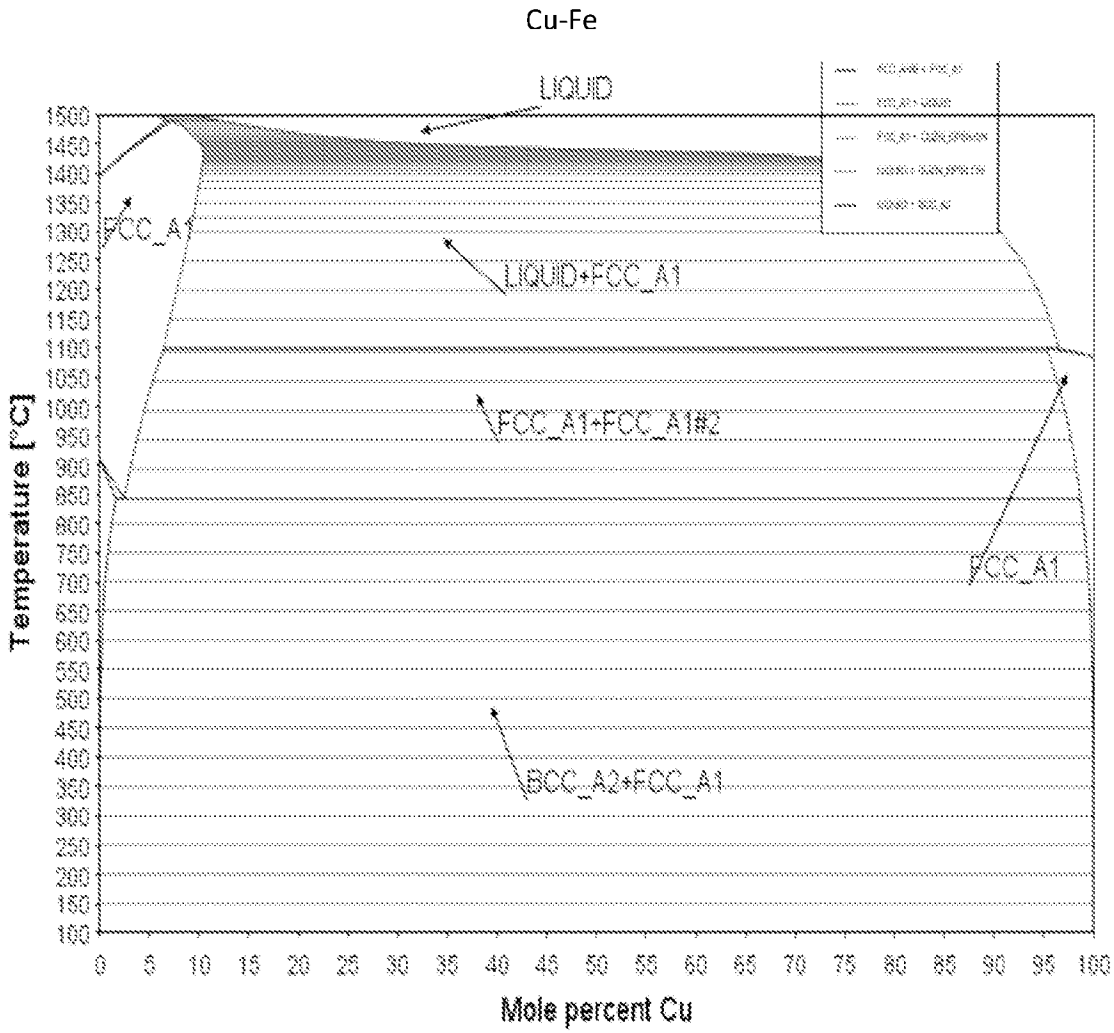
Cu-Fe
LIQUID
FCC_A1
LIQUID+FCC_A1
FCC_A1+FCC_A1#2
FCC_A1
BCC_A2+FCC_A1
Temperature [°C]
Mole percent Cu
1500
1450
1400
1350
1300
1250
1200
1150
1100
1050
1000
950
900
850
800
750
700
650
600
550
500
450
400
350
300
250
200
150
100
0 5 10 15 20 25 30 35 40 45 50 55 60 65 70 75 80 85 90 95 100

FIG. 7B

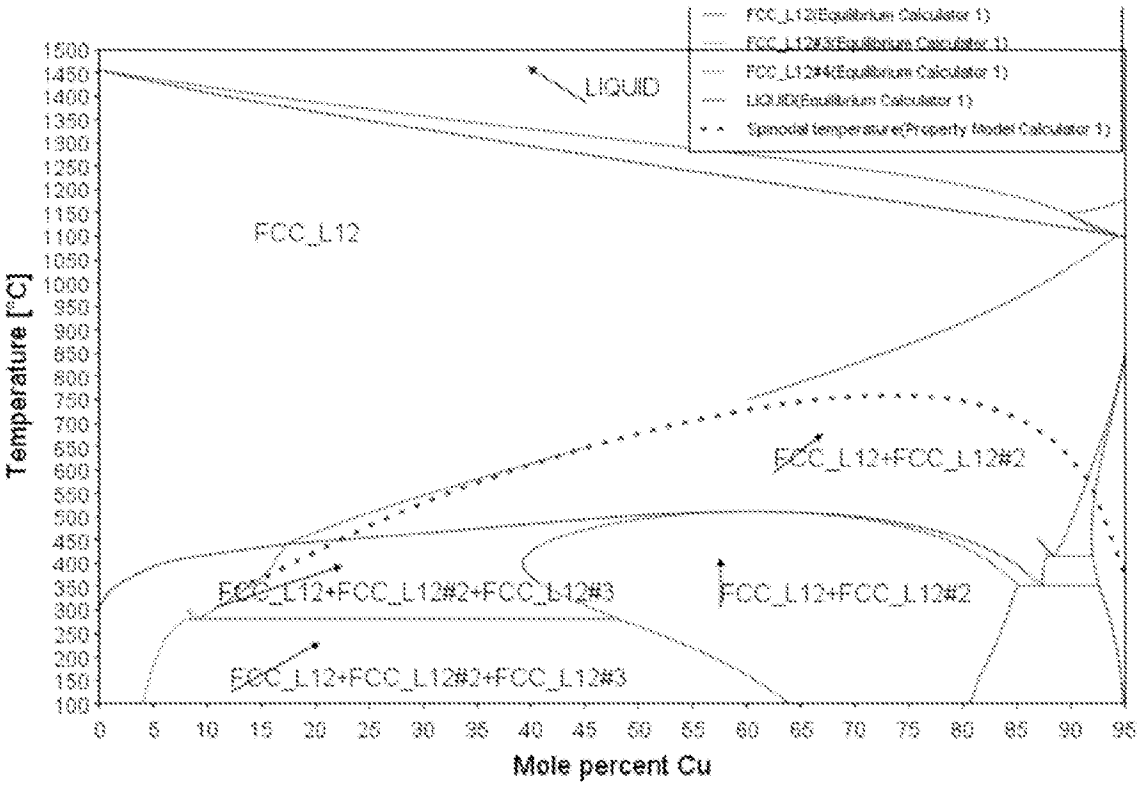
FCC_L12(Equilibrium Calculator 1)
FCC_L12#3(Equilibrium Calculator 1)
FCC_L12#4(Equilibrium Calculator 1)
LIQUID(Equilibrium Calculator 1)
Spinodal temperature(Property Model Calculator 1)
LIQUID
FCC_L12
FCC_L12+FCC_L12#2
FCC_L12+FCC_L12#2+FCC_L12#3
FCC_L12+FCC_L12#2
FCC_L12+FCC_L12#2+FCC_L12#3
Temperature [°C]
Mole percent Cu

FIG. 8A

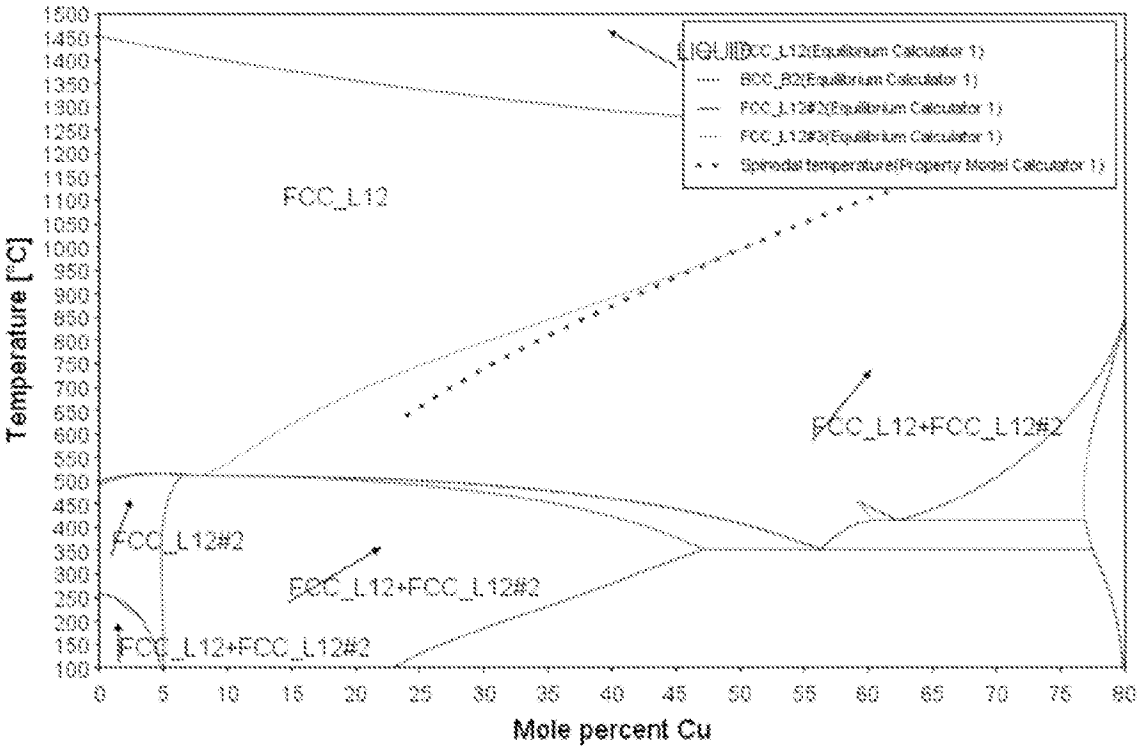
LIQUID(FCC_L12(Equilibrium Calculator 1))
BCC_B2(Equilibrium Calculator 1)
FCC_L12#2(Equilibrium Calculator 1)
FCC_L12#3(Equilibrium Calculator 1)
Spinodal temperature(Property Model Calculator 1)
FCC_L12
FCC_L12+FCC_L12#2
FCC_L12#2
B2+FCC_L12+FCC_L12#2
FCC_L12+FCC_L12#2
Temperature [°C]
Mole percent Cu

FIG. 8B

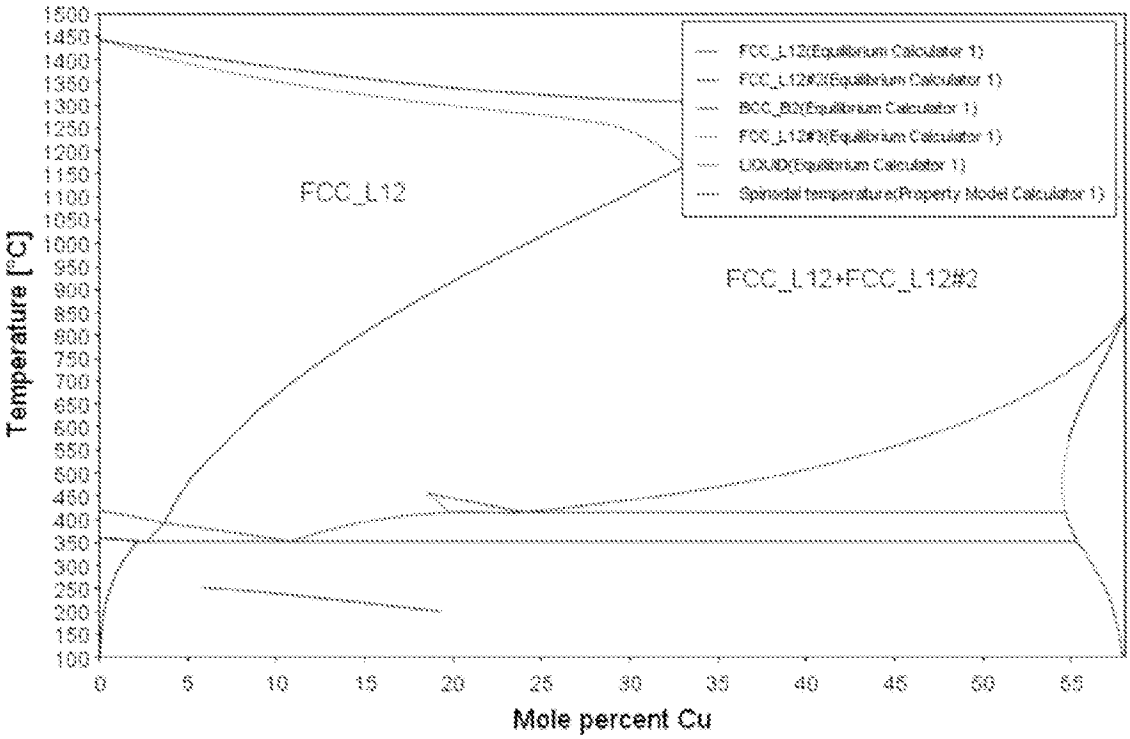
FCC_L12(Equilibrium Calculator 1)
FCC_L12#2(Equilibrium Calculator 1)
BCC_B2(Equilibrium Calculator 1)
FCC_L12#3(Equilibrium Calculator 1)
LIQUID(Equilibrium Calculator 1)
Spinodal temperature(Property Model Calculator 1)
FCC_L12
FCC_L12+FCC_L12#2
Temperature [°C]
Mole percent Cu
1500
1450
1400
1350
1300
1250
1200
1150
1100
1050
1000
950
900
850
800
750
700
650
600
550
500
450
400
350
300
250
200
150
100
0
5
10
15
20
25
30
35
40
45
50
55

FIG. 8C

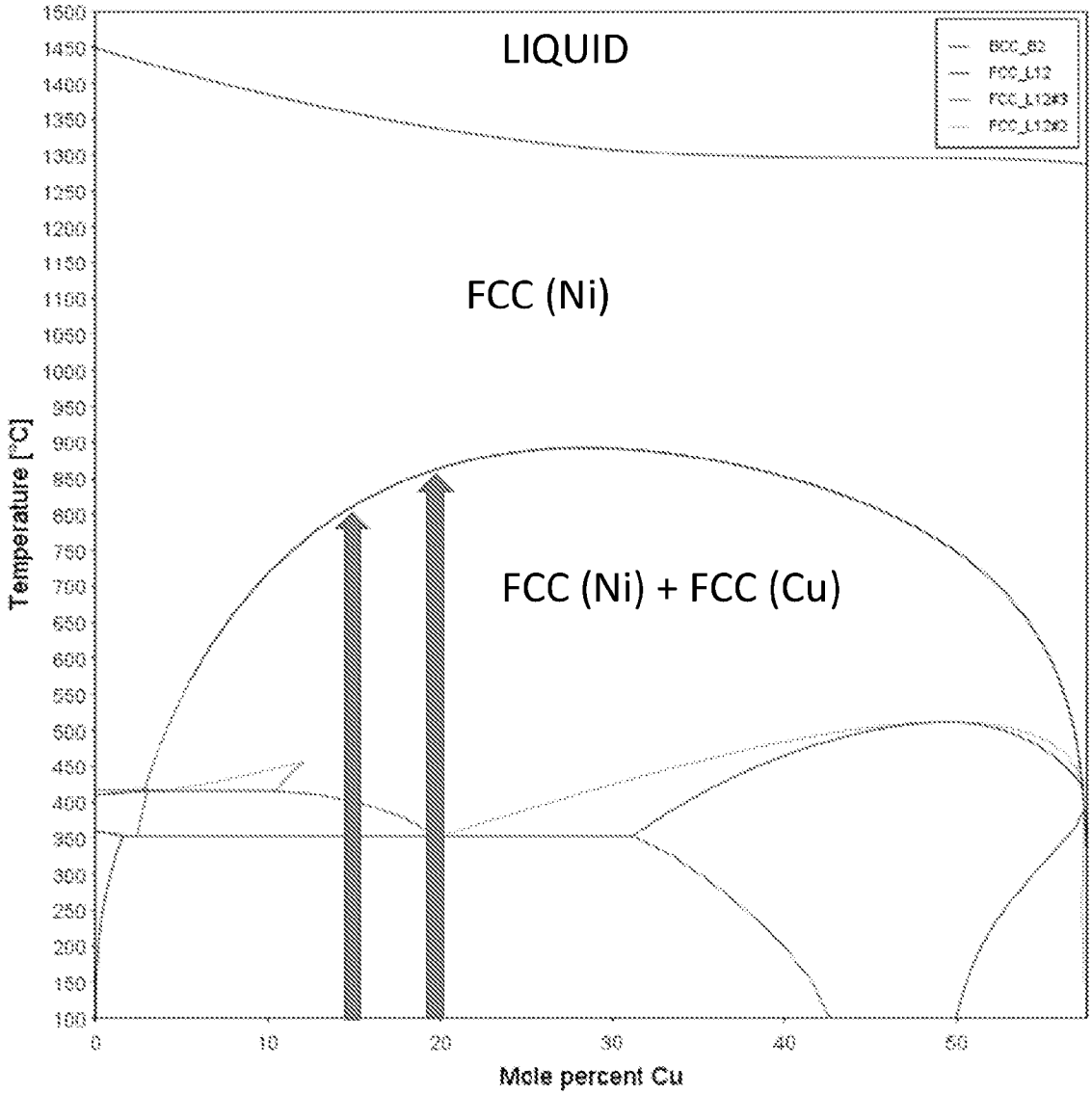
LIQUID
FCC (Ni)
FCC (Ni) + FCC (Cu)
Temperature [°C]
Mole percent Cu
1500
1450
1400
1350
1300
1250
1200
1150
1100
1050
1000
950
900
850
800
750
700
650
600
550
500
450
400
350
300
250
200
150
100
0
10
20
30
40
50

FIG. 8D

For 550C:

Stable Phases

	Moles	Mass	Volume Fraction
FCC (Cu)	0.10254	6.48378	0.10503

Composition

Component	Mole Fraction	Mass Fraction
Cu	0.93710	0.94171
Ni	0.06074	0.05638
Fe	0.00216	0.00191

	Moles	Mass	Volume Fraction
FCC (Ni,Fe)	0.89746	51.72665	0.89497

Composition

Component	Mole Fraction	Mass Fraction
Ni	0.46662	0.47515
Fe	0.47327	0.45857
Cu	0.06012	0.06628

FIG. 8E

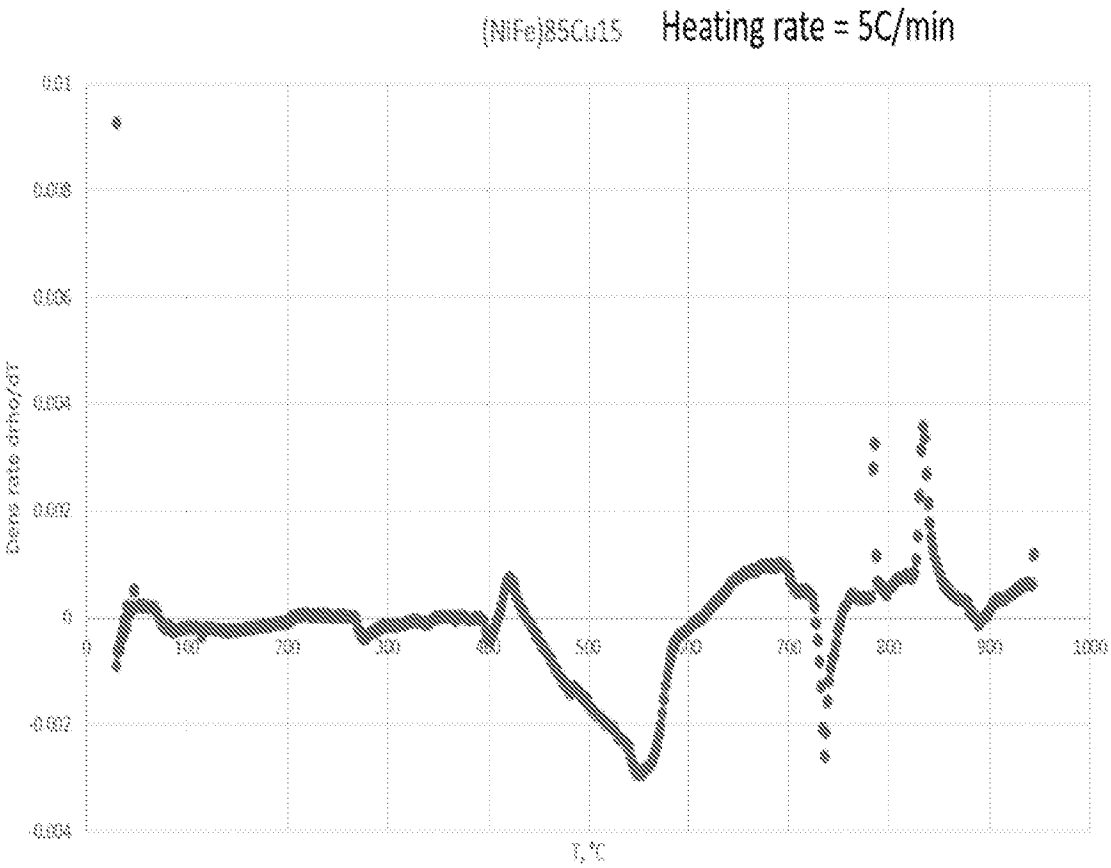
(NiFe)85Cu15
Heating rate = 5C/min
Dens rate drho/dT
T, °C
0.01
0.008
0.006
0.004
0.002
0
-0.002
-0.004
0
100
200
300
400
500
600
700
800
900
1000

FIG. 8F

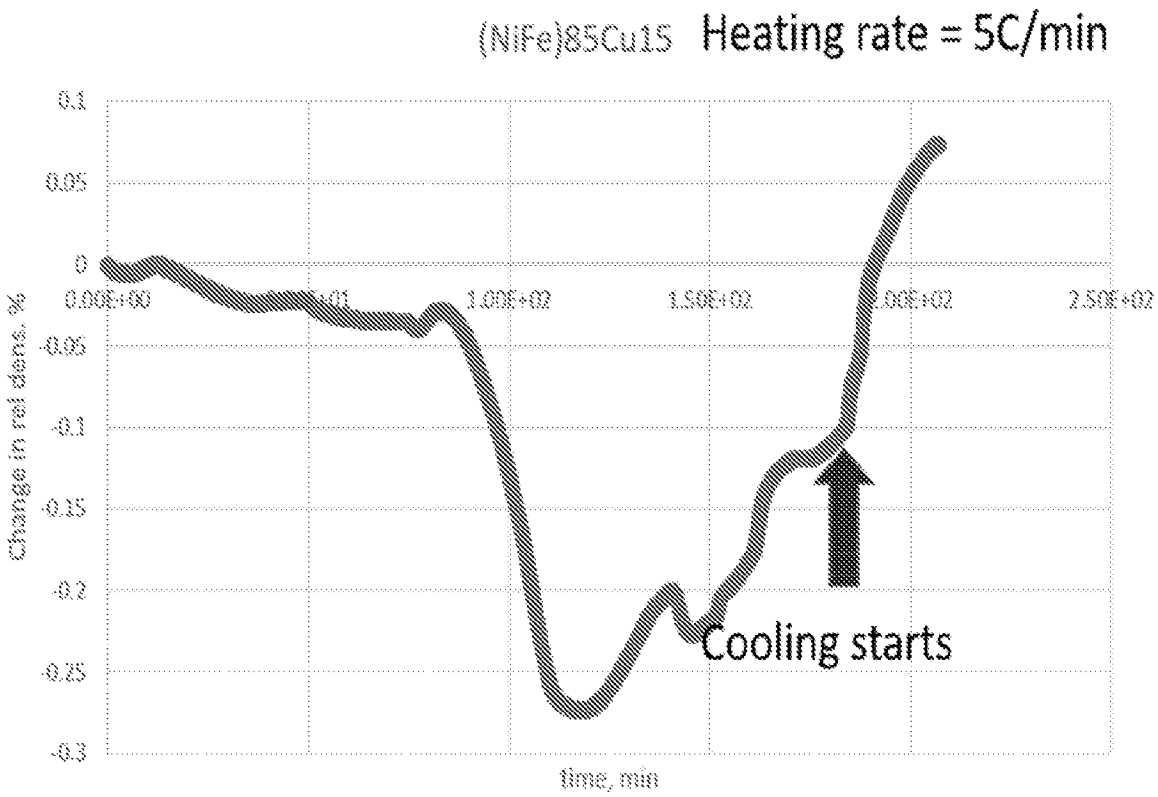
(NiFe)85Cu15 Heating rate = 5C/min
0.1
0.05
0
-0.05
-0.1
-0.15
-0.2
-0.25
-0.3
0.00E+00
1.00E+02
1.50E+02
2.50E+02
Change in rel dens, %
time, min
Cooling starts

FIG. 8G

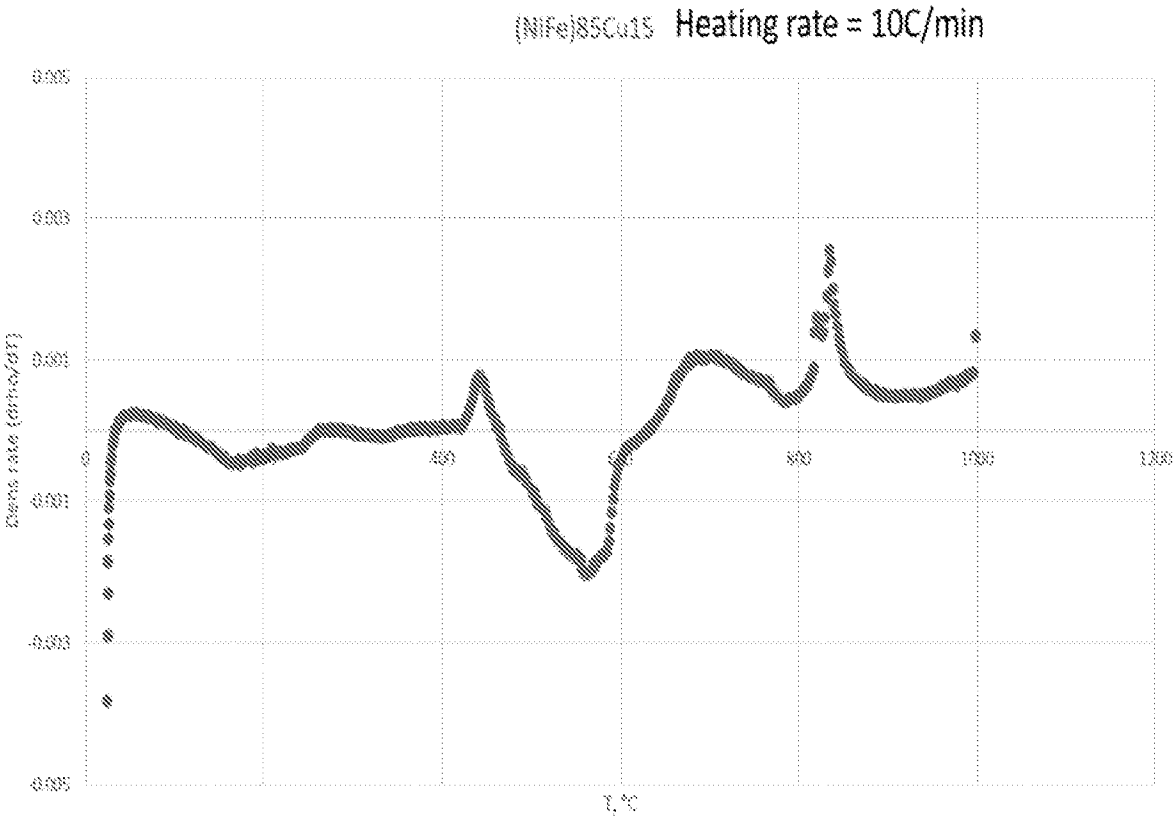
(NiFe)85Cu15 Heating rate = 10C/min
0.005
0.003
0.001
-0.001
-0.003
-0.005
0
400
800
1200
1600
T, °C

FIG. 8H

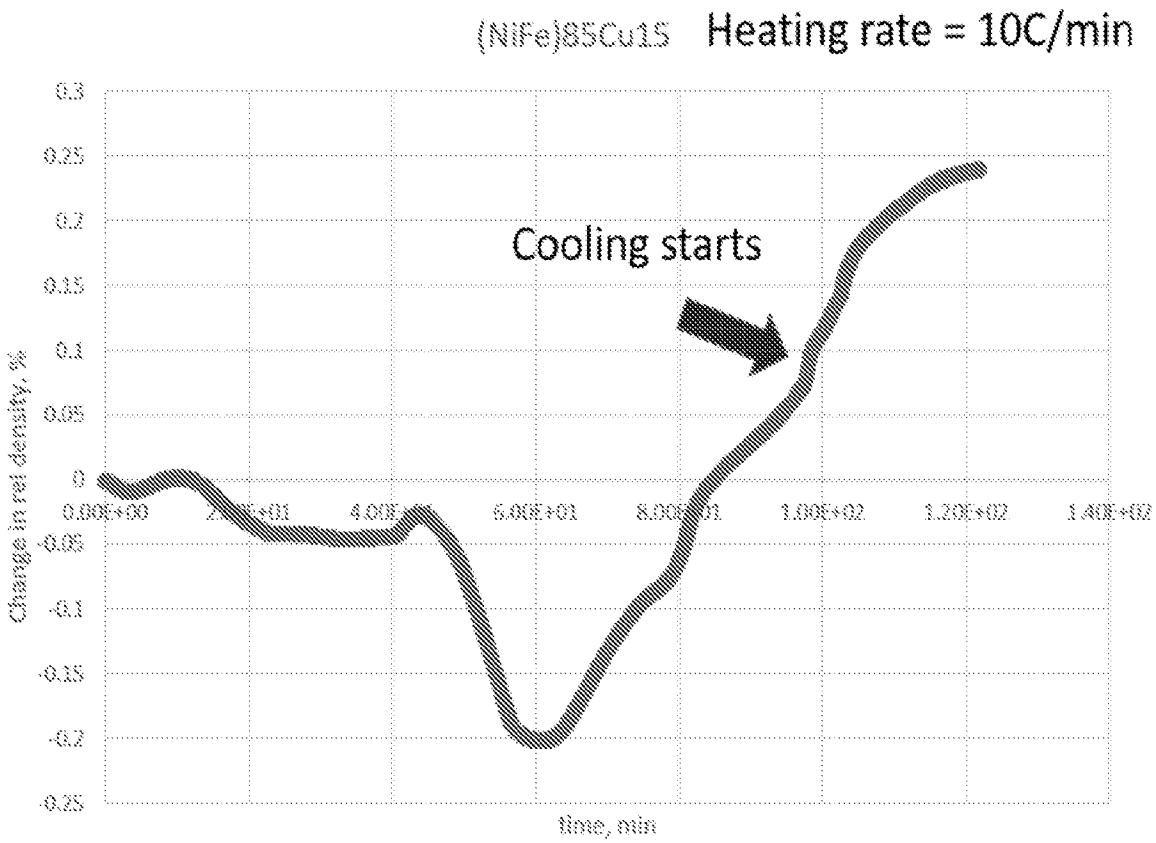
(NiFe)85Cu15
Heating rate = 10C/min
Cooling starts
Change in rel density, %
time, min
0.3
0.25
0.2
0.15
0.1
0.05
0
-0.05
-0.1
-0.15
-0.2
-0.25
0.00E+00
2.00E+01
4.00E+01
6.00E+01
8.00E+01
1.00E+02
1.20E+02
1.40E+02

FIG. 8I

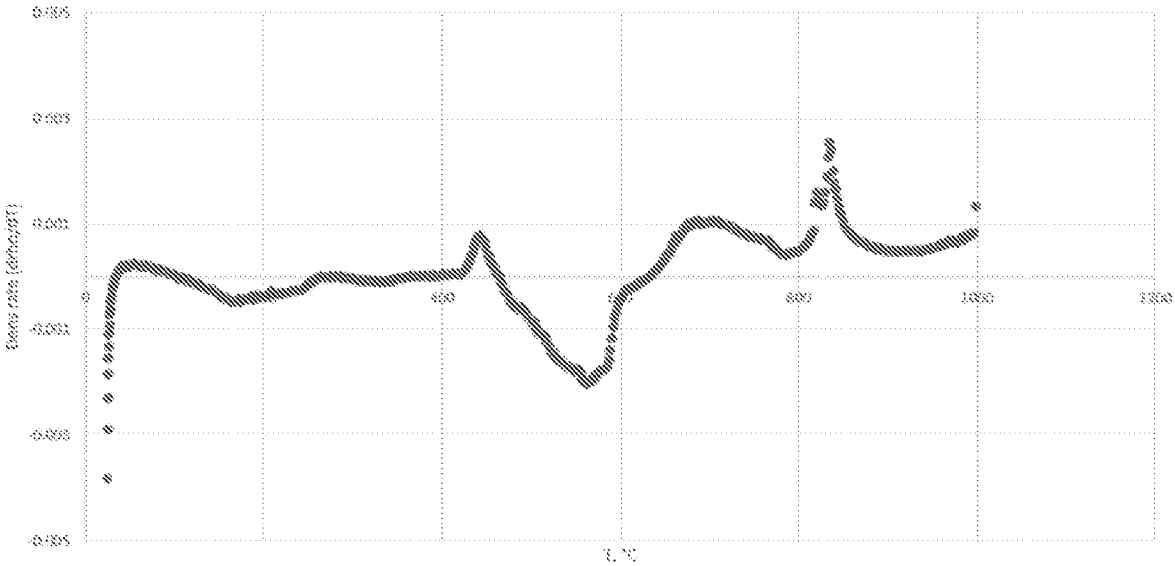
0.005
0.003
0.001
-0.001
-0.003
-0.005
0
400
800
1000
1200
T, °C

FIG. 8J

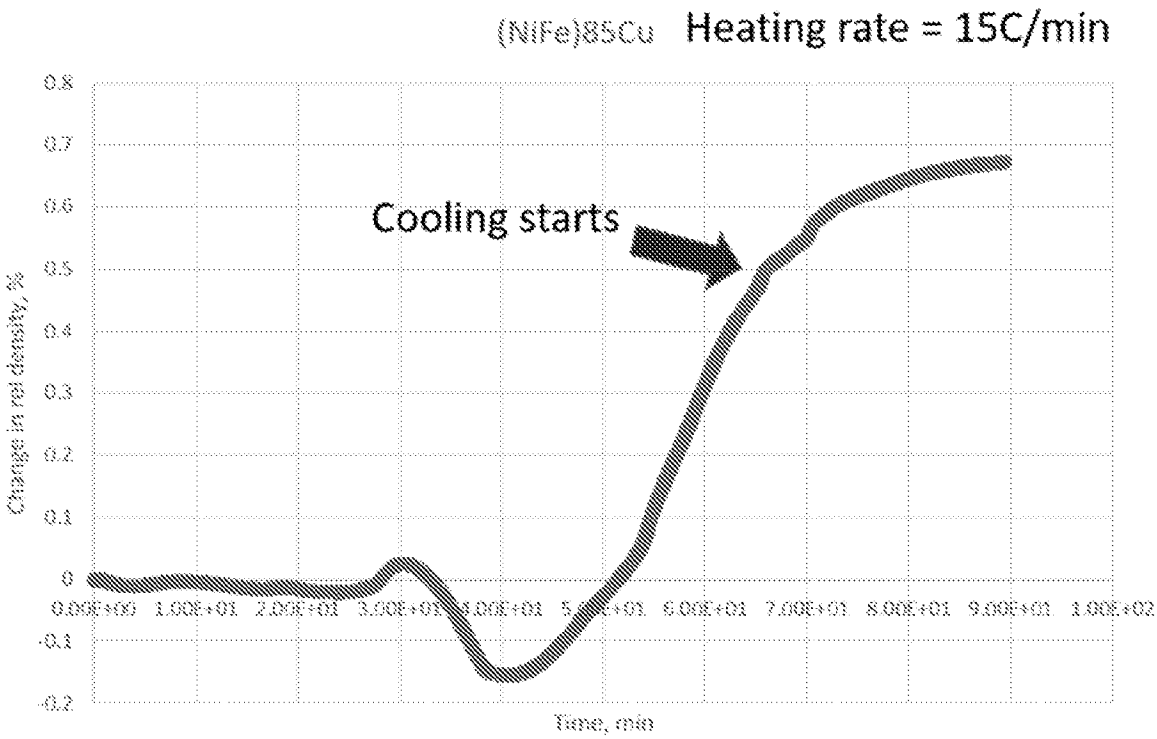
(NiFe)85Cu
Heating rate = 15C/min
Cooling starts
Change in rel density, %
0.8
0.7
0.6
0.5
0.4
0.3
0.2
0.1
0
-0.1
-0.2
0.00E+00
1.00E+01
2.00E+01
3.00E+01
4.00E+01
5.00E+01
6.00E+01
7.00E+01
8.00E+01
9.00E+01
1.00E+02
Time, min

FIG. 8K

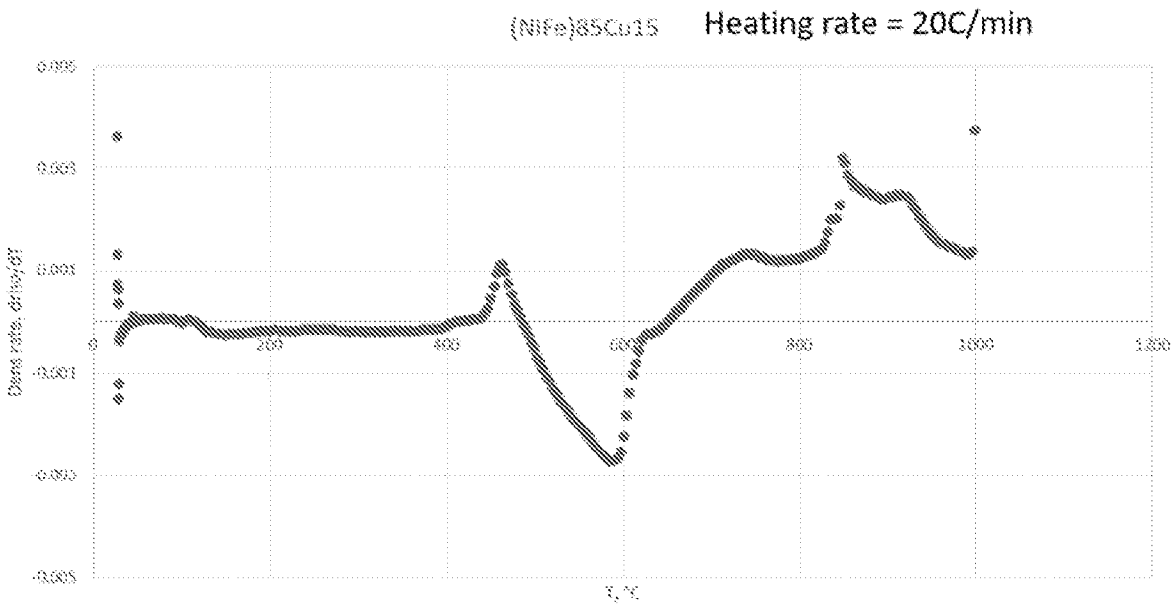
(NiFe)85Cu15
Heating rate = 20C/min
0.005
0.003
0.001
-0.001
-0.003
-0.005
0
200
400
600
800
1000
1200
T, °C

FIG. 8L

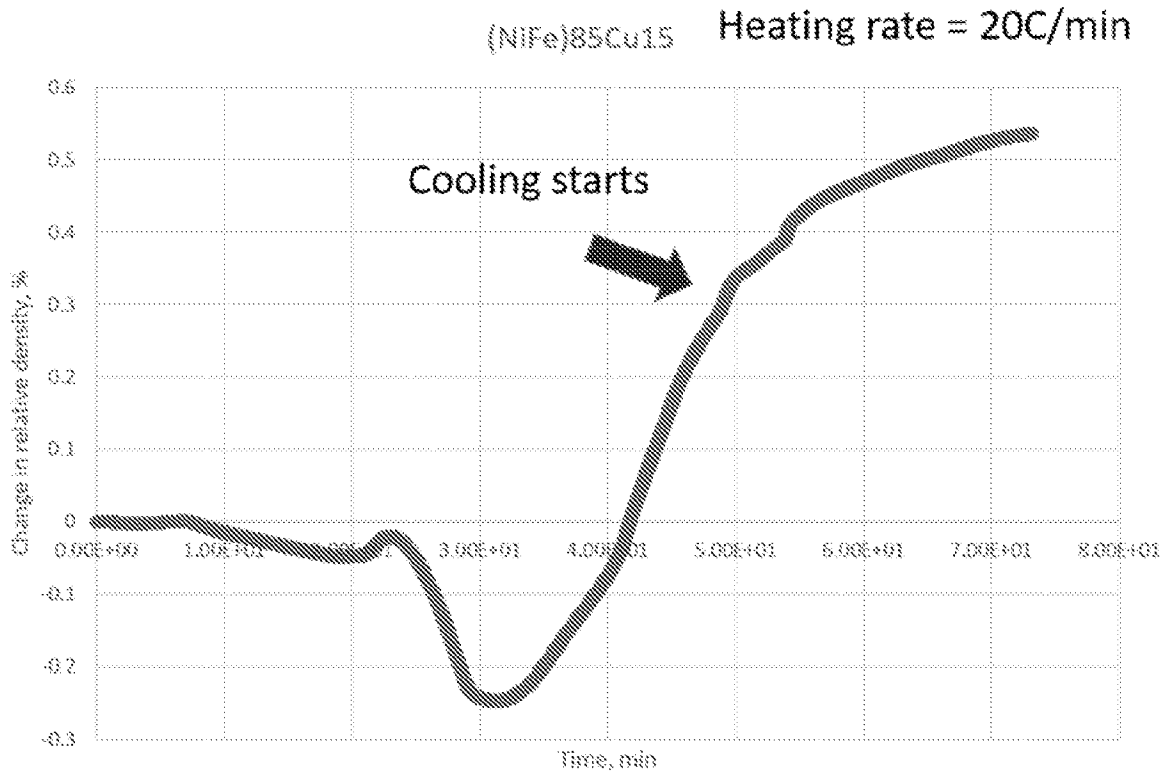
(NiFe)85Cu15
Heating rate = 20C/min
Cooling starts
0.6
0.5
0.4
0.3
0.2
0.1
0
-0.1
-0.2
-0.3
0.00E+00
1.00E+01
3.00E+01
4.00E+01
5.00E+01
6.00E+01
7.00E+01
8.00E+01
Change in relative density, %
Time, min

FIG. 8M

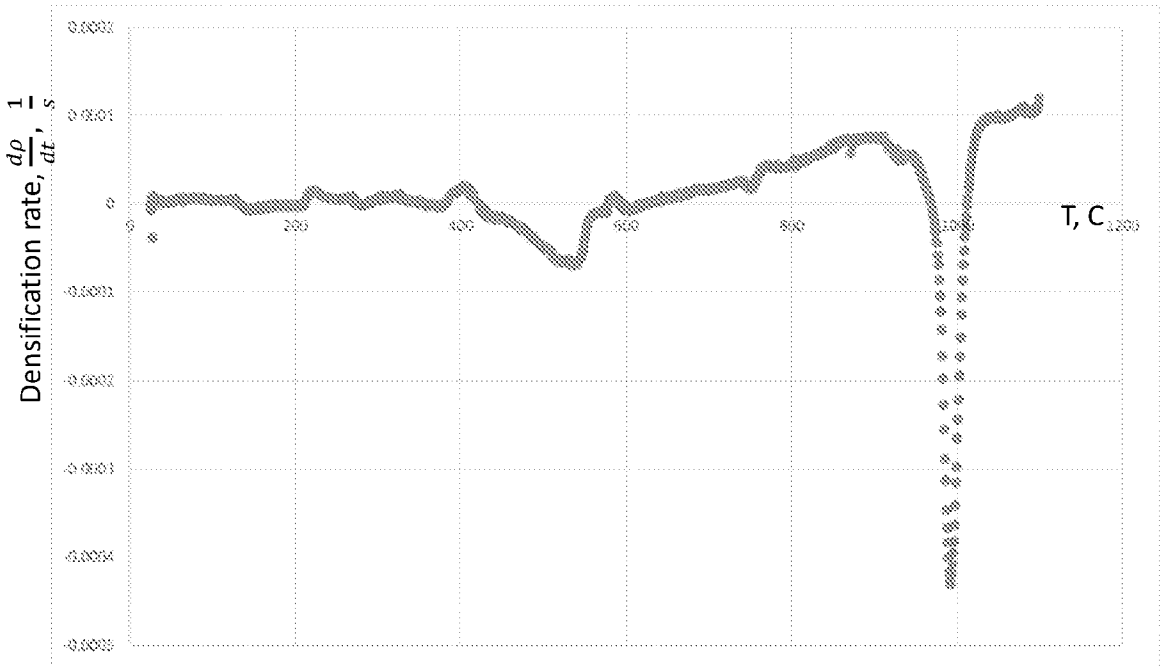
Densification rate, $\frac{d\rho}{dt}, \frac{1}{s}$
T, C

FIG. 8N

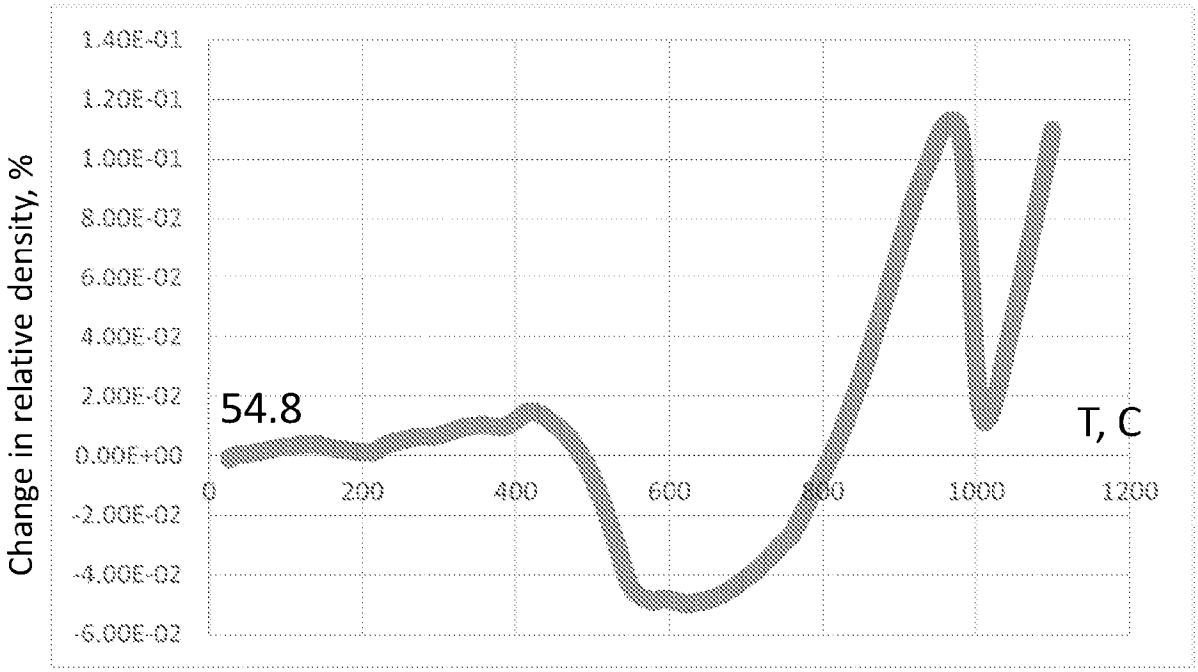
Change in relative density, %
1.40E-01
1.20E-01
1.00E-01
8.00E-02
6.00E-02
4.00E-02
2.00E-02
0.00E+00
-2.00E-02
-4.00E-02
-6.00E-02
0
200
400
600
1000
1200
54.8
T, C

FIG. 8O

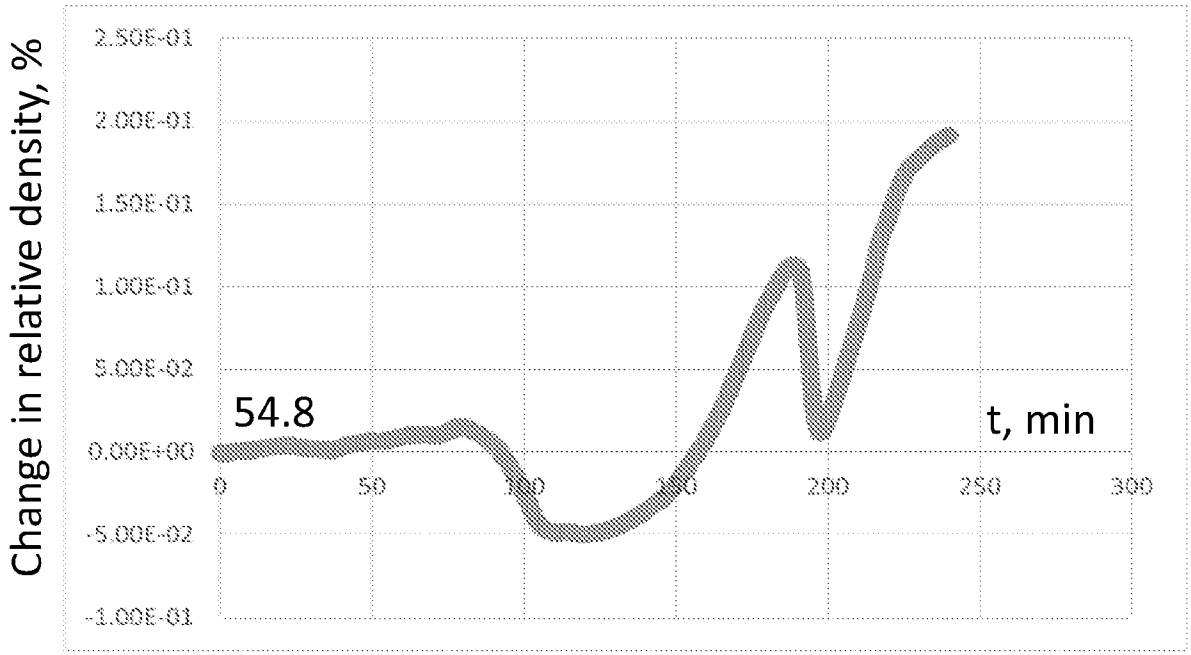
Change in relative density, %
2.50E-01
2.00E-01
1.50E-01
1.00E-01
5.00E-02
0.00E+00
-5.00E-02
-1.00E-01
54.8
t, min
0
50
100
150
200
250
300

FIG. 8P

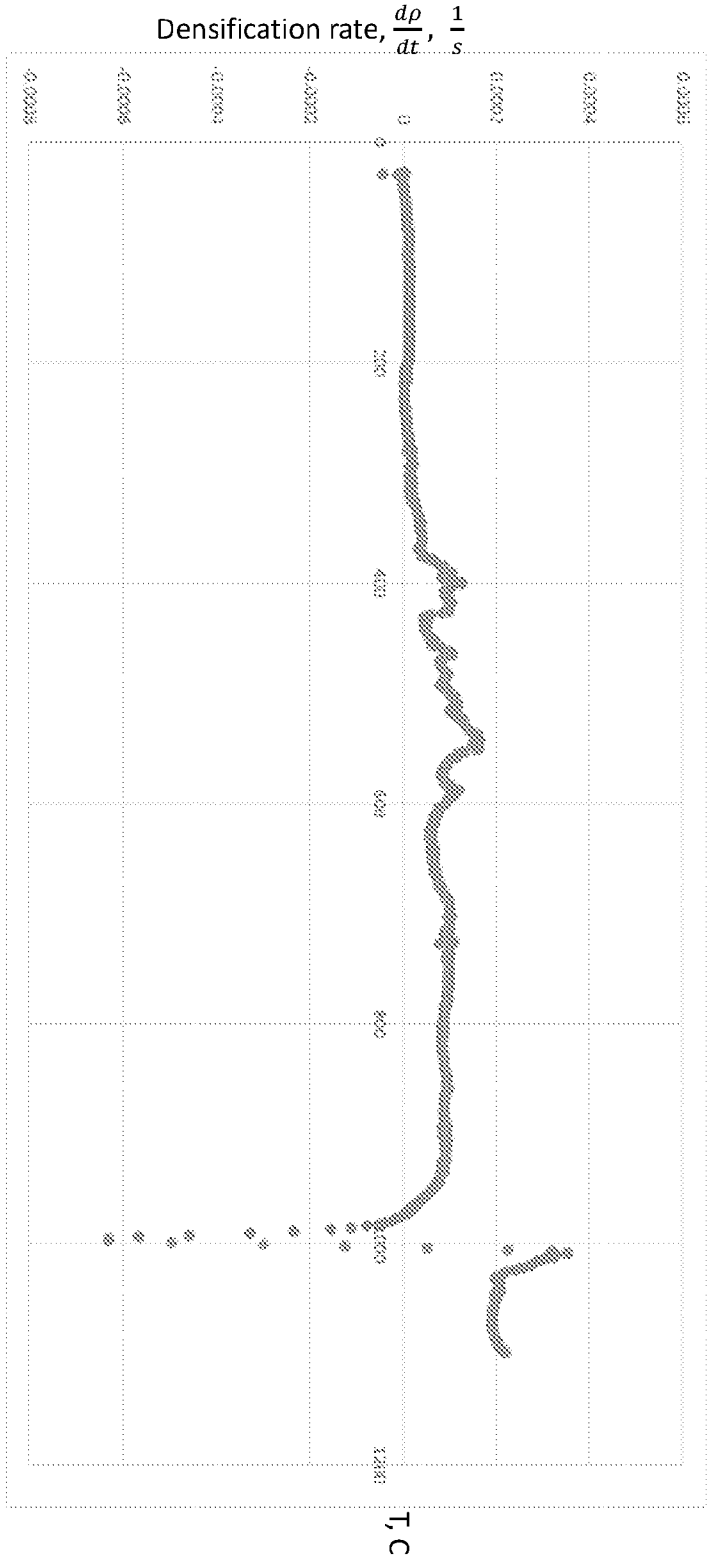
0.0026
0.0024
0.0022
0
-0.0002
-0.0004
-0.0006
-0.0008
0
200
400
600
800
1000
1200
T, C
Densification rate, $\frac{d\rho}{dt}$, $\frac{1}{s}$

FIG. 8Q

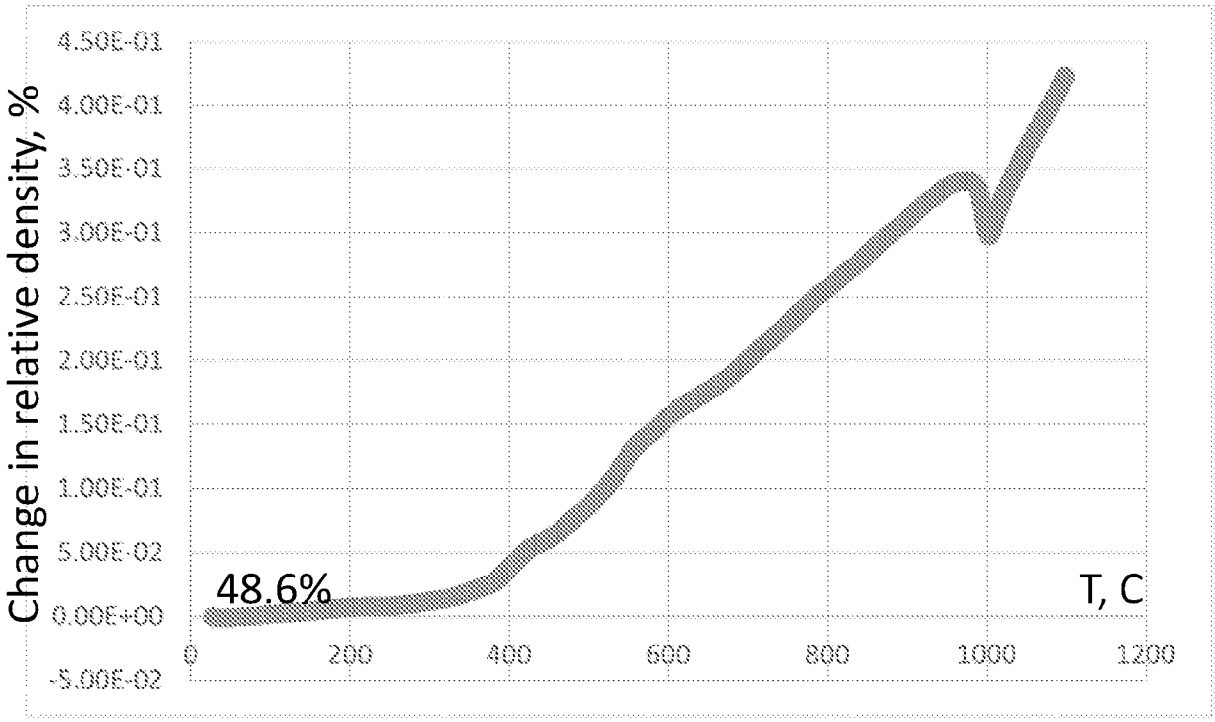
Change in relative density, %
4.50E-01
4.00E-01
3.50E-01
3.00E-01
2.50E-01
2.00E-01
1.50E-01
1.00E-01
5.00E-02
0.00E+00
-5.00E-02
0
200
400
600
800
1000
1200
48.6%
T, C

FIG. 8R

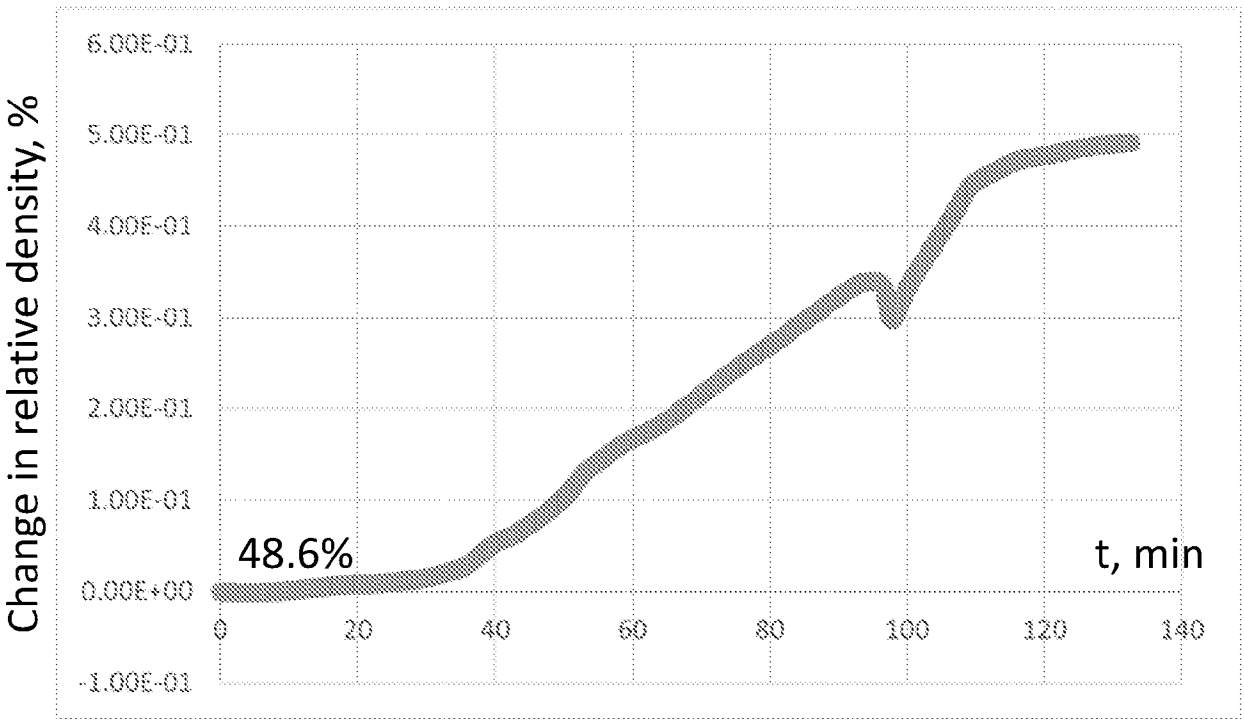
Change in relative density, %
6.00E-01
5.00E-01
4.00E-01
3.00E-01
2.00E-01
1.00E-01
0.00E+00
-1.00E-01
0
20
40
60
80
100
120
140
48.6%
t, min

FIG. 8S

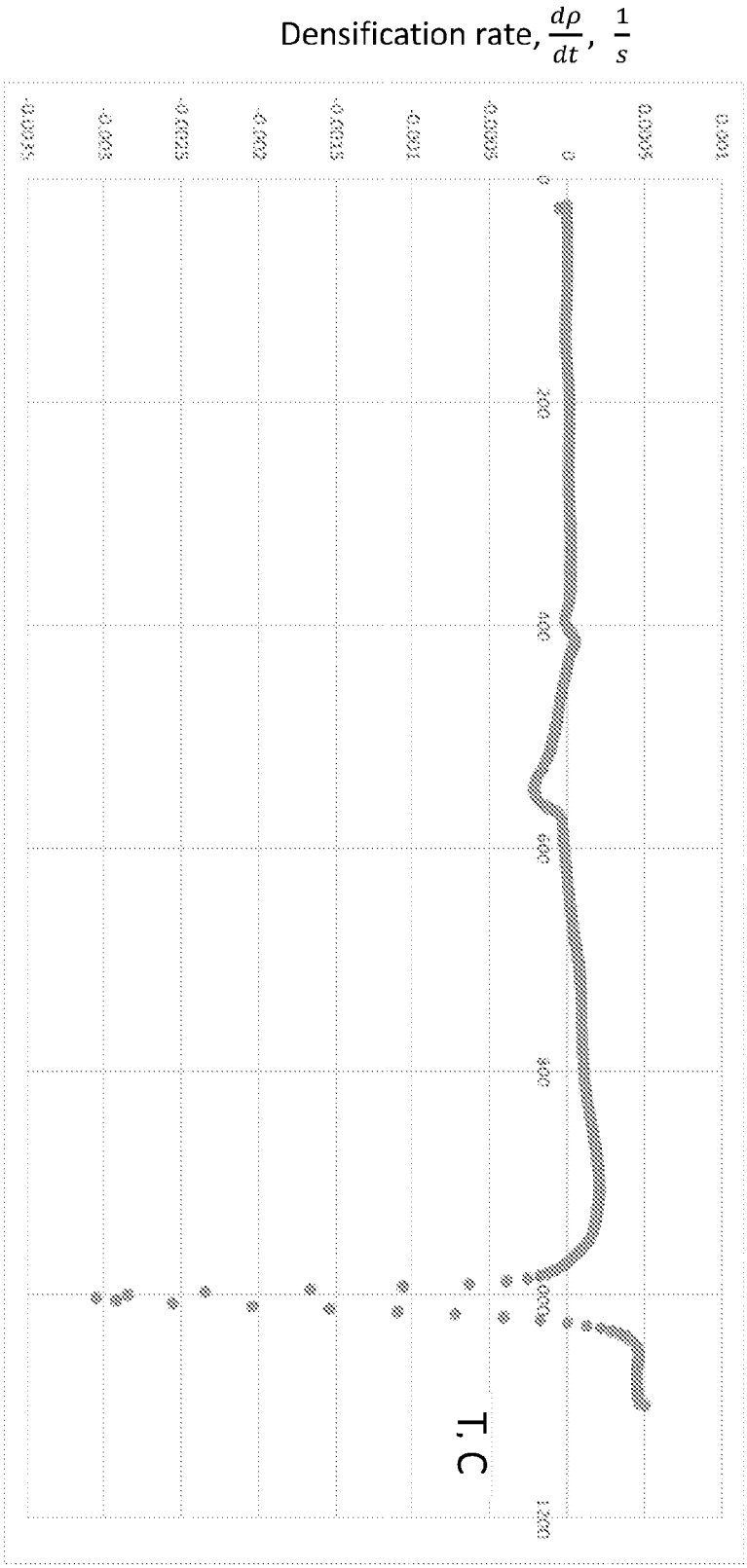
Densification rate, $\frac{d\rho}{dt}$, $\frac{1}{s}$
0.001
0.0005
0
-0.0005
-0.001
-0.0015
-0.002
-0.0025
-0.003
-0.0035
0
200
400
600
800
1000
1200
T, C

FIG. 8T

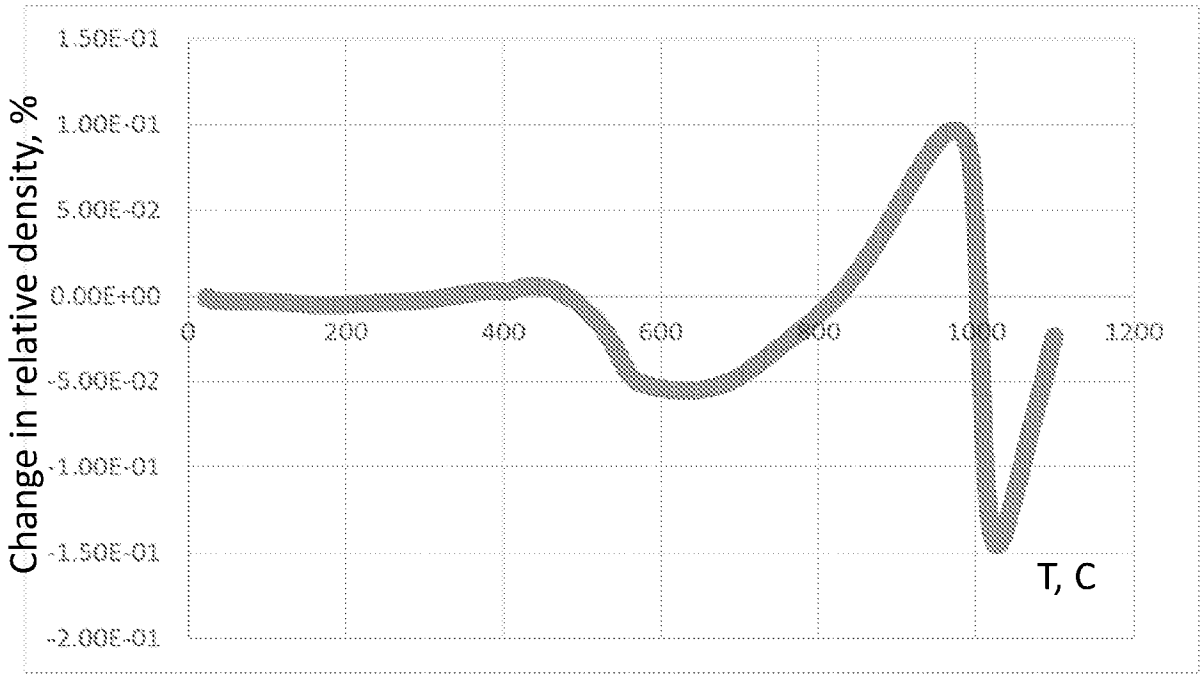
1.50E-01
1.00E-01
5.00E-02
0.00E+00
-5.00E-02
-1.00E-01
-1.50E-01
-2.00E-01
Change in relative density, %
0
200
400
600
1200
T, C

FIG. 8U

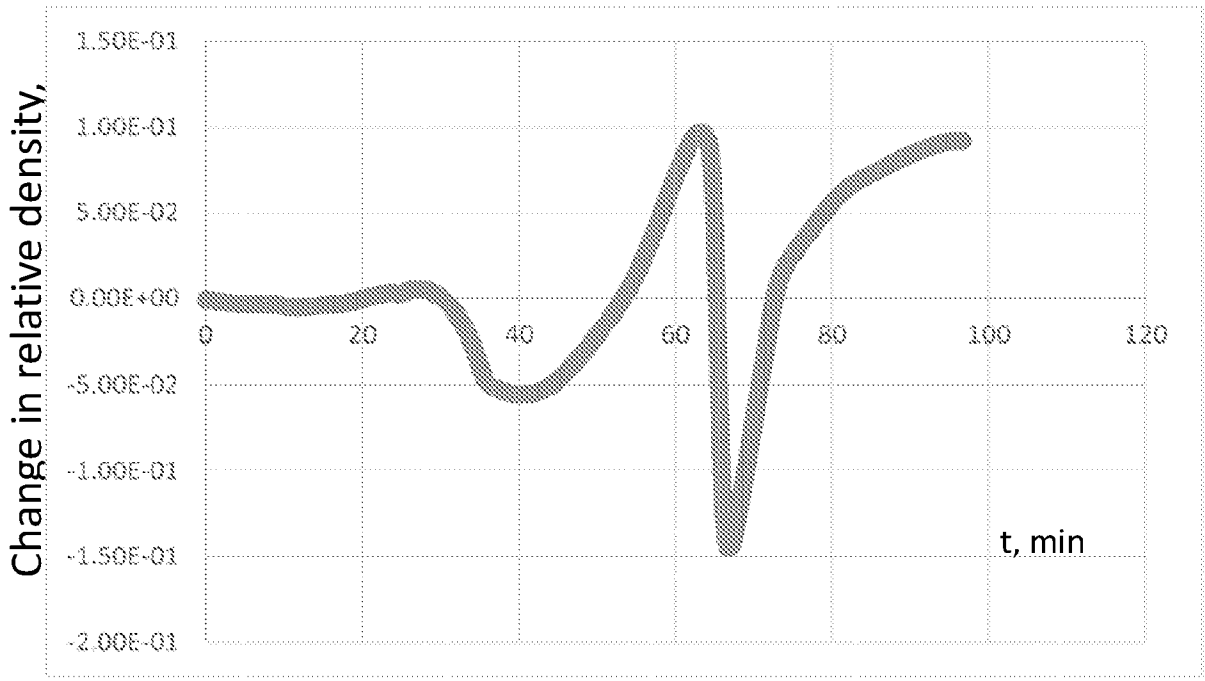
1.50E-01
1.00E-01
5.00E-02
0.00E+00
-5.00E-02
-1.00E-01
-1.50E-01
-2.00E-01
Change in relative density,
0
20
40
60
80
100
120
t, min

FIG. 8V

Ni-Co

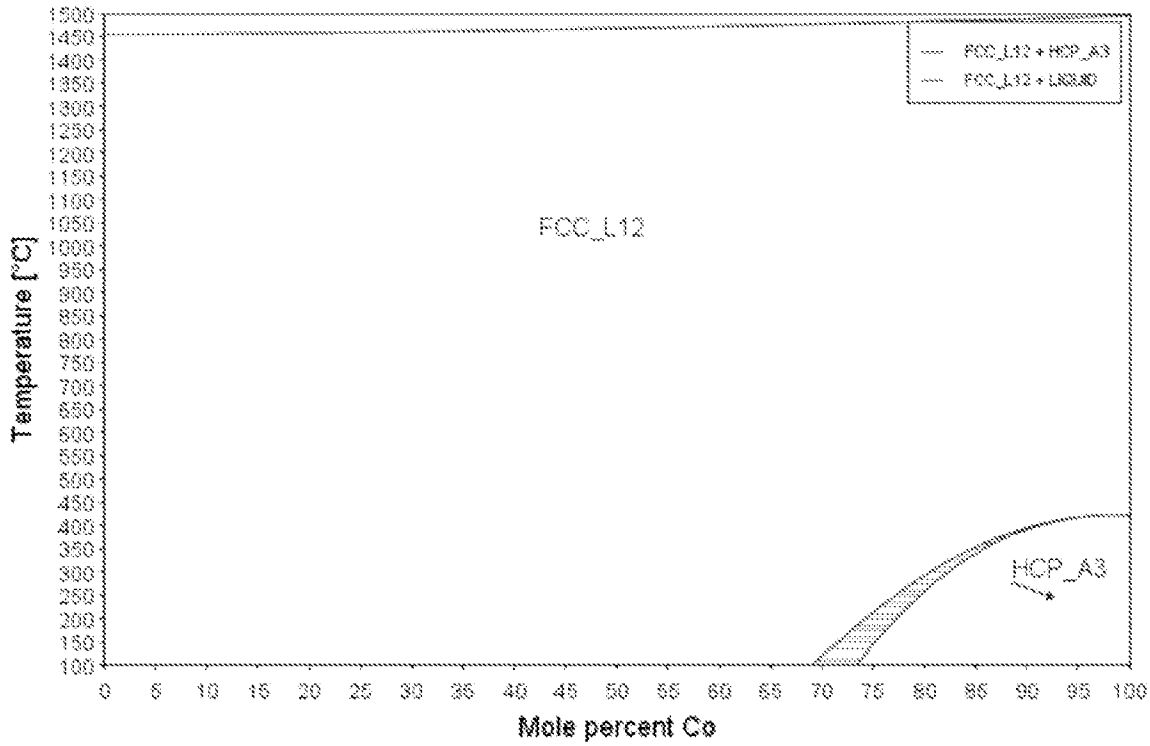
FCC_L12 + HCP_A3
FCC_L12 + LIQUID
FCC_L12
HCP_A3
Temperature [°C]
Mole percent Co
1500
1450
1400
1350
1300
1250
1200
1150
1100
1050
1000
950
900
850
800
750
700
650
600
550
500
450
400
350
300
250
200
150
100
0
5
10
15
20
25
30
35
40
45
50
55
60
65
70
75
80
85
90
95
100

FIG. 9A

Cu-Co

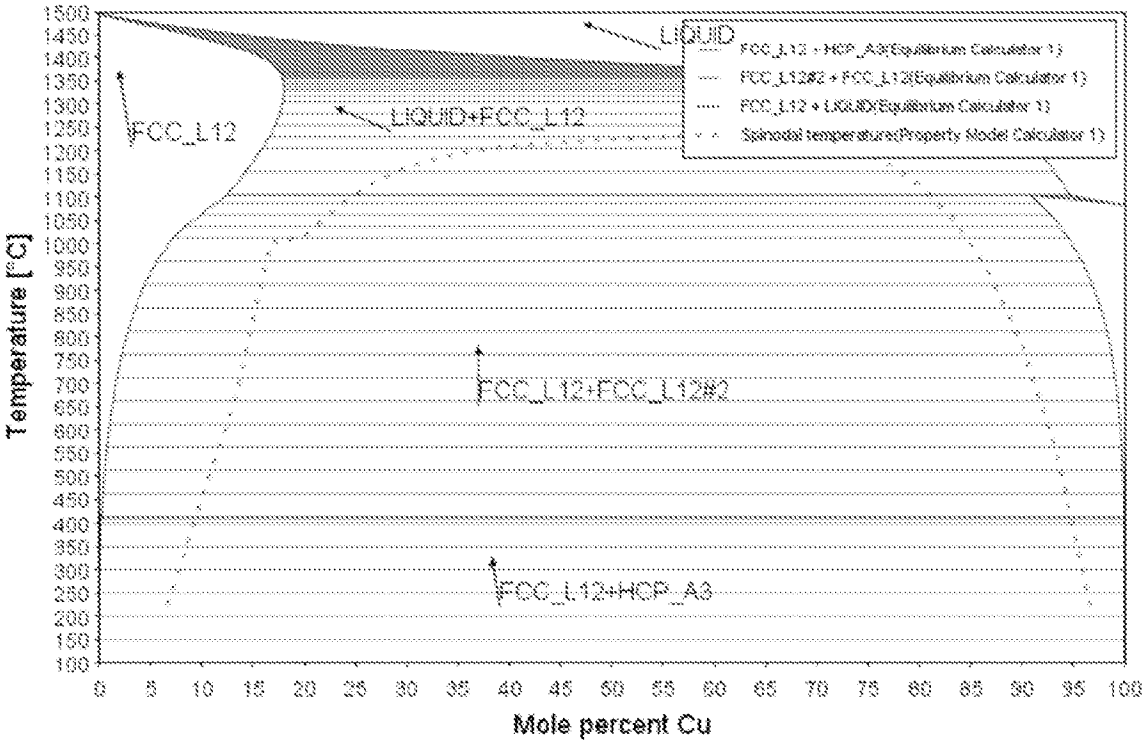
LIQUID
FCC_L12 + HCP_A3(Equilibrium Calculator 1)
FCC_L12#2 + FCC_L12(Equilibrium Calculator 1)
FCC_L12 + LIQUID(Equilibrium Calculator 1)
Spinodal temperature(Property Model Calculator 1)
FCC_L12
LIQUID+FCC_L12
FCC_L12+FCC_L12#2
FCC_L12+HCP_A3
Temperature [°C]
Mole percent Cu

FIG. 9B

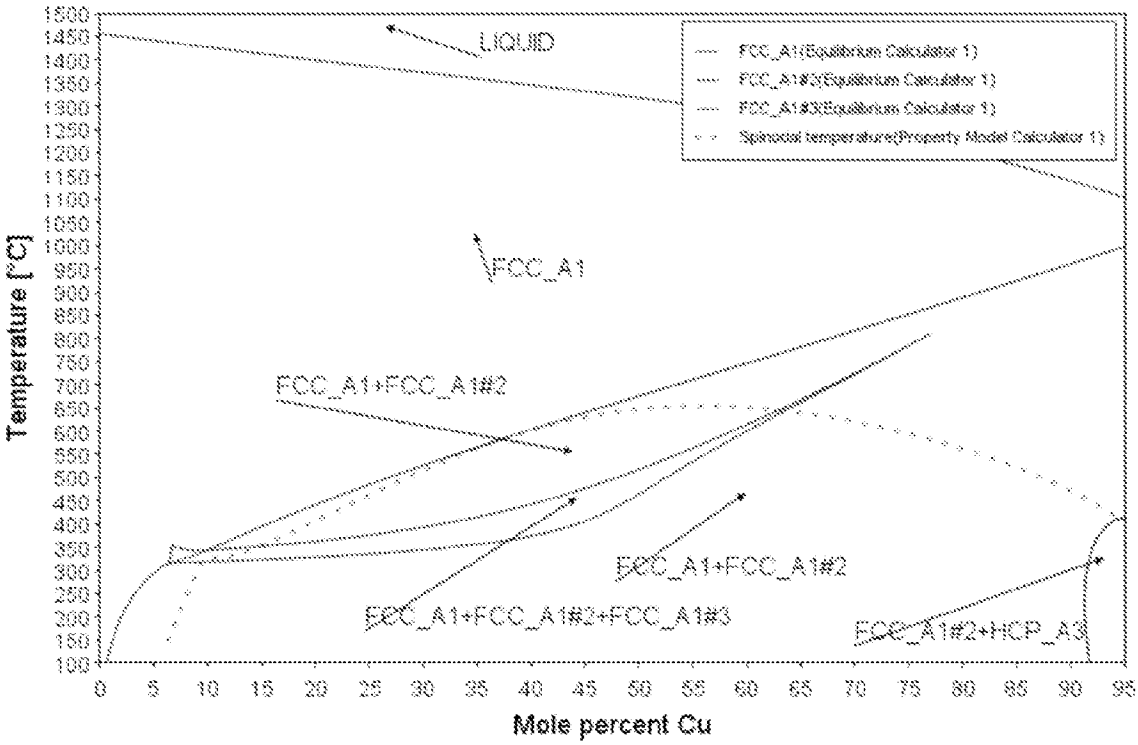
LIQUID
FCC_A1(Equilibrium Calculator 1)
FCC_A1#2(Equilibrium Calculator 1)
FCC_A1#3(Equilibrium Calculator 1)
Spinodal temperature(Property Model Calculator 1)
FCC_A1
FCC_A1+FCC_A1#2
FCC_A1+FCC_A1#2
FCC_A1+FCC_A1#2+FCC_A1#3
FCC_A1#2+HCP_A3
Temperature [C]
Mole percent Cu

FIG. 10A

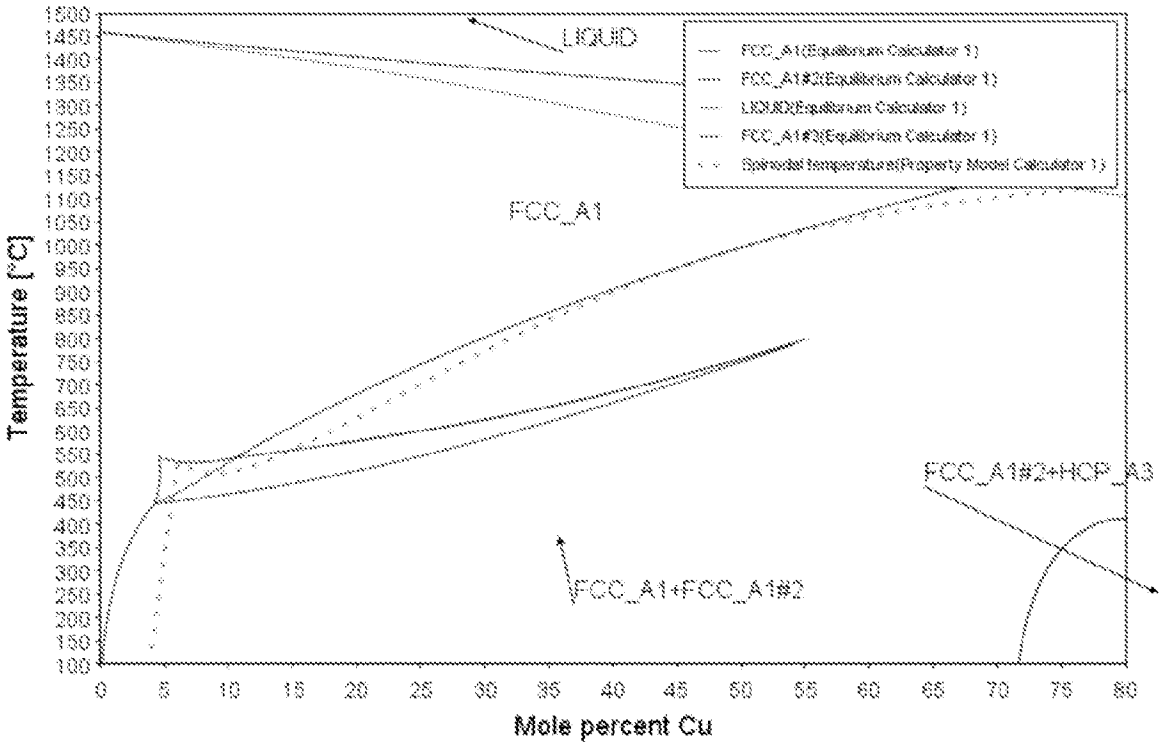
LIQUID
FCC_A1
FCC_A1#2+HCP_A3
FCC_A1+FCC_A1#2
Temperature [°C]
Mole percent Cu

FIG. 10B

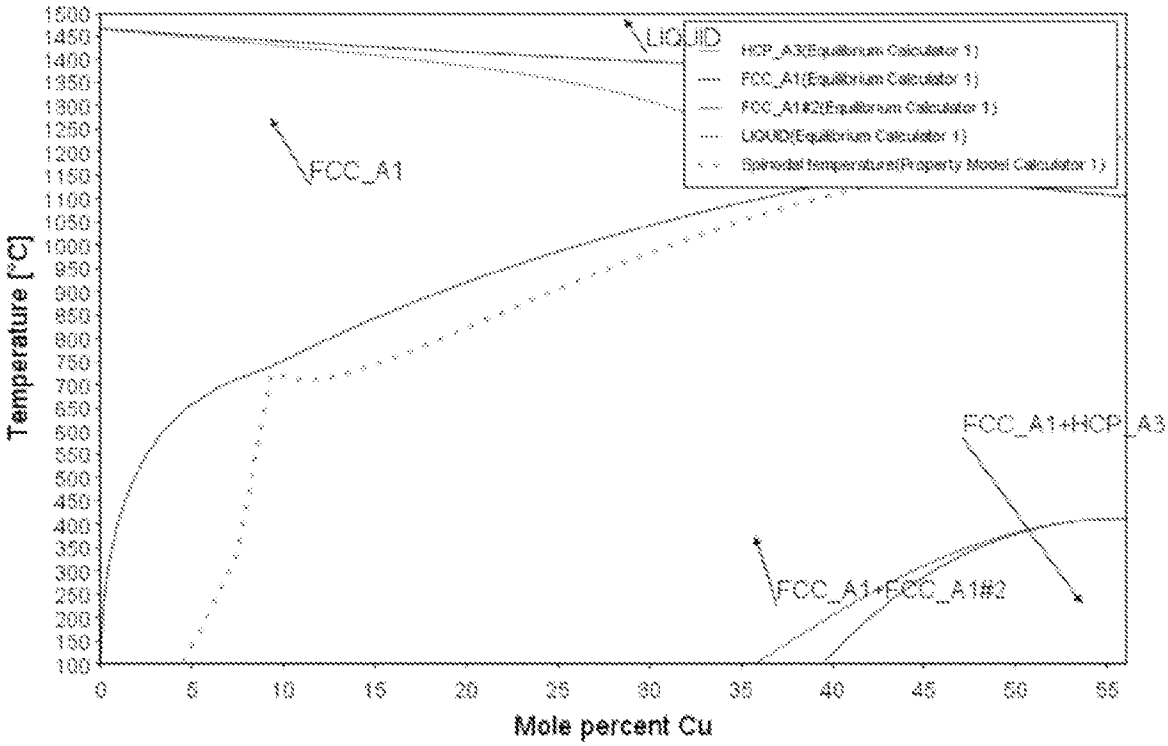
LIQUID
HCP_A3(Equilibrium Calculator 1)
FCC_A1(Equilibrium Calculator 1)
FCC_A1#2(Equilibrium Calculator 1)
LIQUID(Equilibrium Calculator 1)
Spinodal temperature(Property Model Calculator 1)
FCC_A1
FCC_A1+HCP_A3
FCC_A1+FCC_A1#2
Temperature [°C]
Mole percent Cu
1500
1450
1400
1350
1300
1250
1200
1150
1100
1050
1000
950
900
850
800
750
700
650
600
550
500
450
400
350
300
250
200
150
100
0
5
10
15
20
25
30
35
40
45
50
55

FIG. 10C

Ni-V

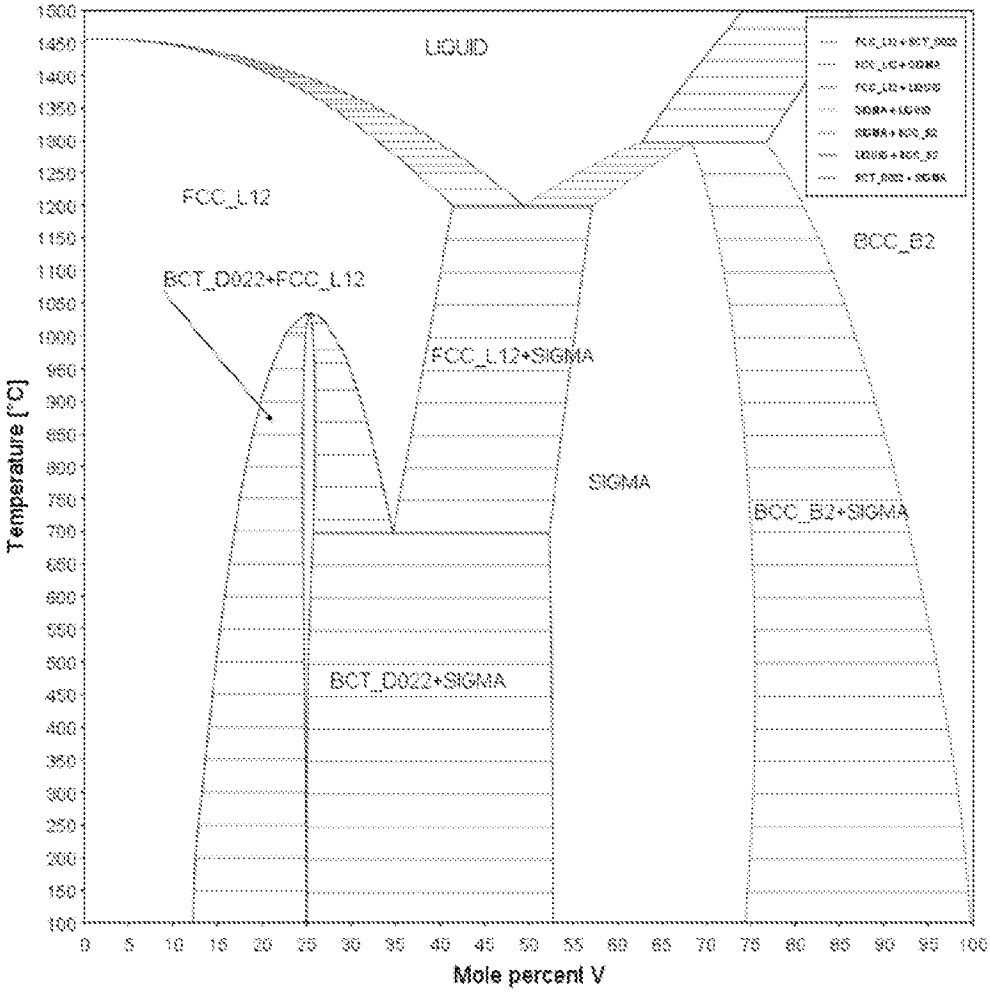
LIQUID
FCC_L12
BCT_D022+FCC_L12
FCC_L12+SIGMA
SIGMA
BCC_B2
BCC_B2+SIGMA
BCT_D022+SIGMA
Temperature [°C]
Mole percent V

FIG. 11A

Cu-V

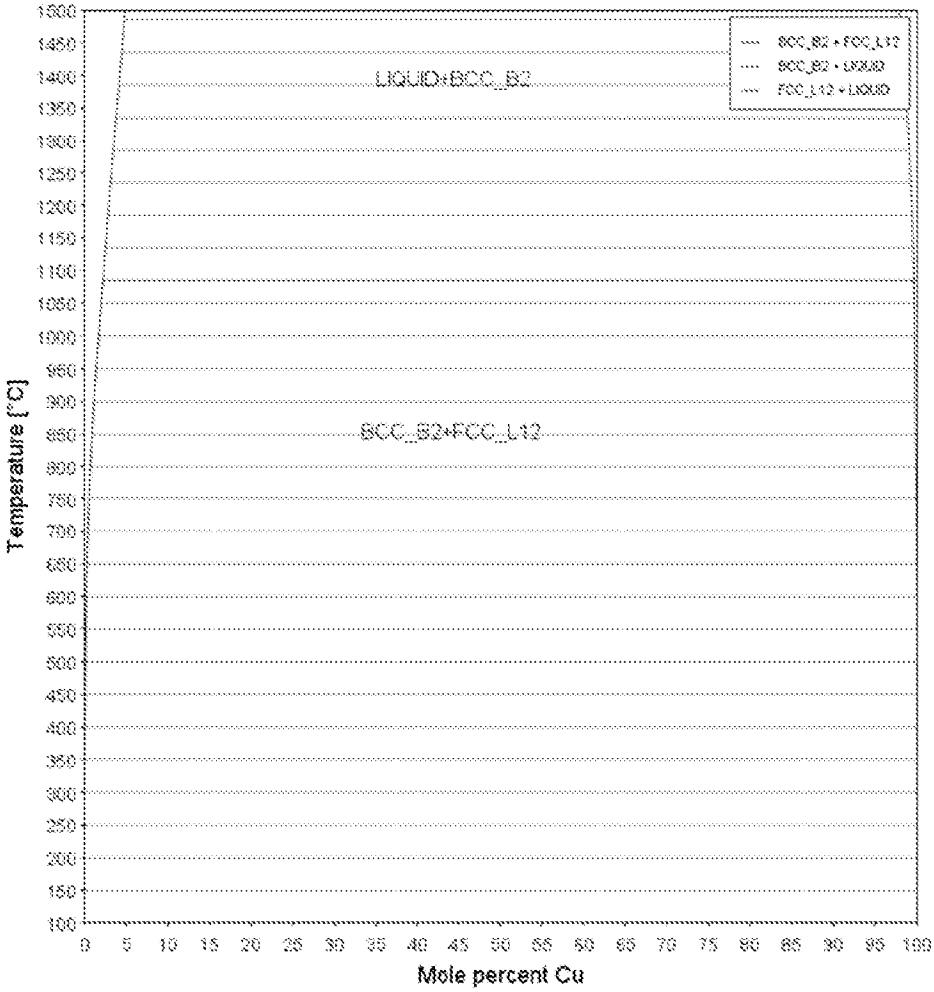

FIG. 11B

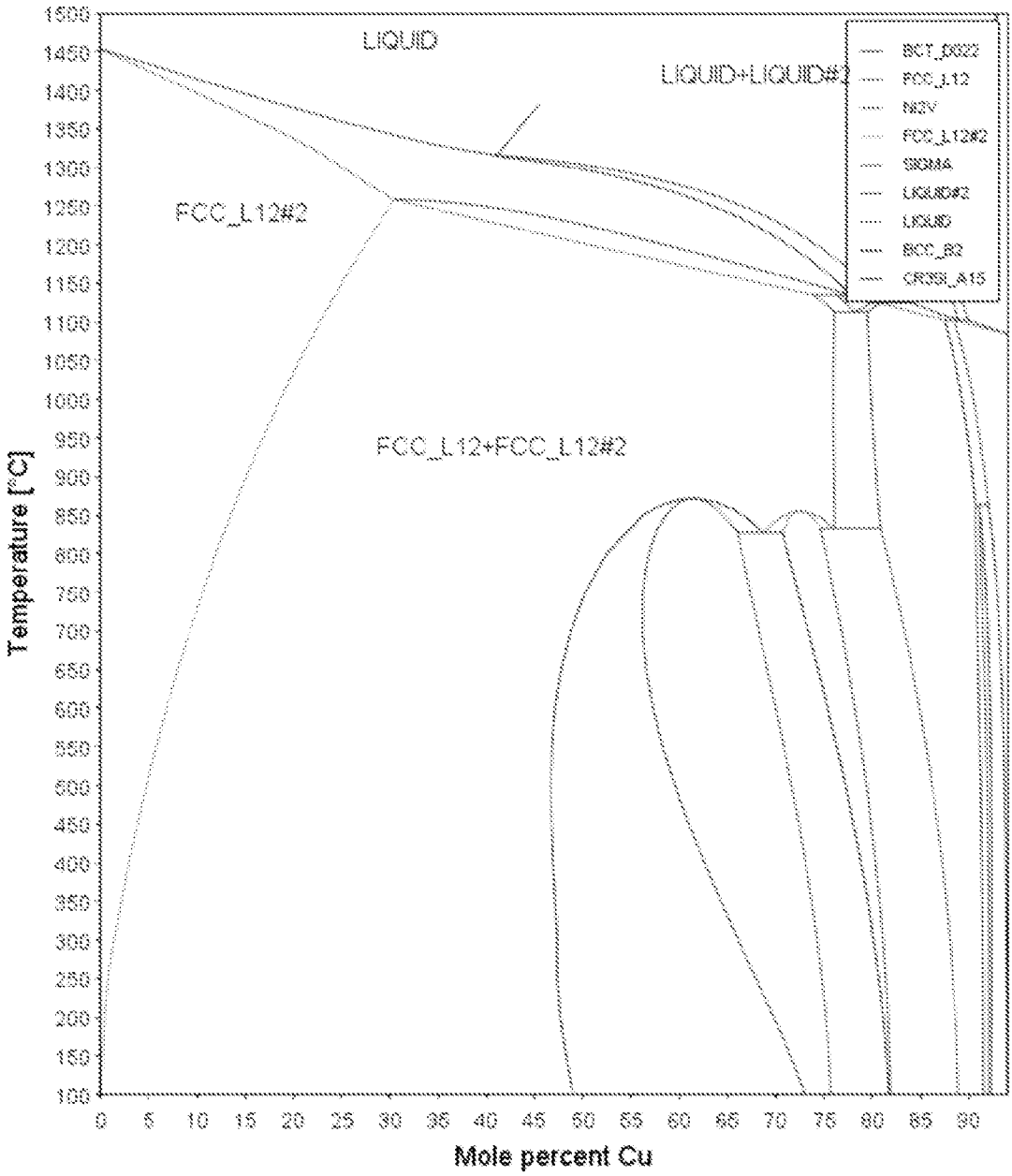
LIQUID
LIQUID+LIQUID#2
FCC_L12#2
FCC_L12+FCC_L12#2
BCT_D022
FCC_L12
N2V
FCC_L12#2
SIGMA
LIQUID#2
LIQUID
BCC_B2
CR3Si_A15
Temperature [°C]
Mole percent Cu
1500
1450
1400
1350
1300
1250
1200
1150
1100
1050
1000
950
900
850
800
750
700
650
600
550
500
450
400
350
300
250
200
150
100
0 5 10 15 20 25 30 35 40 45 50 55 60 65 70 75 80 85 90

FIG. 12A

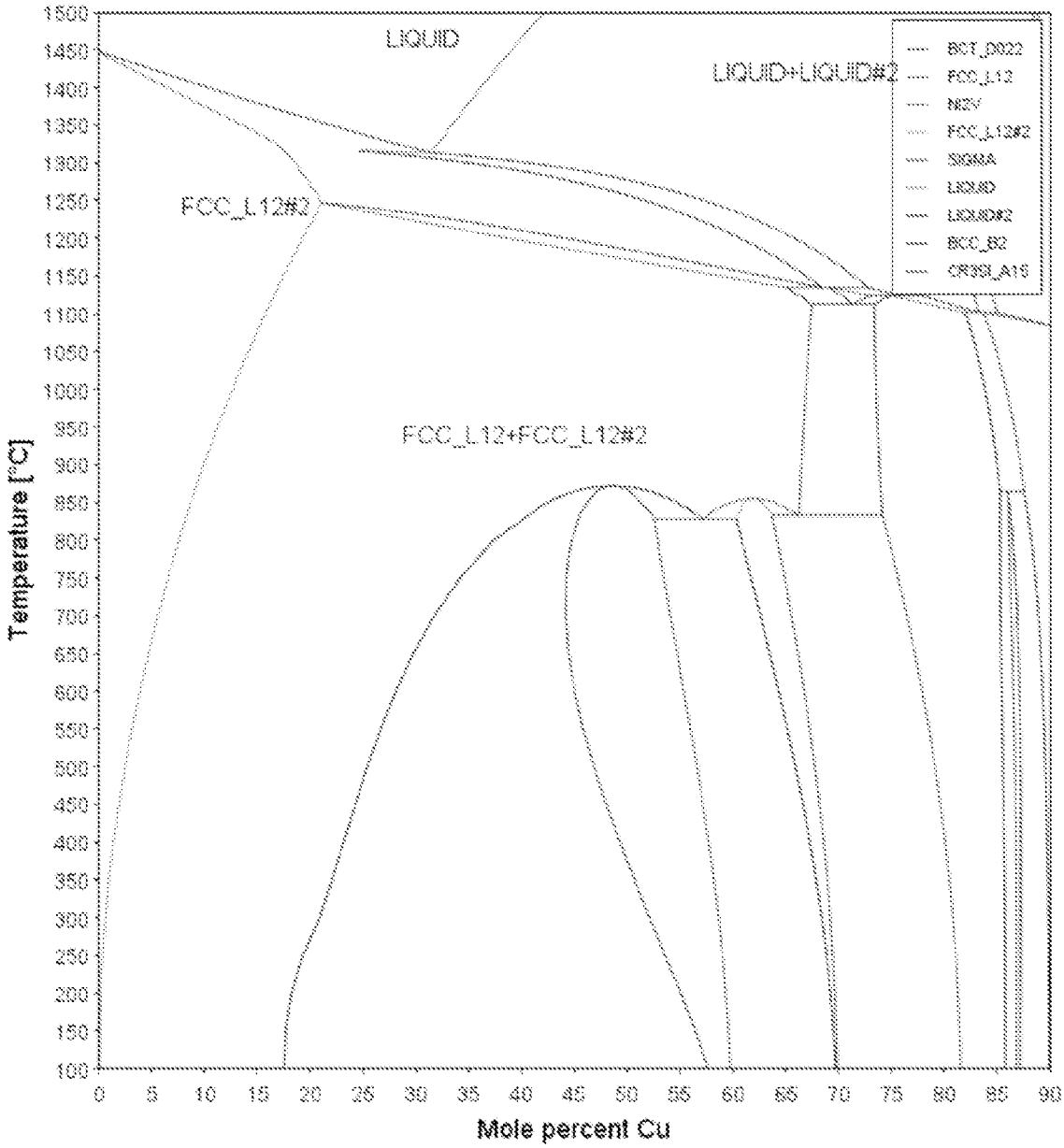
LIQUID
LIQUID+LIQUID#2
FCC_L12#2
FCC_L12+FCC_L12#2
BCT_D022
FCC_L12
NI2V
FCC_L12#2
SIGMA
LIQUID
LIQUID#2
BCC_B2
CR3SI_A15
Temperature [°C]
Mole percent Cu

FIG. 12B

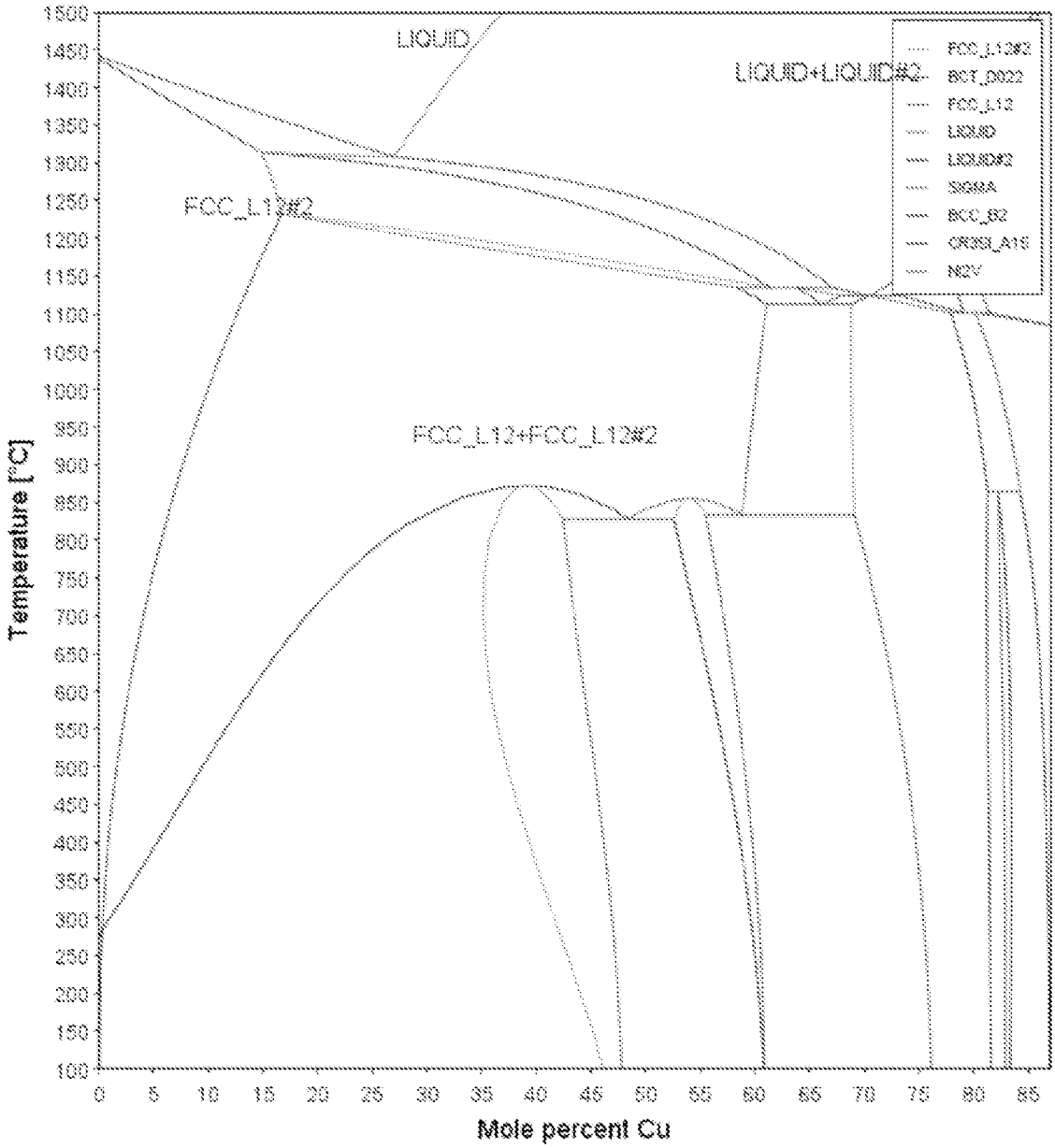
LIQUID
LIQUID+LIQUID#2
FCC_L12#2
FCC_L12+FCC_L12#2
FCC_L12#2
BCT_D022
FCC_L12
LIQUID
LIQUID#2
SIGMA
BCC_B2
CR3SI_A15
NI2V
Temperature [°C]
Mole percent Cu
1500
1450
1400
1350
1300
1250
1200
1150
1100
1050
1000
950
900
850
800
750
700
650
600
550
500
450
400
350
300
250
200
150
100
0
5
10
15
20
25
30
35
40
45
50
55
60
65
70
75
80
85

FIG. 12C

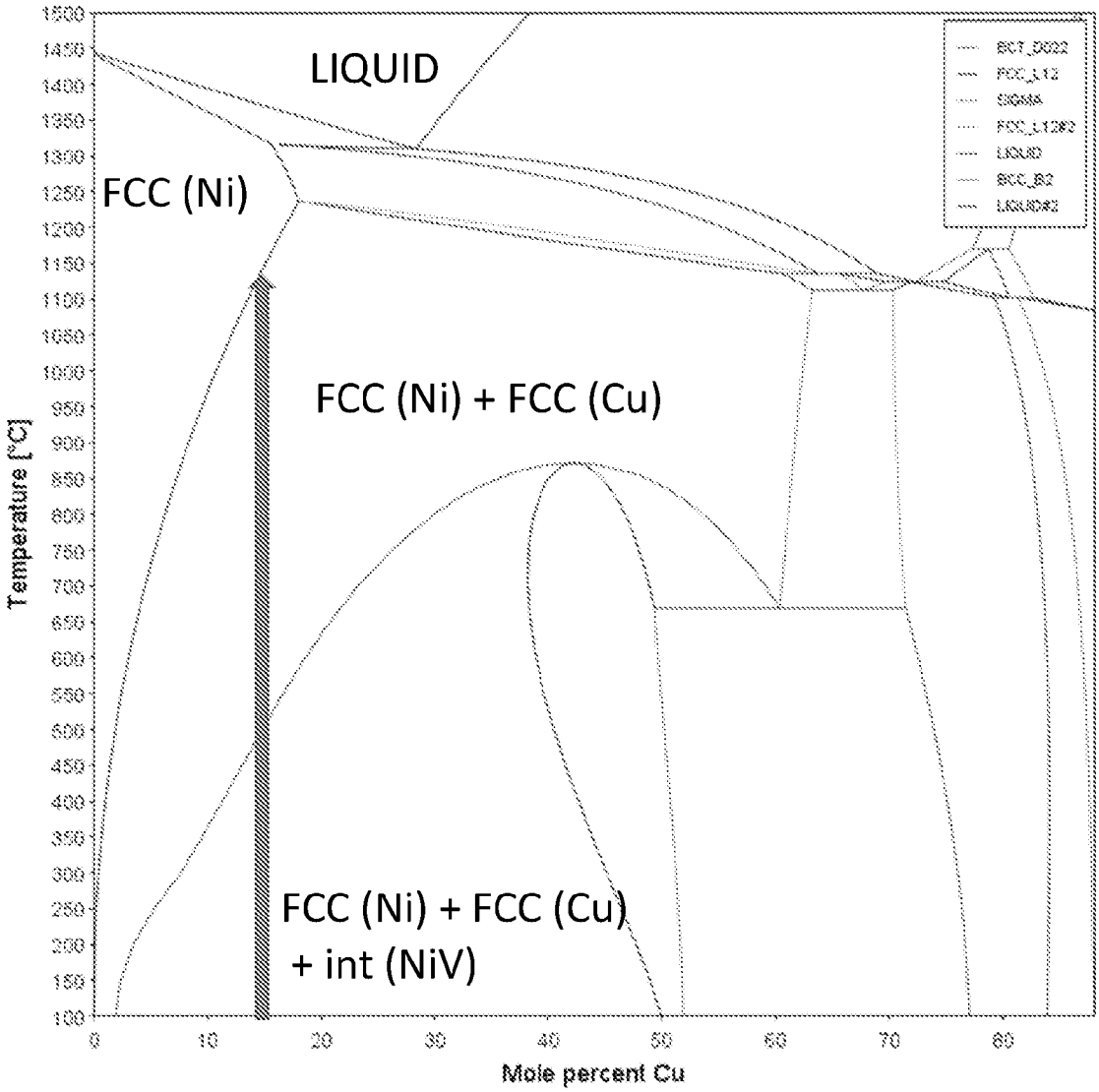
LIQUID
FCC (Ni)
FCC (Ni) + FCC (Cu)
FCC (Ni) + FCC (Cu)
+ int (NiV)
Temperature [°C]
Mole percent Cu
1500
1450
1400
1350
1300
1250
1200
1150
1100
1050
1000
950
900
850
800
750
700
650
600
550
500
450
400
350
300
250
200
150
100
0
10
20
30
40
50
60
70
80

FIG. 12D

Stable Phases

	Moles	Mass	Volume Fraction
FCC_L12#1	0.18028	11.24504	0.18678

Composition

Component	Mole Fraction	Mass Fraction
Cu	0.75878	0.77304
Ni	0.24119	0.22695
V	0.00002	0.00002

	Moles	Mass	Volume Fraction
FCC_L12#2	0.81972	47.25382	0.81322

Composition

Component	Mole Fraction	Mass Fraction
Ni	0.83491	0.85002
V	0.14639	0.12936
Cu	0.01871	0.02062

FIG. 12E

Densification rate, $\frac{d\rho}{dt}$, $\frac{1}{s}$
0.00007
0.00006
0.00005
0.00004
0.00003
0.00002
0.00001
0
-0.00001
-0.00002
0
400
600
800
1000
1200
T, C

FIG. 12F

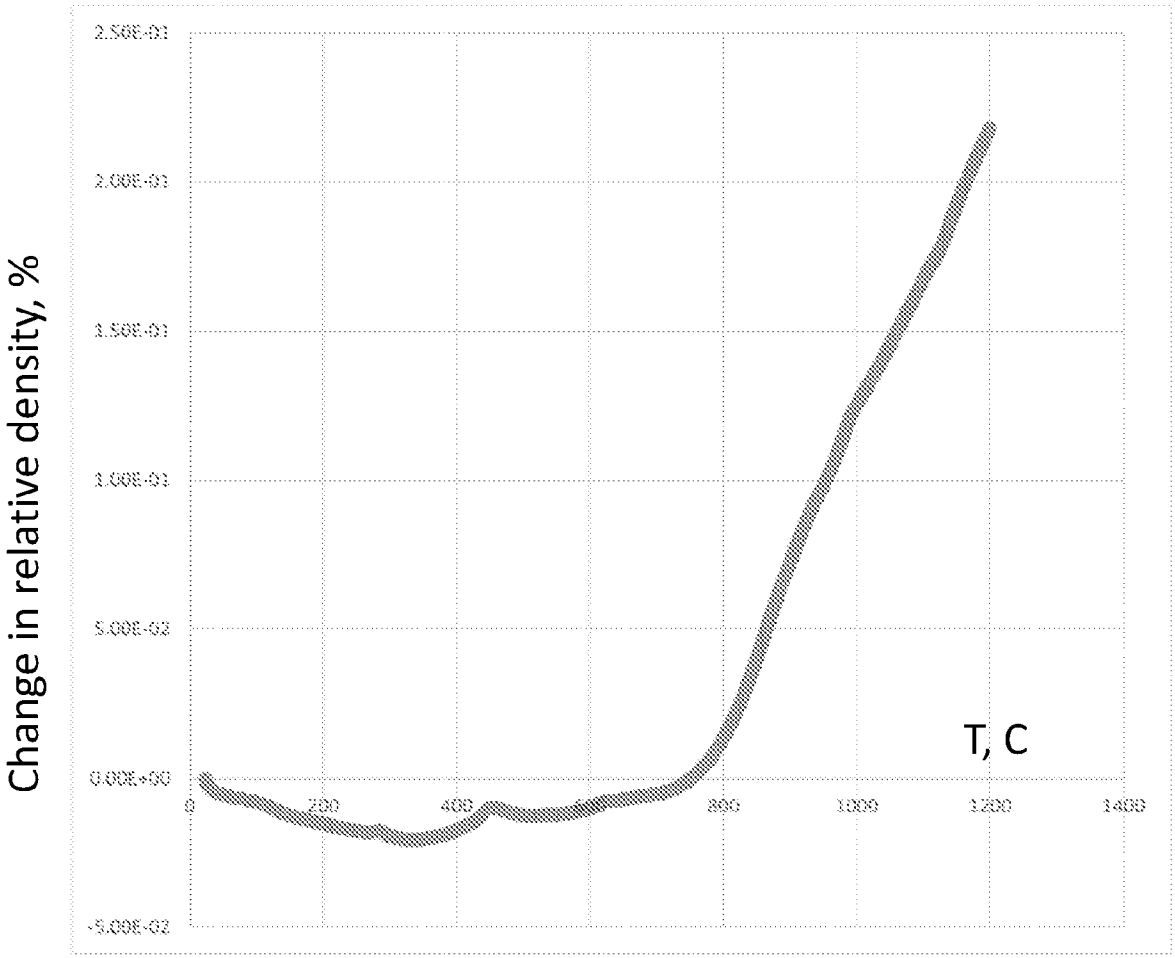
Change in relative density, %
2.50E-01
2.00E-01
1.50E-01
1.00E-01
5.00E-02
0.00E+00
-5.00E-02
0
200
400
600
800
1000
1200
1400
T, C

FIG. 12G

Solute	D_0	Q		T range
Cu	1.5 x 10^-4	258.3		
		257		
		255.5		
	7.24 x 10^-5	250.1		850° to 1050°C
	2.7 x 10^-5	250.1		775-1050C
	5 x 10^-5	231.7		700--1000C
Fe	1 x 10-5	269.4		1200 to 1400C
		252.9		
	4.05 x 10^-5	254.9	in 50:50 Ni-Fe	810 - 1110 °C
	4.8 x 10^-5	256.3		970.5°C to 1200°C
	8 x 10^-5	254.4		900 to 1150C
	3.8 x 10^-5	255.4	in 50:50 Ni-Fe	1000 to 1426C
Cr		272.6		
	1.1 x 10^-4	272-278		1100-1268 C
	1.9x 10^-4	277.6		
	2x 10^-4	270.6		
V		278.4		
	8.7 x 10^-5	272.7		800-1300
Ni	9.2 x 10^-5	276.5		540-920
		273.9		
		284		

FIG. 13

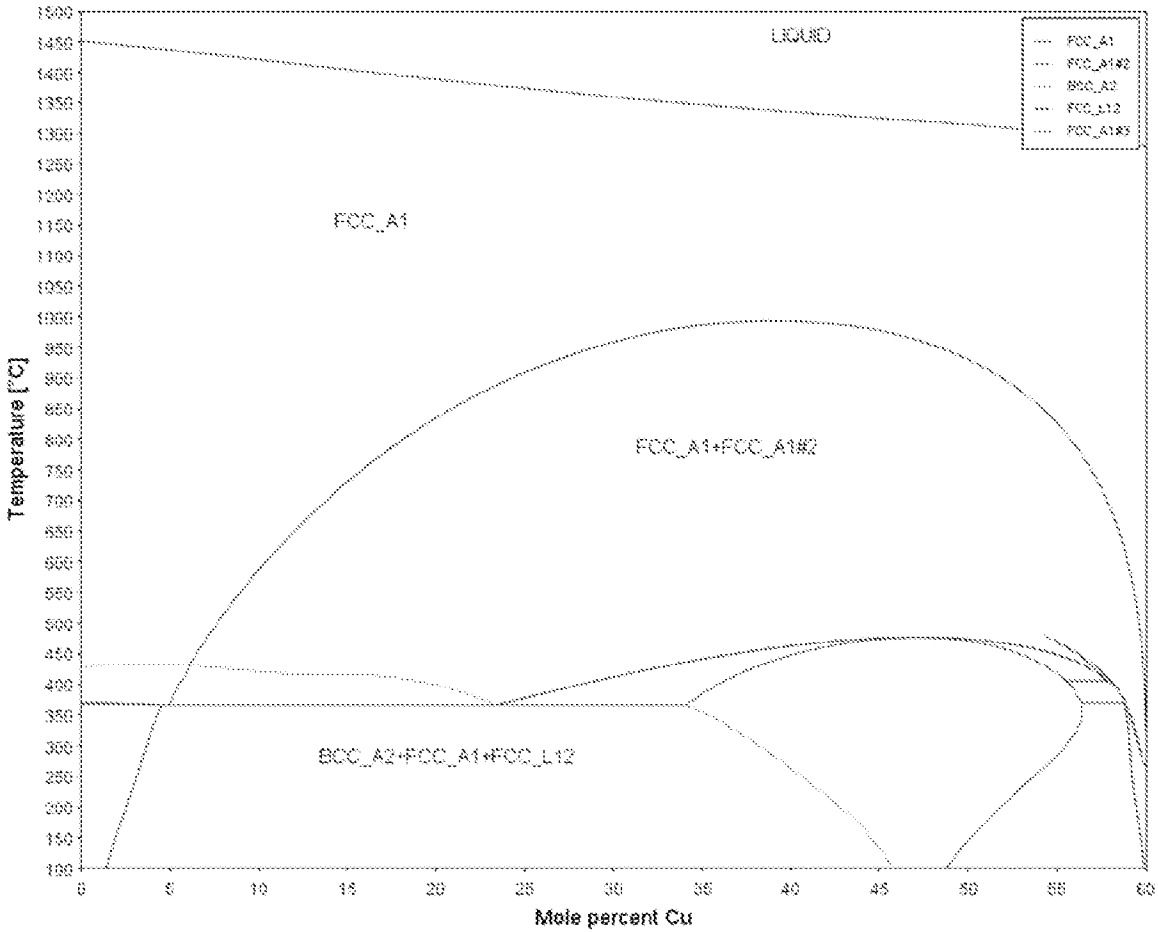
LIQUID
FCC_A1
FCC_A1#2
BCC_A2
FCC_L12
FCC_A1#3
FCC_A1
FCC_A1+FCC_A1#2
BCC_A2+FCC_A1+FCC_L12
Temperature [°C]
Mole percent Cu

FIG. 14A

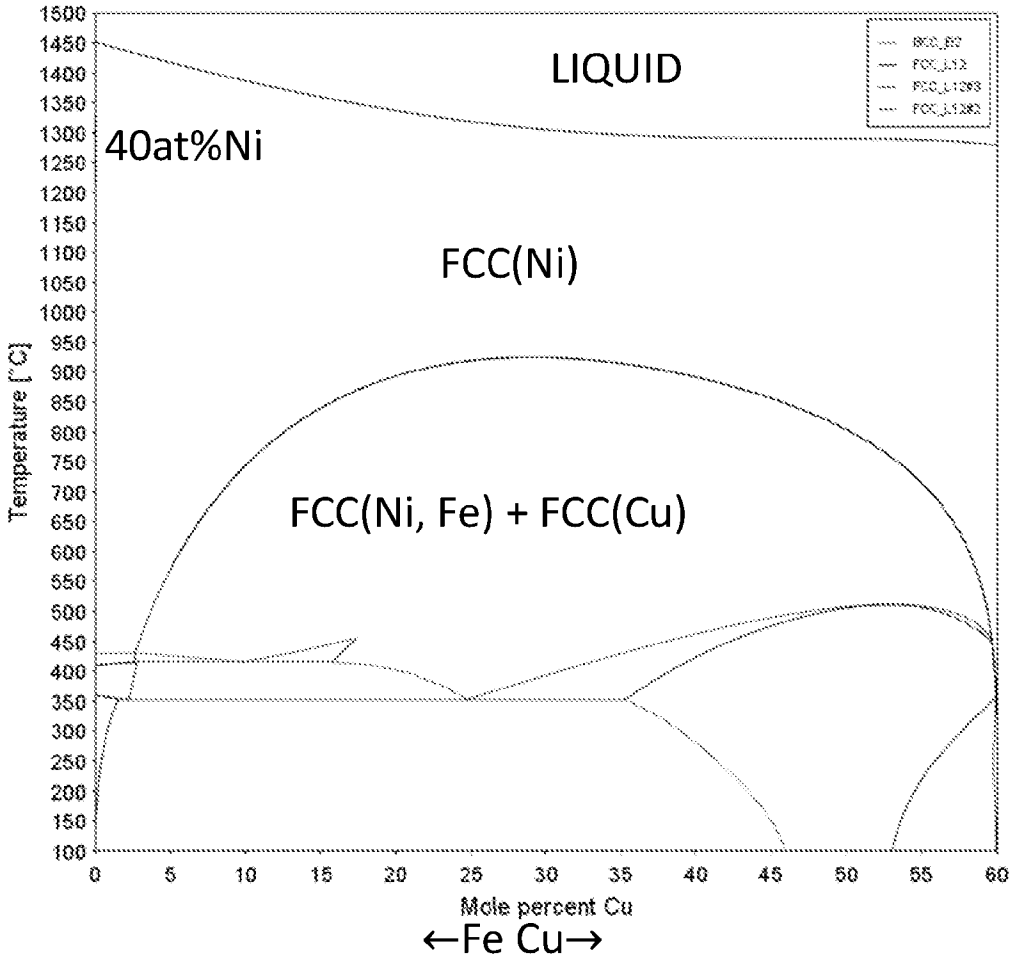
LIQUID
40at%Ni
FCC(Ni)
FCC(Ni, Fe) + FCC(Cu)
Temperature [°C]
Mole percent Cu
←Fe Cu→

FIG. 14B

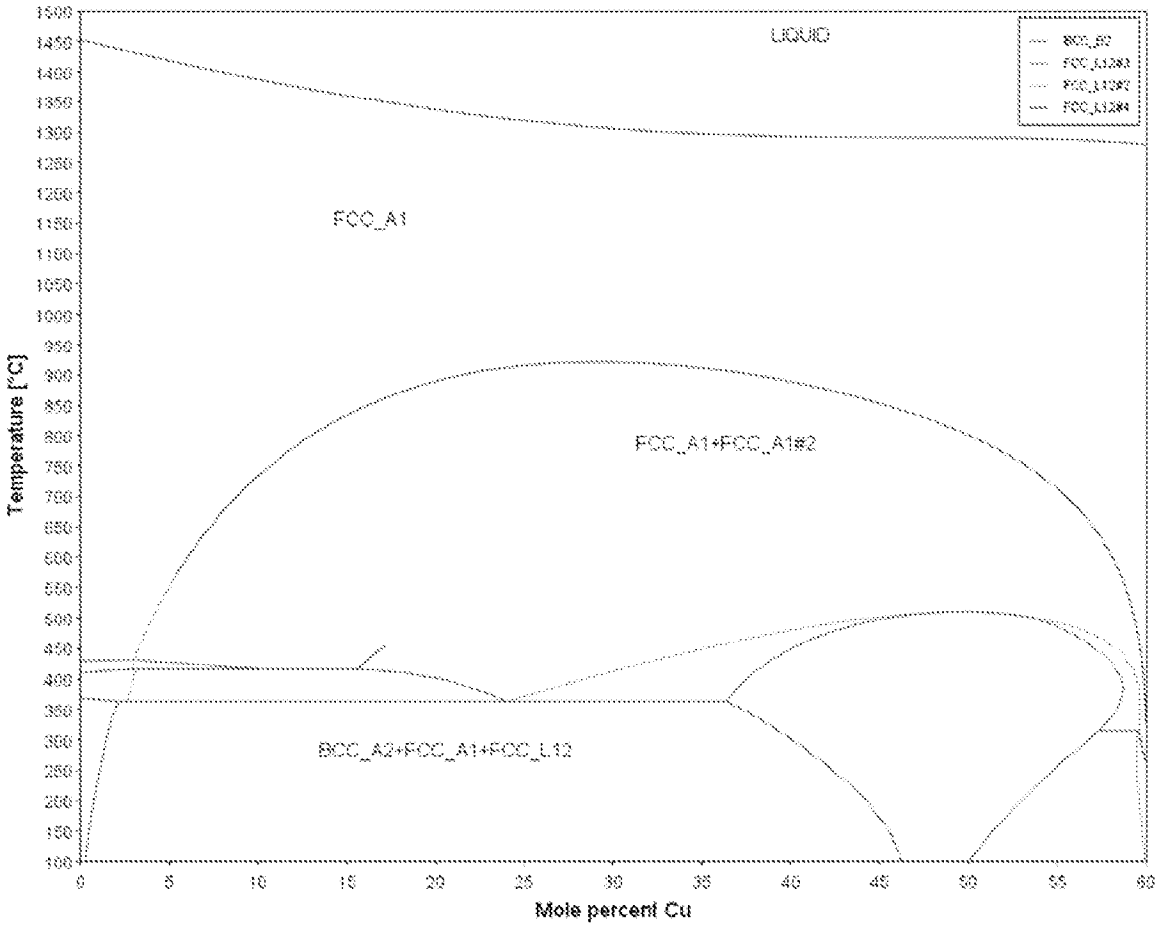
LIQUID
FCC_A1
FCC_A1+FCC_A1#2
BCC_A2+FCC_A1+FCC_L12
Temperature [°C]
Mole percent Cu

FIG. 14C

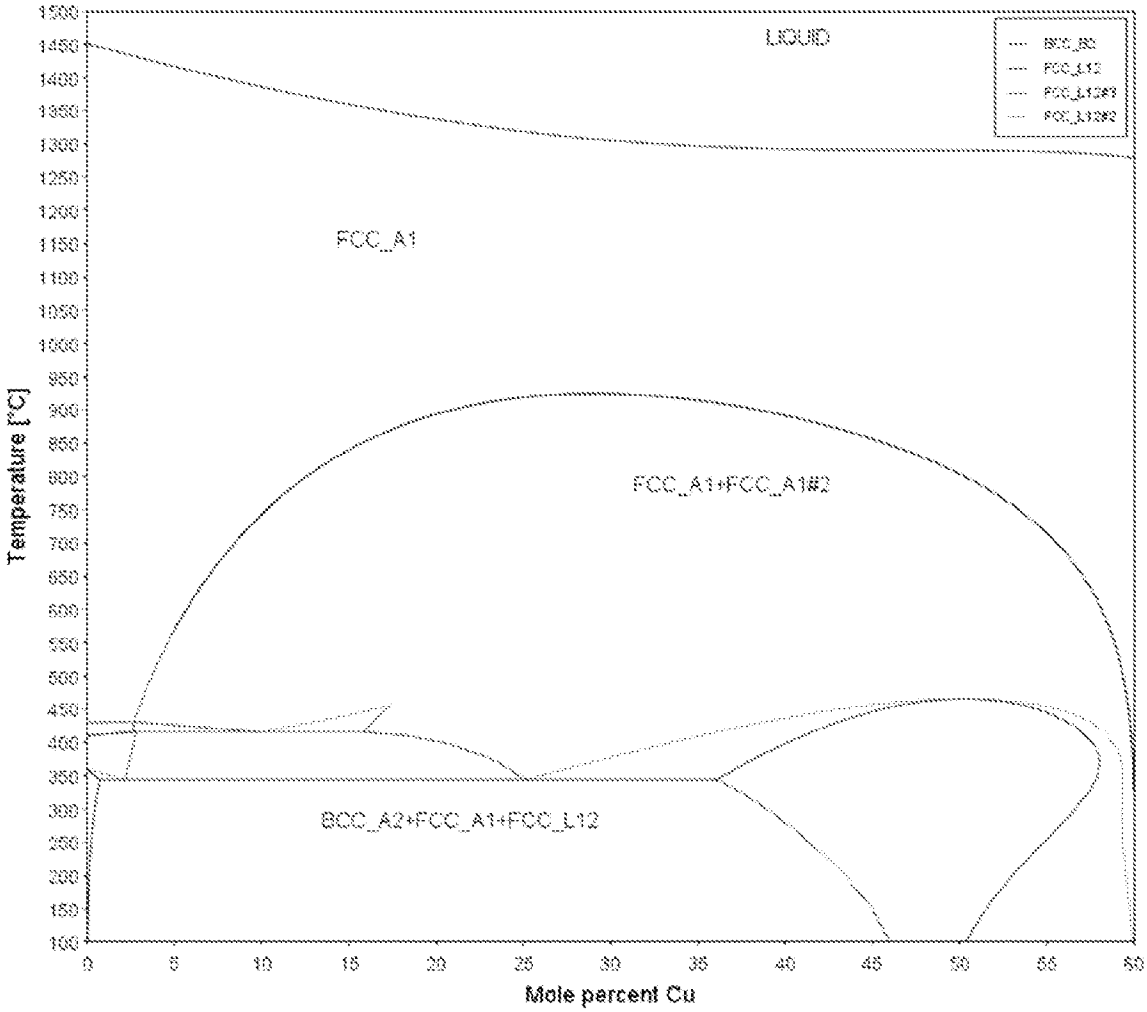
LIQUID
FCC_A1
FCC_A1#2
FCC_A1+FCC_A1#2
BCC_A2+FCC_A1+FCC_L12
Temperature [°C]
Mole percent Cu

FIG. 14D

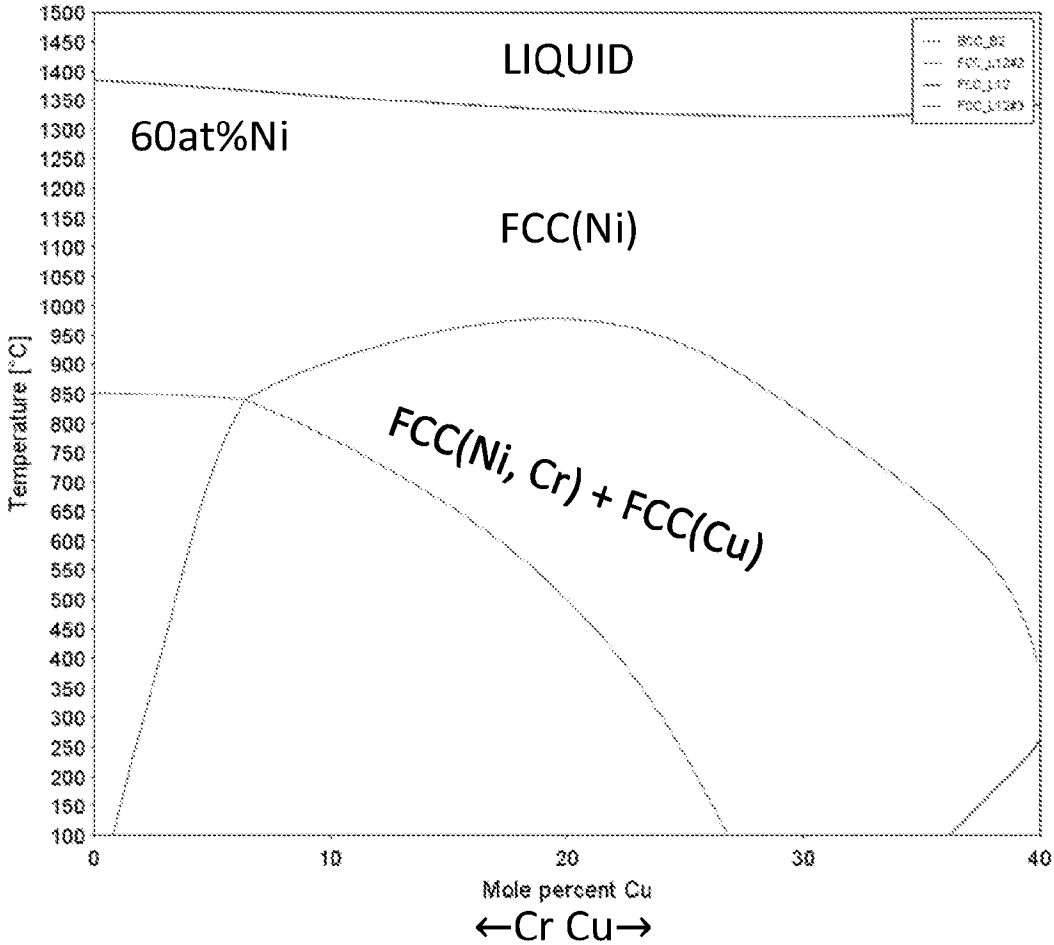
LIQUID
60at%Ni
FCC(Ni)
FCC(Ni, Cr) + FCC(Cu)
Temperature [°C]
1500
1450
1400
1350
1300
1250
1200
1150
1100
1050
1000
950
900
850
800
750
700
650
600
550
500
450
400
350
300
250
200
150
100
0
10
20
30
40
Mole percent Cu
←Cr Cu→

FIG. 15

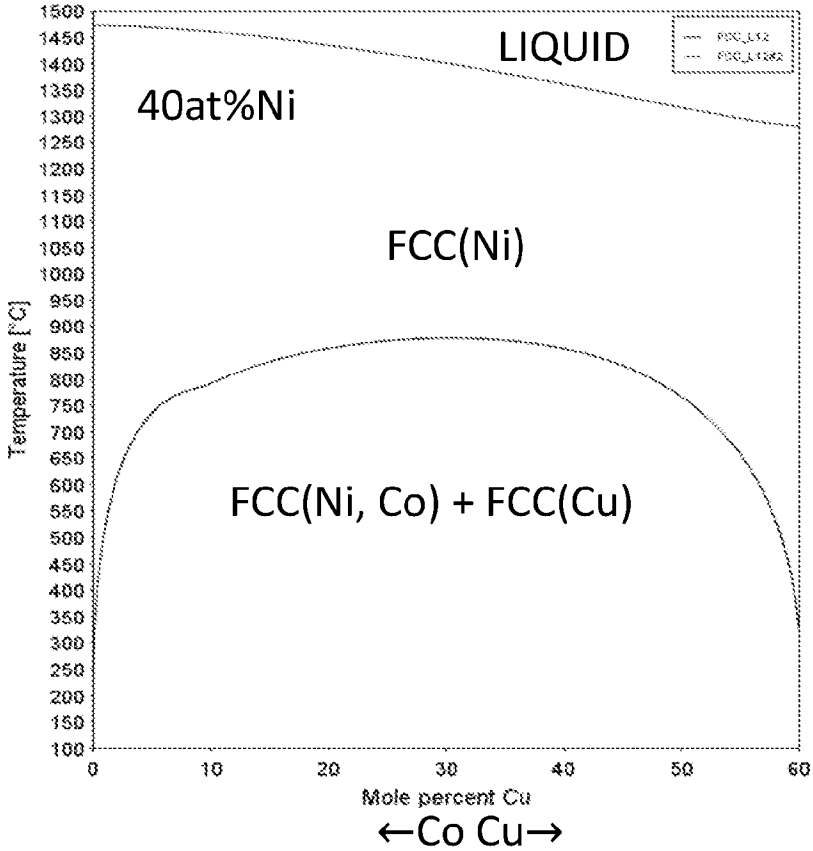
LIQUID
40at%Ni
FCC(Ni)
FCC(Ni, Co) + FCC(Cu)
Temperature [°C]
Mole percent Cu
←Co Cu→

FIG. 16

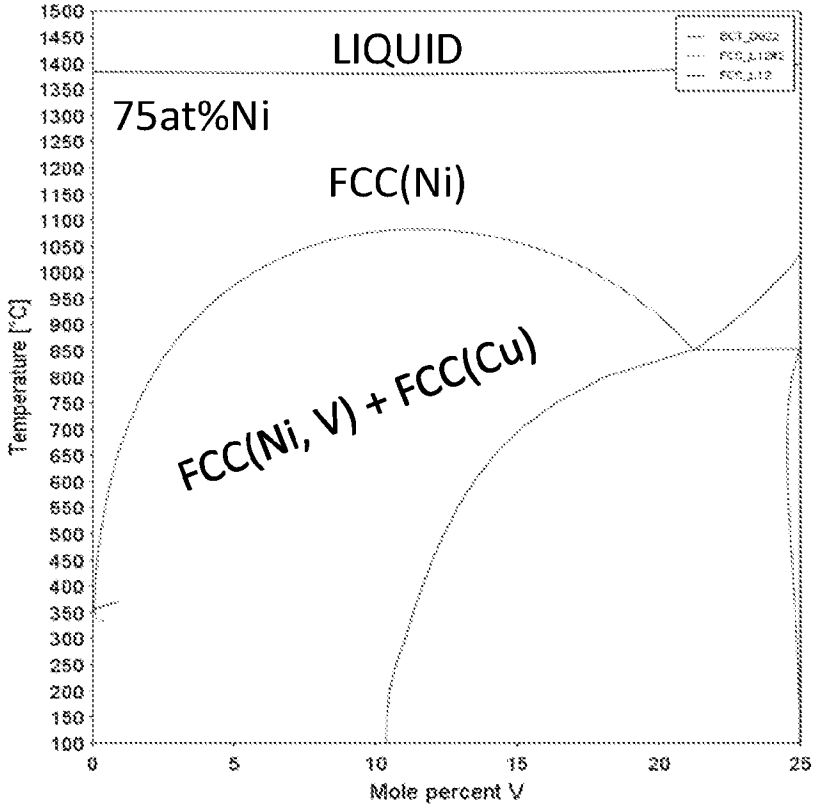
LIQUID
75at%Ni
FCC(Ni)
FCC(Ni, V) + FCC(Cu)
Temperature [°C]
Mole percent V
1500
1450
1400
1350
1300
1250
1200
1150
1100
1050
1000
950
900
850
800
750
700
650
600
550
500
450
400
350
300
250
200
150
100
0
5
10
15
20
25

←Cu V→

FIG. 17

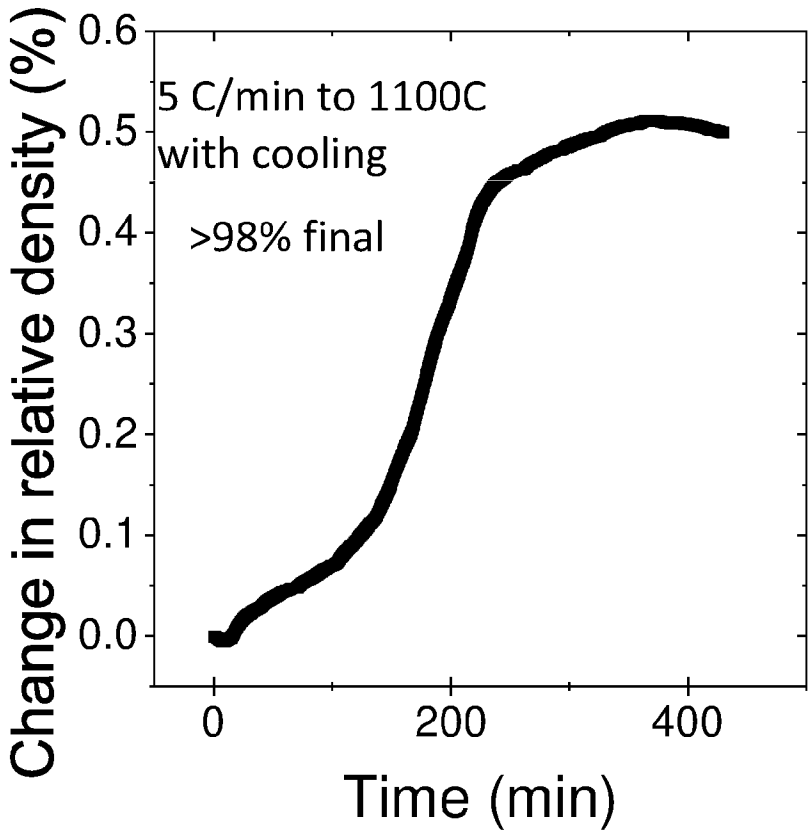
5 C/min to 1100C
with cooling
>98% final
Change in relative density (%)
0.6
0.5
0.4
0.3
0.2
0.1
0.0
0
200
400
Time (min)

FIG. 18A

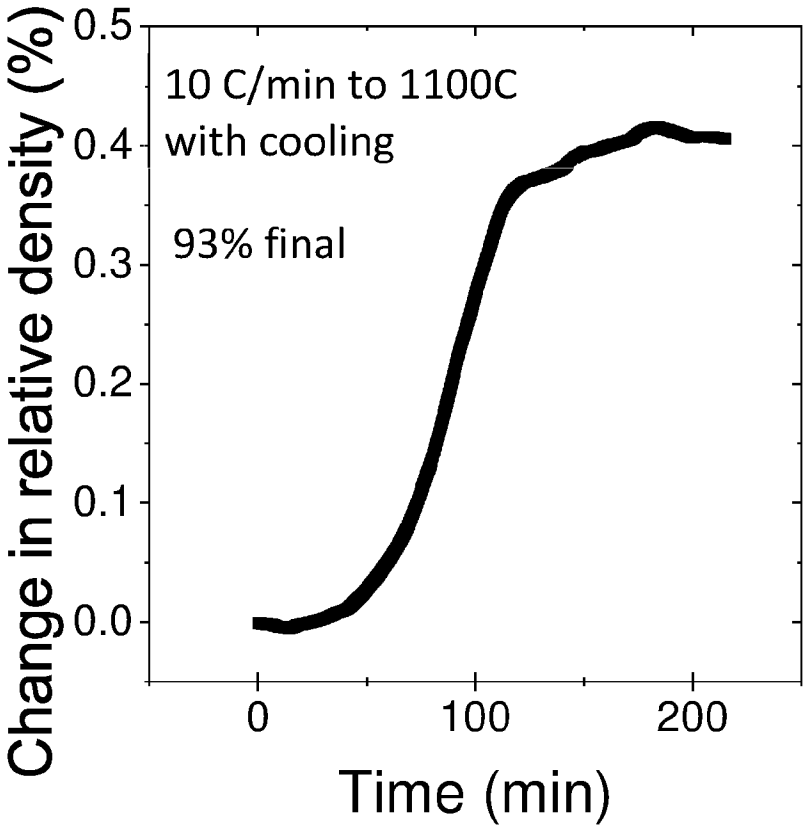
10 C/min to 1100C
with cooling
93% final
Change in relative density (%)
0.5
0.4
0.3
0.2
0.1
0.0
0
100
200
Time (min)

FIG. 18B

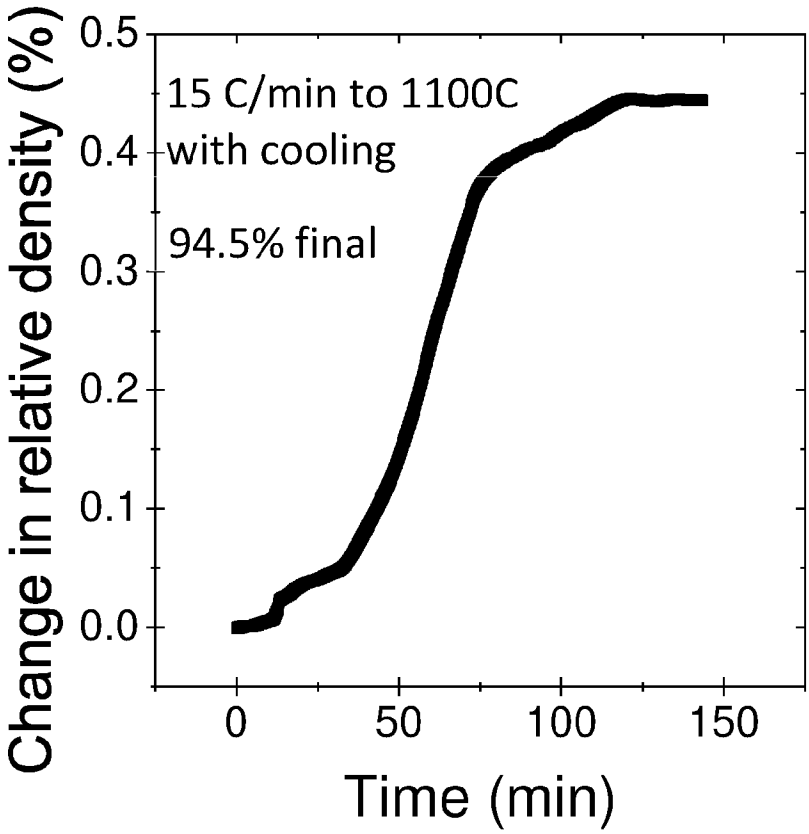
15 C/min to 1100C
with cooling
94.5% final
Change in relative density (%)
0.5
0.4
0.3
0.2
0.1
0.0
0
50
100
150
Time (min)

FIG. 18C

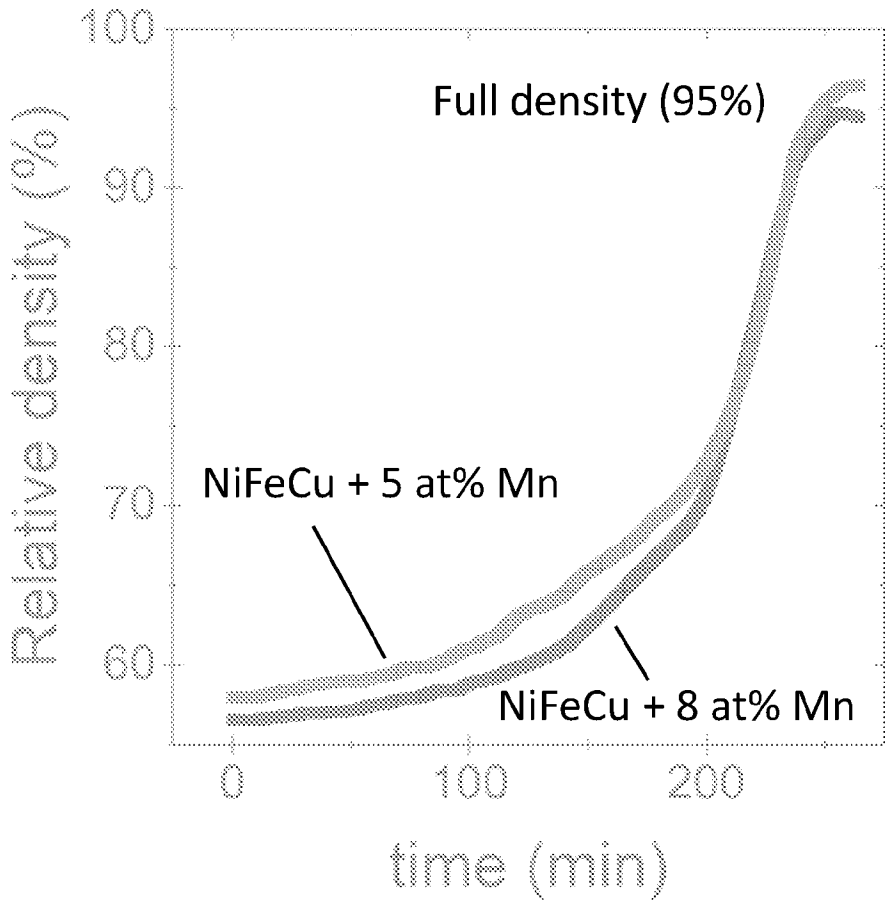
Full density (95%)
NiFeCu + 5 at% Mn
NiFeCu + 8 at% Mn
Relative density (%)
100
90
80
70
60
0
100
200
time (min)

FIG. 19

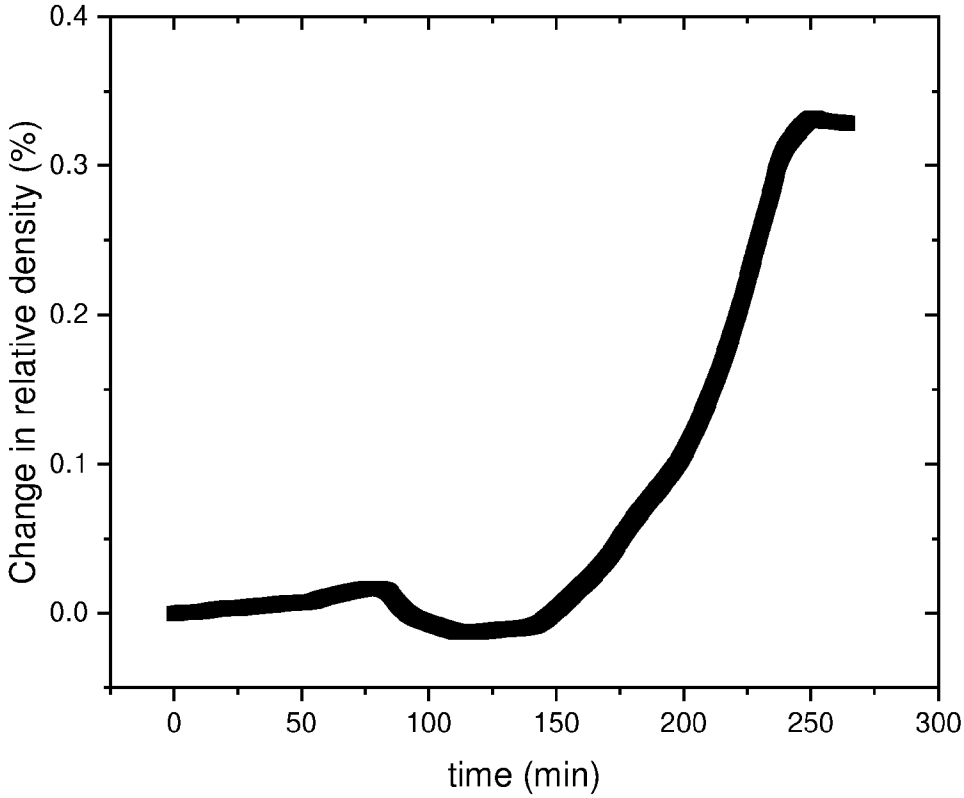
0.4
0.3
0.2
0.1
0.0
Change in relative density (%)
0
50
100
150
200
250
300
time (min)

FIG. 20

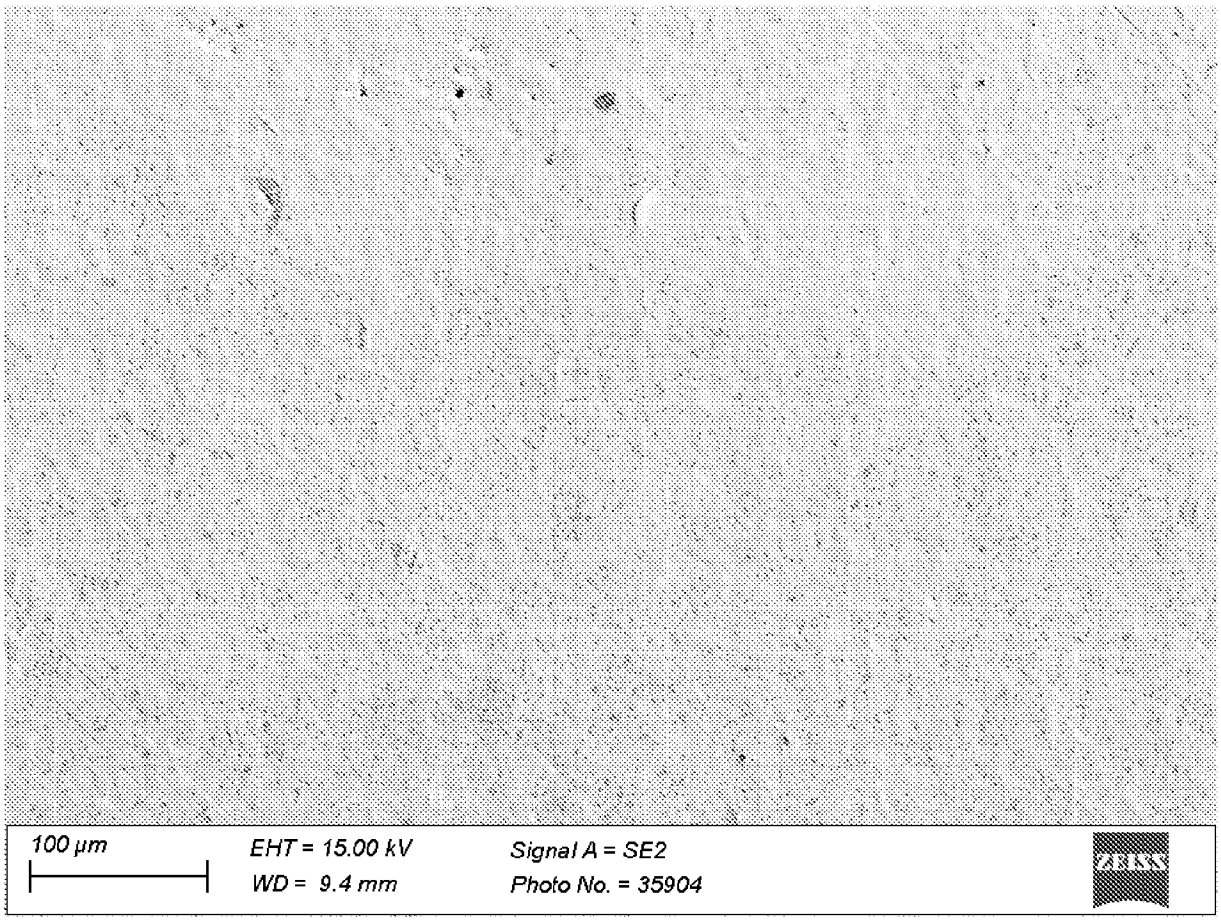

FIG. 21

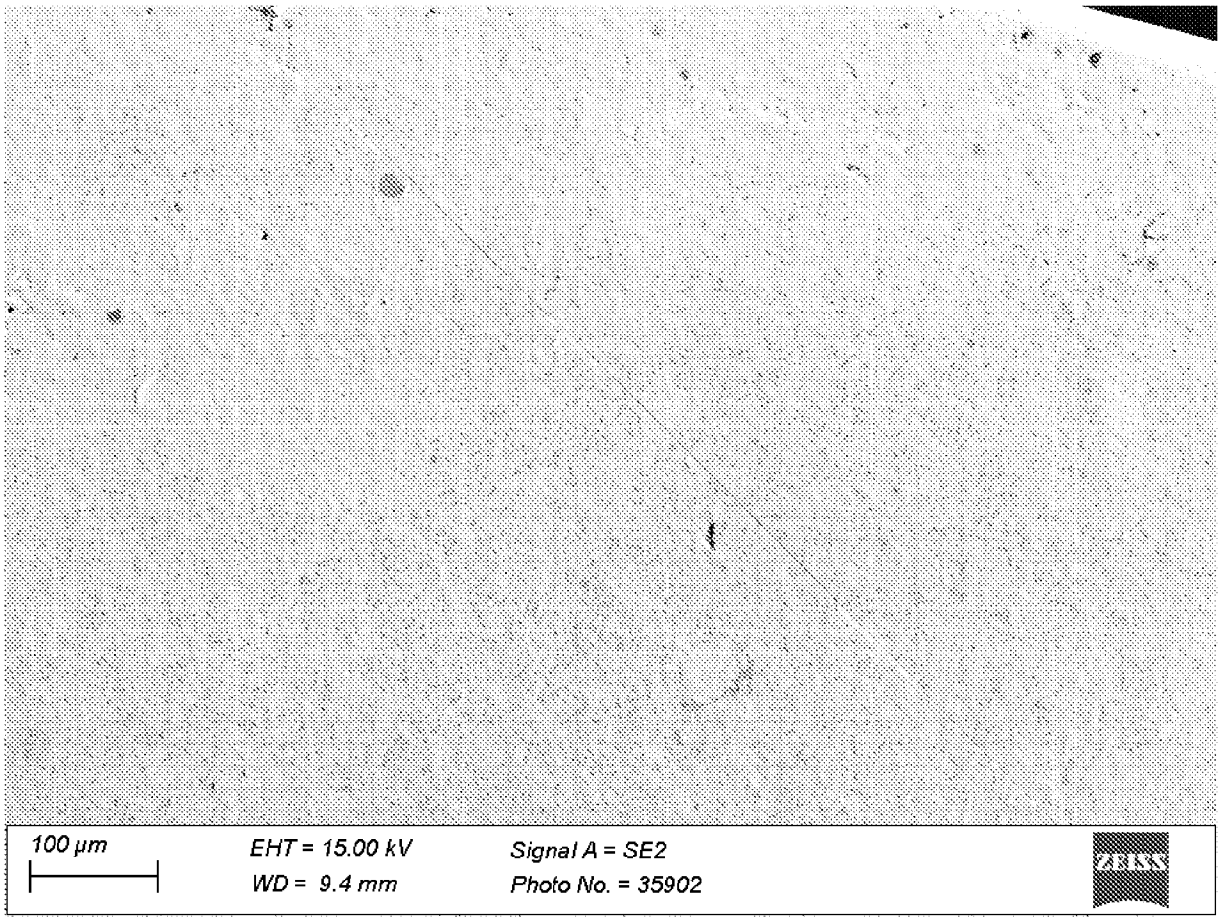

FIG. 22

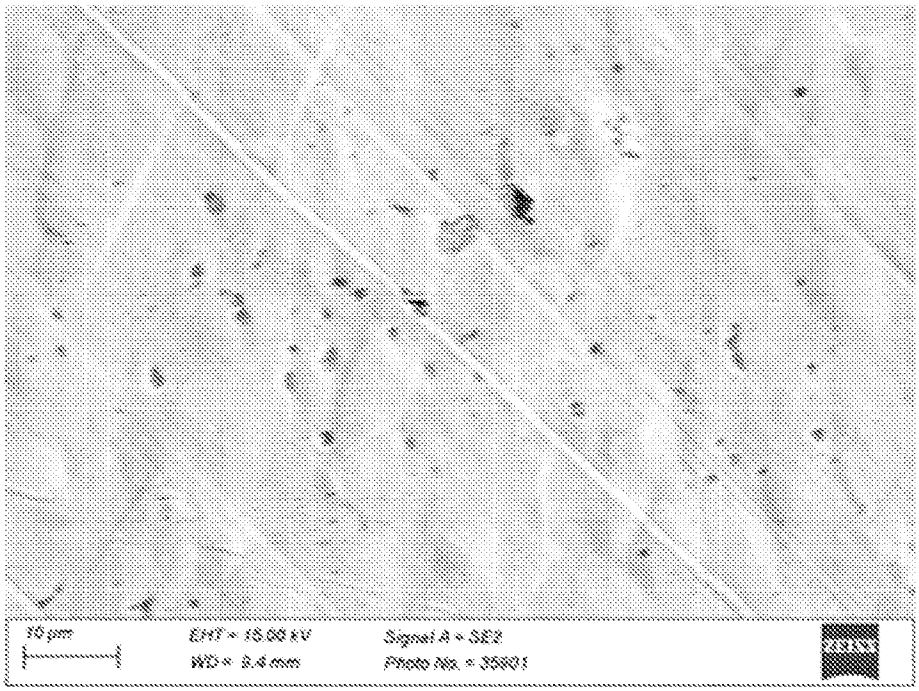
10 µm
EHT = 15.00 kV
WD = 9.4 mm
Signal A = SE2
Photo No. = 35001

FIG. 23

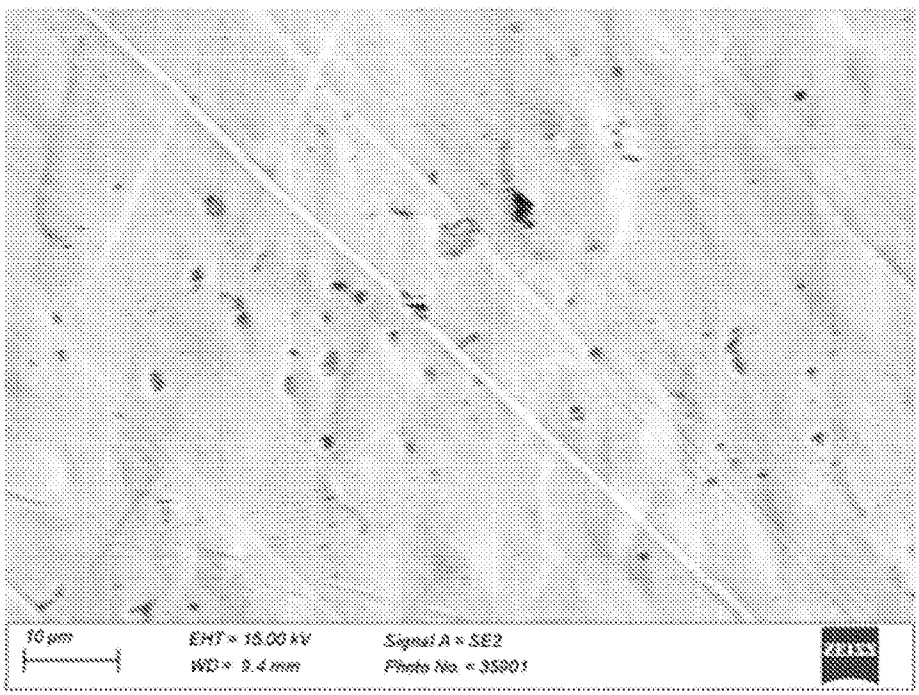
10 µm
EHT = 15.00 kV
WD = 9.4 mm
Signal A = SE2
Photo No. = 35001

FIG. 24

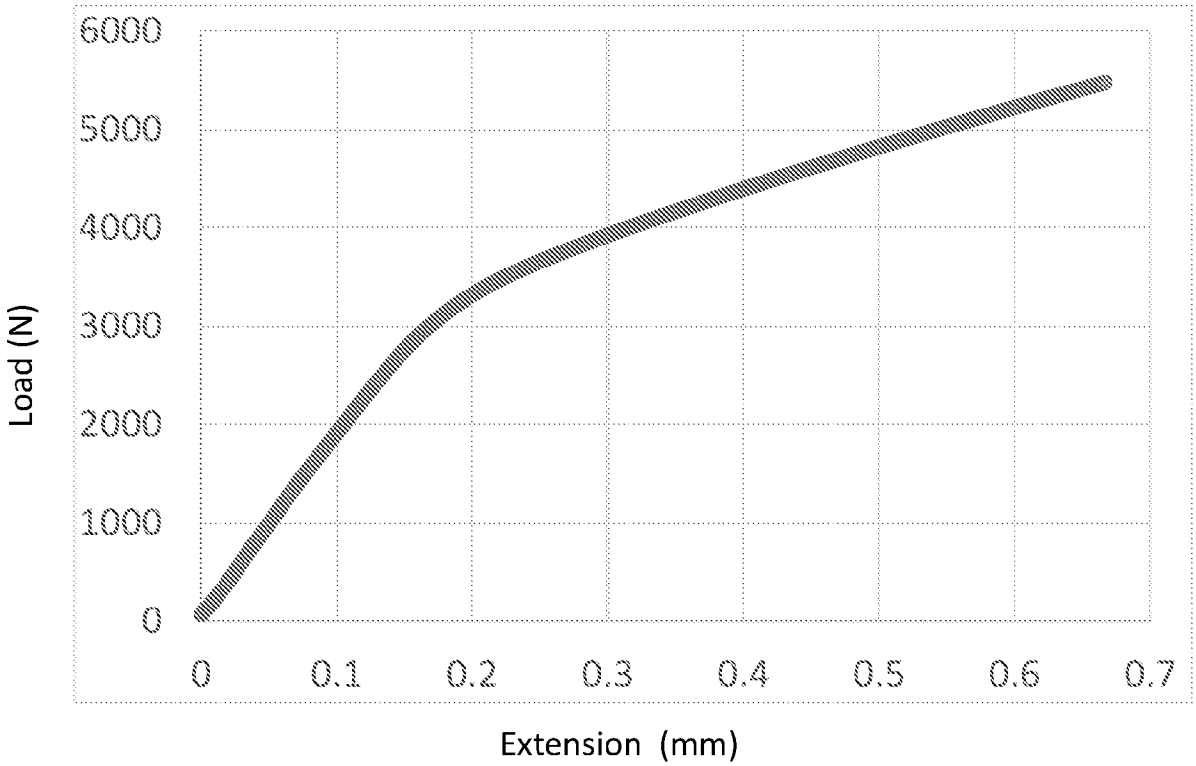
6000
5000
4000
3000
2000
1000
0
Load (N)
0
0.1
0.2
0.3
0.4
0.5
0.6
0.7
Extension (mm)

FIG. 25

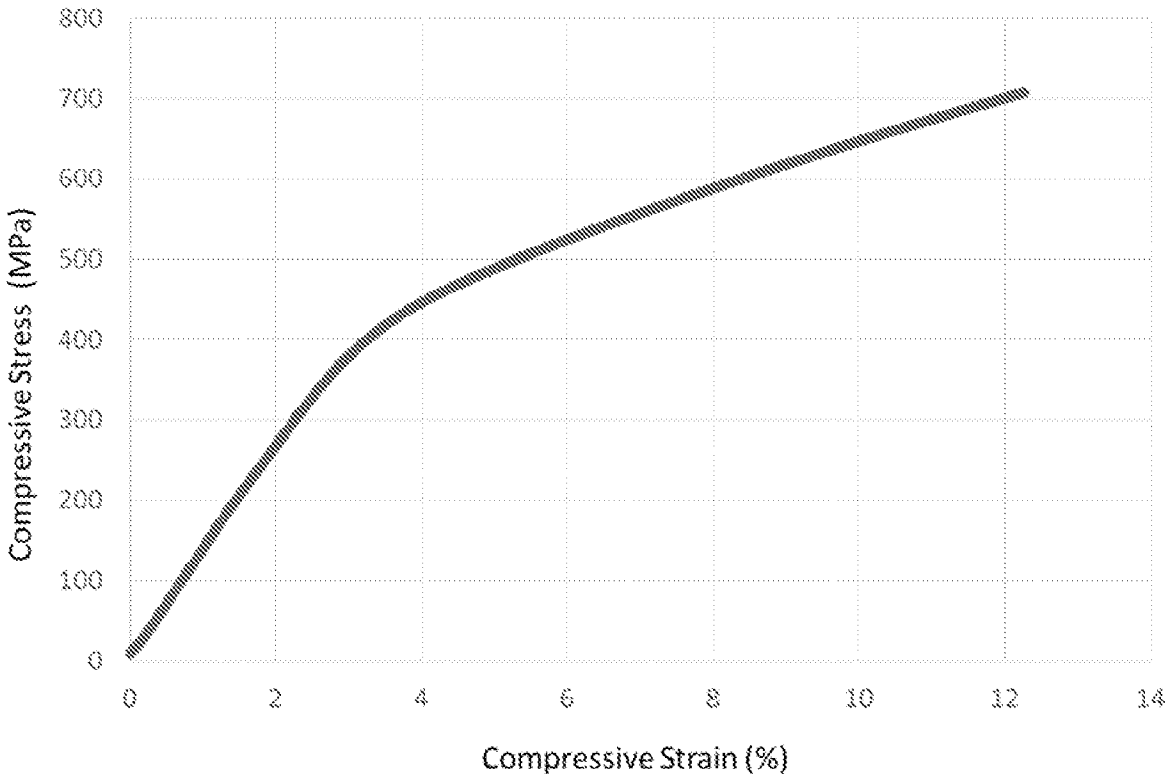
800
700
600
500
400
300
200
100
0
Compressive Stress (MPa)
0
2
4
6
8
10
12
14
Compressive Strain (%)

FIG. 26

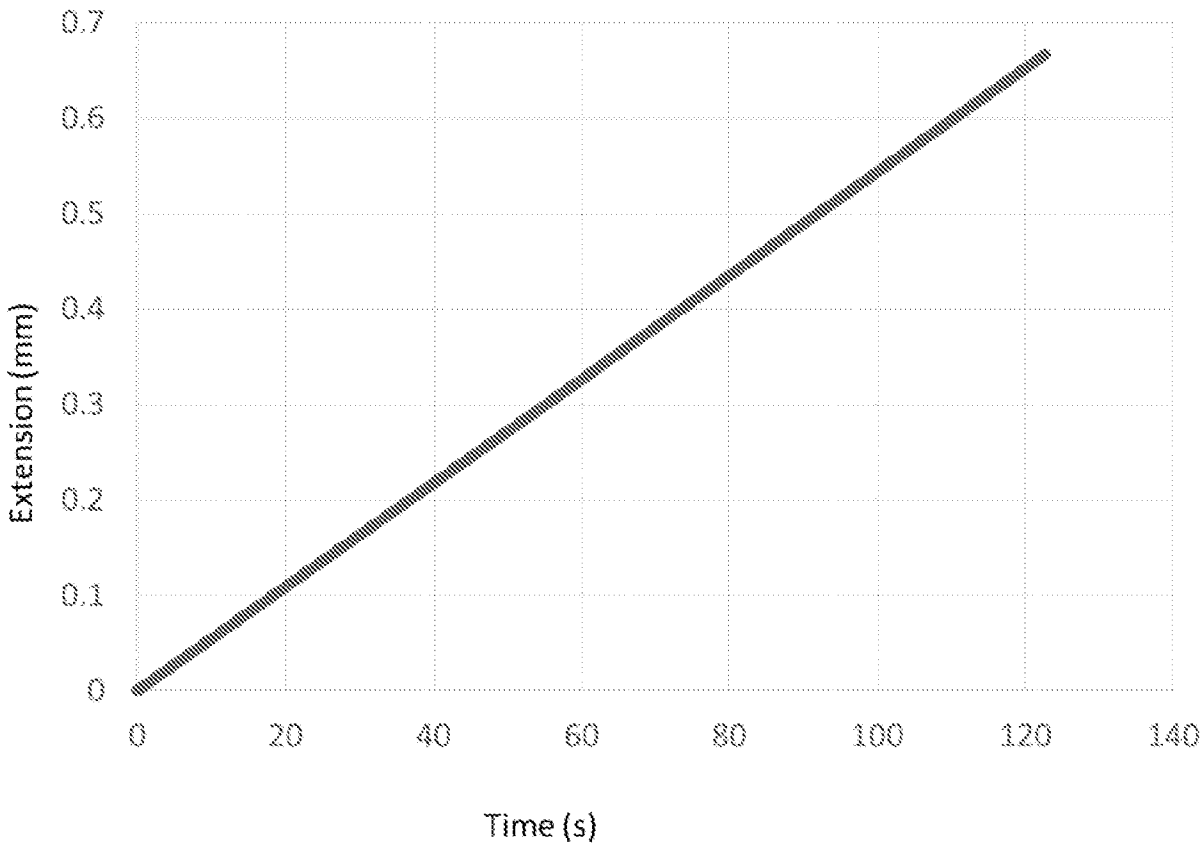

FIG. 27

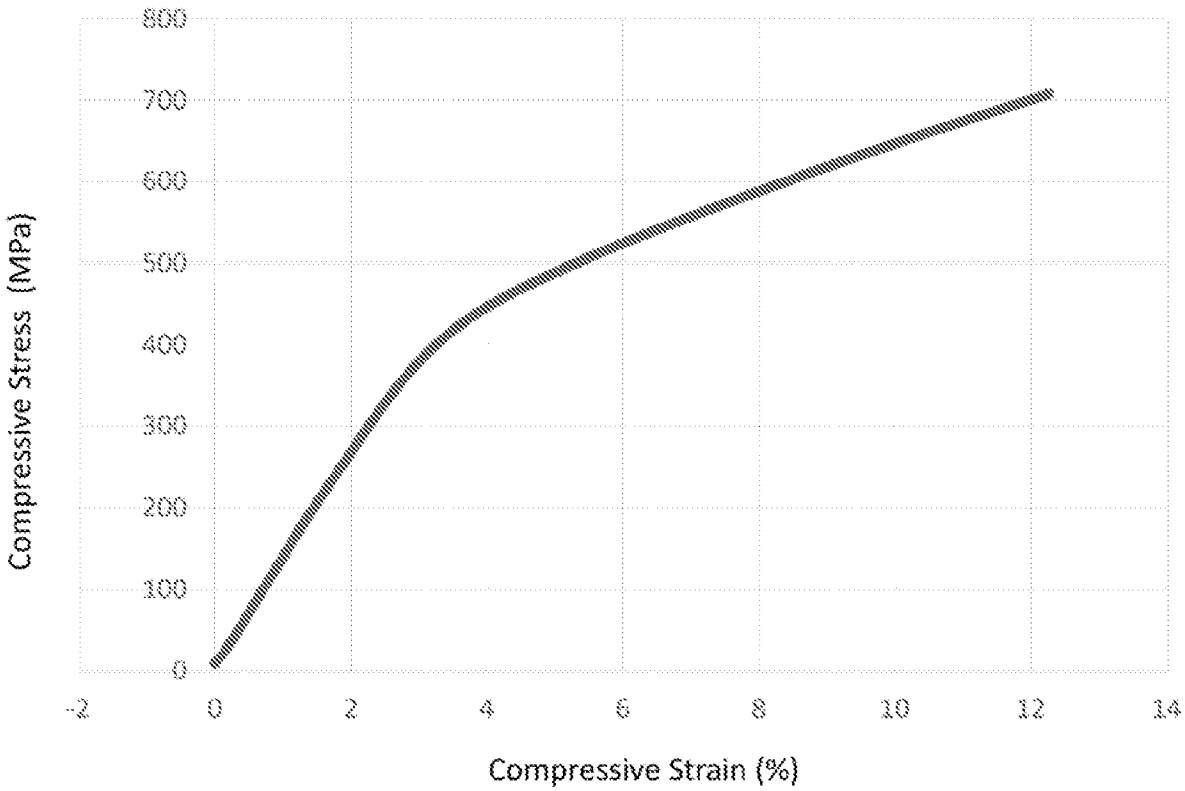
800
700
600
500
400
300
200
100
0
Compressive Stress (MPa)
-2
0
2
4
6
8
10
12
14
Compressive Strain (%)

FIG. 28